153
COMPLETED

NUREG/CR-4861
UCID-20980

ORIGINAL

Development of Site Specific Response Spectra

Prepared by D. L. Bernreuter, J. C. Chen, J. B. Savy

Lawrence Livermore National Laboratory

Prepared for
U.S. Nuclear Regulatory
Commission

BEST COPY AVAILABLE

NOTICE

This report was prepared as an account of work sponsored by an agency of the United States Government. Neither the United States Government nor any agency thereof, or any of their employees, makes any warranty, expressed or implied, or assumes any legal liability or responsibility for any third party's use, or the results of such use, of any information, apparatus, product or process disclosed in this report, or represents that its use by such third party would not infringe privately owned rights.

NOTICE

Availability of Reference Materials Cited in NRC Publications

Most documents cited in NRC publications will be available from one of the following sources:

1. The NRC Public Document Room, 1717 H Street, N.W.
Washington, DC 20555
2. The Superintendent of Documents, U.S. Government Printing Office, Post Office Box 37082,
Washington, DC 20013-7082
3. The National Technical Information Service, Springfield, VA 22161

Although the listing that follows represents the majority of documents cited in NRC publications, it is not intended to be exhaustive.

Referenced documents available for inspection and copying for a fee from the NRC Public Document Room include NRC correspondence and internal NRC memoranda; NRC Office of Inspection and Enforcement bulletins, circulars, information notices, inspection and investigation notices; Licensee Event Reports; vendor reports and correspondence; Commission papers; and applicant and licensee documents and correspondence.

The following documents in the NUREG series are available for purchase from the GPO Sales Program: formal NRC staff and contractor reports, NRC-sponsored conference proceedings, and NRC booklets and brochures. Also available are Regulatory Guides, NRC regulations in the *Code of Federal Regulations*, and *Nuclear Regulatory Commission Issuances*.

Documents available from the National Technical Information Service include NUREG-series reports and technical reports prepared by other federal agencies and reports prepared by the Atomic Energy Commission, forerunner agency to the Nuclear Regulatory Commission.

Documents available from public and special technical libraries include all open literature items, such as books, journal and periodical articles, and transactions. *Federal Register* notices, federal and state legislation, and congressional reports can usually be obtained from these libraries.

Documents such as theses, dissertations, foreign reports and translations, and non-NRC conference proceedings are available for purchase from the organization sponsoring the publication cited.

Single copies of NRC draft reports are available free, to the extent of supply, upon written request to the Division of Technical Information and Document Control, U.S. Nuclear Regulatory Commission, Washington, DC 20555.

Copies of industry codes and standards used in a substantive manner in the NRC regulatory process are maintained at the NRC Library, 7920 Norfolk Avenue, Bethesda, Maryland, and are available there for reference use by the public. Codes and standards are usually copyrighted and may be purchased from the originating organization or, if they are American National Standards, from the American National Standards Institute, 1430 Broadway, New York, NY 10018.

NUREG/CR-4861
UCID-20980
RA

Development of Site Specific Response Spectra

Manuscript Completed: July 1986
Date Published: March 1987

Prepared by
D. J. Bernreuter, J. C. Chen, J. B. Savy

Lawrence Livermore National Laboratory
7000 East Avenue
Livermore, CA 94550

Prepared for
Division of Engineering Safety
Office of Nuclear Regulatory Research
U.S. Nuclear Regulatory Commission
Washington, DC 20555
NRC FIN A0454

BEST COPY AVAILABLE

BLANK

DEVELOPMENT OF SITE SPECIFIC RESPONSE SPECTRA

ABSTRACT

For a number of years the United States Nuclear Regulatory Commission (NRC) has employed site specific spectra (SSSP) in their evaluation of the adequacy of the Safe Shutdown Earthquake (SSE). These spectra were developed only from the spectra of the horizontal components of the ground motion and from a very limited data set. As the data set has considerably increased for Eastern North America (ENA) and as more relevant data has become available from earthquakes occurring in other parts of the world (e.g., Italy), together with the fact that recent data indicated the importance of the vertical component, it became clear that an update of the SSSP's for ENA was desirable.

The methodology used in this study is similar to the previous ones in that it used actual earthquake ground motion data with magnitudes within a certain range and recorded at distances and at sites similar to those that would be chosen for the definition of an SSE.

An extensive analysis of the origin and size of the uncertainty is an important part of this study. The results of this analysis of the uncertainties is used to develop criteria for selecting the earthquake records to be used in the derivation of the SSSP's.

We concluded that the SSSPs were not very sensitive to the distribution of the source to site distance of the earthquake records used in the analysis. That is, the variability (uncertainty) introduced by the range of distances was relatively small compared to the variability introduced by other factors. We also concluded that the SSSP are somewhat sensitive to the distribution of the magnitudes of these earthquakes, particularly at rock sites and, by inference, at shallow soil sites. We found that one important criterion in selecting records to generate SSSP is the depth of soil at the site.

BEST COPY AVAILABLE

BLANK PAGE

TABLE OF CONTENTS

ABSTRACT iii
LIST OF TABLES vi
LIST OF FIGURES vii
EXECUTIVE SUMMARY xv
1. Introduction 1

2. Review of Theoretical-Numerical Studies 6
2.1 Introduction 6
2.2 Effect of Rupture Depth on Spectral Shape 6
2.3 Effect of Rupture Depth and Magnitude on Spectral Values 7
2.4 The Effect of Rupturing to the Surface 7
2.5 Topography and 1-D Versus 3-D Analysis Effects 8

3. Uncertainties in Ground Motion Data Collection 15
3.1 Introduction 15
3.2 Ground Motion Instruments 15
3.3 Errors in Digitized Signals 16

4. Effect of Shallow Soil, Weathered Bedrock, Travel Path and Magnitude on Ground Motion 20
4.1 Introduction 20
4.2 Effect of Shallow Soil Layers for ENA Earthquake Records 20
4.3 Effect of Weathered Bedrock on Recorded Motion 21
4.4 Effect of Traveling Path 23
4.5 Effect of Earthquake Magnitudes 24
4.6 Conclusions 25

5. Uncertainties in Ground Motion Prediction and Criteria for Selection of the Data Set 49
5.1 Introduction 49
5.2 Site Specific Spectra Approach 49
5.3 Model for the Uncertainty 51
5.4 Uncertainty Introduced by the Travel Path 52
5.5 Uncertainty Introduced by the Source 53
5.6 Uncertainty Introduced by the Site 54
5.7 Uncertainties Introduced by the Range for M and R Used 59

6. Development of Site Specific Spectra for ENA 69
6.1 Criteria for Selecting Records 69
6.2 Potential Errors Introduced by Site Classification Schemes 71
6.3 Development of Base Cases 74
6.4 Sensitivities of the SSSP 76

7. Discussions and Conclusions 117

8. References 119

BEST COPY AVAILABLE

LIST OF TABLES

TABLE		PAGE NO.
2.1	Generalized Crustal Models in EUS, (Apsel et al. 1983).....	9
3.1	Summary of Instrument Characteristics.....	18
4.1	ENA Earthquake Records Used for This Study.....	27
4.2	WUS Earthquake Motions Recorded on Hard Rock.....	28
4.3	Earthquake with Compatible Magnitude and Distance as Compared to ENA Earthquakes.....	29
6.1	Rock Records Used.....	80
6.2	Records Selected for Deep Soil Case for the Ensemble of Earthquakes Centered at m_{bLg} = 5.25.....	81
6.3	Records Selected for the Deep Soil Case for the Ensemble of Earthquakes Centered at m_{bLg} = 5.75.....	82
6.4	Records Selected for Shallow Soil Cases.....	83
6.5	Data for the Earthquakes Identified in Tables 6.2, 6.3 and 6.4.....	84
6.6	Deep Soil Stations, Site Information for Sites Identified in Tables 6.2 and 6.3.....	86
6.7	Site Information for Shallow Soil Sites.....	88

BEST COPY AVAILABLE

LIST OF FIGURES

FIGURE		PAGE NO.
1.1a	Comparison of the 5% damped relative velocity spectra for both horizontal components for the New Brunswich earthquake recorded at Mitchell Lake Road and the Daley City earthquake recorded at Golden Gate Park.....	3
1.1b	Comparison of the 5% damped relative velocity spectra for both horizontal components for the New Hampshire earthquake recorded at the downstream station at Franklin Falls Dam and the Daley City earthquake recorded at Golden Gate Park.....	4
1.2	5% damped relative velocity spectra of both horizontal components for the magnitude 4.25 June 13, 1975 earthquake recorded at New Madrid.....	5
2.1	Response spectral ratios for magnitude 4.5 rupture depth study in the stiff soil crustal model for 0-2 km rupture normalized by deeper rupture (4-6 km). (R.J. Apsel et al., 1983).....	10
2.2	Pseudo-velocity response spectral values (2 percent damping) at site distance of 5 km in the stiff-soil crustal model compared for M4.5 ruptures at 0-2 km (601 and 611), 2-4 km (701 and 711) 4-6 km (801 and 811) and 13-15 km (901 and 911) depths and M5.5 ruptures at 10-15 km depth. (R.J. Apsel et. al, 1983).....	11
2.3	Same as Figure 2.2 for site distance of 20 km. (R.J. Apsel et al., 1983).....	12
2.4	Representation of a sediment-filled valley by a sine-type model, (Bard and Bouchon 1984).....	13
2.5	Dependence of the maximum spectral amplification (b) and the corresponding frequency on the shape ratio h/l for five surface sites (from x/l=0., center, to x/l = 0.64,edge.) Both sets of results are compared with the corresponding one-dimensional (1D)	

BEST COPY AVAILABLE

FIGURE PAGE

values, displayed on the left. The geometrical and mechanical characteristics of the valleys are detailed in the test. (Bard and Bouchon, 1984)..... 14

3.1 Schematic Diagram of Mechanical-Optical Photographic Strong-Motion Accelerograph (from Hudson, 1980)..... 19

4.1 The envelope, 50th and 85th percentile relative velocity spectra for estimated rock-outcrop motions from the corresponding ENA earthquake motions recorded on shallow soil sites..... 30

4.2 The envelope, 50th and 84th percentile acceleration spectra for estimated rock-outcrop motions from the corresponding ENA earthquake motions recorded on shallow soil sites..... 31

4.3 Comparison of 50th percentile (medians) 5% damped relative velocity response spectra between the recorded motions at very shallow soil sites and the corresponding rock outcrop motions..... 32

4.4 Comparison of 50th and 84th percentile normalized velocity spectra between the recorded motions at shallow site and the corresponding rock outcrop motions..... 33

4.5 Comparison of 50th, 84th percentile normalized acceleration spectra between the recorded motions at shallow sites and the corresponding rock outcrop motions..... 34

4.6 The velocity profiles of three weathered rock sites..... 35

4.7 Variation of shear modulus with shear strain for rocks at the DCPP site based on 1977 laboratory test data..... 36

4.8 Variation of damping ratio with shear strain for rocks at the DCPP site based on 1977 laboratory test data..... 37

4.9 Comparison of median and 84th percentile spectra between the group of input motions and

BEST COPY AVAILABLE

FIGURE		PAGE
	the group of output responses at the CIT Seismological Lab site.....	38
4.10	Comparison of median and 84th percentile spectra between the group of input motions and the group of output responses at the Golden Gate park.....	39
4.11	Comparison of the 50th and the 80th percentile spectra between the group of input motions and the group of output responses at the Diablo Canyon Power Plant site.....	40
4.12	The effect of material energy absorption factor Q, on the response of one dimensional wave propagation through a hard rock medium.....	41
4.13	The combined effect of material stiffness and energy absorption factor on the response of 1-D wave propagation through rock media.....	42
4.14	Comparison of the median and 84th percentile normalized velocity spectra between motions from the strong WUS earthquake group and the smaller ENA earthquake group, both groups of earthquake data were recorded on hard rock.....	43
4.15	Comparison of the median and 84th percentile normalized acceleration spectra between motions from the strong WUS earthquake group and the smaller ENA earthquake group, both groups of earthquake data were recorded on hard rock.....	44
4.16	Comparison of the 50th and the 84th percentile velocity spectra between motions from the ENA group and the combined Oroville & Ancona group.....	45
4.17	Comparison of the 50th and the 84th percentile acceleration spectra between motions from the ENA group and the combined Oroville & Ancona group.....	46
4.18	Comparison of the 50th and the 84th percentile normalized velocity spectra between motions from the ENA group and the combined Oroville & Ancona group.....	47

BEST COPY AVAILABLE

FIGURE		PAGE
4.19	Comparison of the 50th and the 84th percentile normalized acceleration spectra between motions from the ENA group and the combined Oroville & Ancona group.....	48
5.1.a	Over plot of all of the suite of spectra selected to define the SSSP for a deep soil site having a SSI of MMVII.....	60
5.1b	The Median and 84th percentile spectra of the suite of records shown in Fig. 5.1.a.....	61
5.2	Over plot of both radial and tangential components of 5 UNE recorded at a single deep soil station. These 5 UNE all had a yield of $\pm$ 5 kilotons of each other at a distance of 55 $\pm$ 2km from the recording station.....	62
5.3	The envelope, median and 84th percentile spectra of the suite of spectra shown in Fig. 5.2.....	63
5.4	Comparison of the spectra from two earthquakes located within a few kilometers of each other with similar M_L and recorded at the Oroville Airport.....	64
5.5	Comparison of the spectra from two earthquakes located within a few kilometers of each other with similar magnitudes and recorded at the Brawley Airport. Event numbers and magnitudes from Johnson and Hanks (1976).....	65
5.6	Comparison of Exp (σ_i) obtained from a covariance analysis accounting for each site to that obtained by Lynch (1969) which does not include site factors.....	66
5.7	Comparison of the radial component of the spectra from two nearby stations TMT (Tonopah motel, shallow alluvium) and TCH (Tonopah chruch, rock).....	66
5.8	Comparison of Exp (σ_i) for the covariance analysis for Pahute Mesa UNE (Fig. 6.1) to that for Yucca Flat UNE.....	67
5.9	Normalized peak accelerations recorded at El Centro and Ferndale site compared with McGuire's (1978) correlation.	67

BEST COPY AVAILABLE

FIGURE		PAGE
5.10	Normalized peak horizontal acceleration for the Oroville data set. The data for Johnson Ranch are denoted by J and for the Oroville Airport by A. The data from the other stations are denoted by *	68
6.1a	Schematic representation of the overall computation scheme used by Bernreuter et al. (1985)	89
6.1b	Schematic representation of the overall simulation approach used in Bernreuter et al. (1985) to model the range of sites with category	90
6.2	The median amplification factors for the sand-like site categories S-1,S-2 and S-3 defined in Bernreuter et al. (1985)	90
6.3	A comparison of the median amplification factor for a fixed site falling into category S-2 and the median amplification factor based on the range of sites in category S-2	92
6.4a	Envelope, 84th percentile and median spectra of the set of records falling into the MM VII case for rock sites- horizontal components	93
6.4b	Envelope, 84th percentile and median spectra of the set of records falling into the MM VII case for rock sites- vertical components	94
6.5a	Envelope, 84th percentile and median spectra of the set of records falling into the MM VIII case for rock sites- horizontal component	95
6.5b	Envelope, 84th percentile and median spectra of the set of records falling into the MM VIII case for rock sites- vertical components	96
6.6a	Envelope, 84th percentile and median spectra of the set of records falling into the MM VII case for deep soil sites-horizontal components	97
6.6b	Envelope, 84th percentile and median spectra of the set of records falling into the MM VII case for deep soil sites-vertical components	98

BEST COPY AVAILABLE

FIGURE		PAGE
6.7a	Envelope, 84th percentile and median spectra of the set of records falling into the MM VIII case for deep soil sites-horizontal components	99
6.7b	Envelope, 84th percentile and median spectra of the set of records falling into the MM VIII case for deep soil sites-vertical components	100
6.8a	Envelope, 84th percentile and median spectra of the set of records falling into the MM VII case for shallow soil sites-horizontal components	101
6.8b	Envelope, 84th percentile and median spectra of the set of records falling into the MM VII case for shallow soil sites-vertical components	102
6.9	Comparison of the median SSSP for a deep soil site weathered to a rock site for the MM VII case	103
6.10	Comparison of the median SSSP for a deep soil site to a rock site for the MM VIII case	104
6.11	Comparison of the median SSSP for a shallow soil site to a deep site for the MM VII case.	105
6.12	The uncertainty of the SSSP estimate as measured by for deep soil and rock sites for deep soil and rock sites for the MM VII case	106
6.13	The uncertainty of the SSSP estimate as measkured by for records obtained at the Oroville Airport site based on six earthquakes	107
6.14	Comparison of the median and 84th percentile spectra predicted by the regression model fit to the MM VII data for rock sites using distance of 8.4 km and a magnitude of 5.2 to the median and 84th percentile spectra for the SSSP for rock sites for the MM VVII case.	108
6.15	Same as Fig. 6.14, except the prediction is for a distance of 15 km and a magnitude of 5.2	109

BEST COPY AVAILABLE

FIGURE		PAGE
6.16	Comparison of the median and 84th percentile spectra predicted by the regression model fit to the MM VII data for deep soil sites using a distance of 10.9 km and a magnitude of 5.1.....	110
6.17a	Same as Fig. 6.16, except the prediction is for a distance of 15 km and a magnitude of 5.1.....	111
6.17b	Comparison between the median and 84th percentile SSSP for deep soil sites for the MM VII case and the median and 84th percentile spectra obtained by the weighted averaging approach. The weights were based on four rings.....	112
6.18	Comparison of the median spectrum of the rock set with magnitudes 5.1 or less to the set with magnitudes between 5.3 and 5.7.....	113
6.19	Comparison of the median SSSP for rock sites for the MM VII and MM VIII cases.....	114
6.20	Comparison of the median SSSP for deep soil sites for the MM VII and MMM III cases.....	115
6.21	Comparison of the median and 84th percentile spectra for the shallow soil SSSP to the median and 84th percentile spectra obtained using all of the records with magnitudes less than 5.8 in Table 6.4.....	116

BEST COPY AVAILABLE

BLANK PAGE

EXECUTIVE SUMMARY

The United States Nuclear Regulatory Commission (NRC) has employed site specific spectra (SSSP) in their evaluation of the adequacy of the Safe Shutdown Earthquake (SSE) for a number of years. Since these spectra were first developed, a number of additional records from both the Eastern and Western U.S. and other areas have become available and should be incorporated into the existing sets of spectra. In the original applications of SSSP, only horizontal spectra were used. However, recent data indicate that it may be appropriate to compare the vertical component of the SSE design spectra to an appropriate vertical SSSP. One basic concept behind the development of SSSP is that earthquakes in Eastern North America (ENA) have the same average range of source parameters as those in other parts of the world, most notably the Western United States (WUS). This implies that on the average, the only differences in ground motion records from earthquakes in different regions are due to differences in regional attenuation. Based on this assumption, sets of SSSP are developed for ENA sites by selecting sets of earthquakes recorded on similar site conditions within distances where the differences in regional attenuation are thought to be small. The available data used in these studies are primarily from the WUS and some records from other parts of the world are also used. The development and use of the SSSP is complicated by two factors: first, in actual practice, it is difficult to match site conditions, and still find sufficient number of records from earthquakes with the proper distance and magnitude ranges to develop statistically significant sets of SSSP; and secondly, data from several recent ENA earthquakes suggest that ENA earthquakes may be richer in high frequency energy than is typical of earthquakes in the WUS.

It is observed that the short period spectral content of several ENA records is much higher than for typical WUS records. Several factors may lead to the observed differences:

1. Earthquake source mechanism differences.
2. Effect of local site conditions, e.g., very shallow soil over an unweathered bedrock with a high shear wave velocity (high when compared with WUS).
3. The instruments for collecting the strong motion data and the methods used to correct for instrument response introduces errors in the digitized strong motion data.

It is of some interest to note that all ENA records do not appear to exhibit the same enhanced high frequency content.

The purpose of the study reported here is principally to develop new sets of SSSP applicable to several categories of site conditions, thus updating previous work. In addition, the methodology is applied to the vertical component of the strong motion.The approach adopted consists of five parts. In the first part (Section 2) we review some of the work that has been performed to mathematically model source, travel path and the local site conditions that sheds some light on the issues at hand. The results from

BEST COPY AVAILABLE

these studies, along with the modeling studies of Section 4 are used to assist in understanding the comparisons that are made between the spectra from ENA earthquakes and other world wide data.

In the second part, we point out some of the physical limitations present in the ground motion data due to the data collection techniques, including the instruments used in the ground motion data equipment.

The third part, reported in Section 4, consists of a set of analyses performed using simple modeling to better understand the importance and effect of shallow soil layers, weathered rock and deep softer rock columns typical of WUS sites

In the fourth part, reported in Section 5, we examine the contribution to the uncertainty associated with our SSSP and attempt to determine which factors are the most significant as a guide to the development of criteria to select suites of records to represent a given category.

In the fifth part, reported in Section 6, we present the results of calculations for the updated SSSP for the various site categories considered and examine the sensitivity of the SSSP to the makeup of the sets.

The major conclusion reached in this study is that the ground motion at a site will exhibit large variability between earthquakes due to source and travel path variabilities. Thus, any approach used to estimate the ground motion at a site will have large uncertainties and the only way to reduce these uncertainties is to include the important source and travel path parameters in the model. We also found that site parameters are very important and should be modeled. These are not new conclusions, but we believe that in Section 5 we have better defined the relative contribution of each of the major sources of uncertainty in the method used to estimate the ground motion. We found that the uncertainty, expressed by the standard deviation of the logarithm of the acceleration, for a fixed site was approximately .5 and the uncertainty introduced by having a variety of site is .3, which is in agreement with results obtained independently by very different methods by other researchers. (i.e., McCann, 1983). The uncertainty introduced by the paths was found to be on the order of .2 and that of the source was found to be on the order of .3.

Because of large and, at present, unreducible uncertainties, it is not possible to reach conclusions on EUS vs WUS ground motions based on relatively small data sets. For example, in Section 1 we noted that some of the ENA records have more short period energy than WUS records. In Section 2 we noted that this could, in part, be due to the relatively shallow depth of the ENA earthquakes. In Section 4 we found high frequencies are not due to site effect, but the quality factor Q could have some effect, and given the large variabilities between earthquakes of the same magnitude, it is not possible to test this observation in a meaningful way. We also noted that smaller earthquakes appear to have relatively more short period energy than large earthquakes.

The main task of this report was to update the existing SSSP and generate vertical SSSP. New records were added to the sets initially generated in Bernreuter (1981) where only rock and soil sets of SSSP were generated. In

BEST COPY AVAILABLE

the present study this was refined to include rock, shallow soil and deep soil SSSP as well as vertical spectra.

We concluded that the SSSP were not very sensitive to the distance distribution. That is, the variablity (uncertainty) introduced by the range of distances, from the earthquake sources to where the records were collected, was relatively small compared to the variability introduced by other factors. We also concluded that the SSSP are not very sensitive to the distribution of magnitudes used. At rock and, by inference, at shallow soil sites, we found that one important criterion in selecting records to generate SSSP is the depth of soil.

We also concluded that in generating estimates of the ground motion, it is necessary to include data from as many earthquakes as possible with a large number of travel paths. It is also important not to use too much data from a single earthquake.

As more data becomes available, (both strong motion data and equally important data about the soil and rock conditions at the recording site), it will be possible to update and improve the SSSP developed in this report. It is unlikely that the relative difference between the median and 84th percentile spectra will change significantly (i.e., it is unlikely that the uncertainty will be significantly reduced) with the addition of new data. However, it is likely that the absolute location of the medians and other central tendency measures, will change (more so for the rock and shallow soil SSSP than for the deep soil SSSP). With new data, it should be possible to subdivide the rock set and introduce new shallow soil categories. It should be noted that this will only be possible if the new data includes boring logs and shear wave velocity data.

BEST COPY AVAILABLE

1. INTRODUCTION

The United States Nuclear Regulatory Commission (NRC) has employed site specific spectra (SSSP) in their evaluation of the adequacy of the Safe Shutdown Earthquake (SSE) for a number of years. Considerable use has been made of the sets of SSSP contained in Bernreuter (1981). Since these spectra were developed, a number of additional records from both the Eastern and Western U.S. and other areas have become available and should be incorporated into the existing sets of spectra. This updating effort was started in the study of the Limerick and Hope Creek sites, (Bernreuter (1983), and Bernreuter et al. (1984)). In the original applications of SSSP, only horizontal spectra were used. However, recent data indicate that it may be appropriate to compare the vertical component of the SSE design spectra to an appropriate vertical SSSP.

One basic concept behind the development of SSSP is that earthquakes in Eastern North America (ENA) have the same average range of source parameters as those in other parts of the world, most notably the Western United States (WUS). This implies that on the average, the only differences in ground motion records from earthquakes in different regions are due to differences in regional attenuation. Based on this assumption sets of SSSP are developed for ENA sites by selecting sets of earthquakes recorded on similar site conditions within distances where the differences in regional attenuation are thought to be small. The available data used in these studies are primarily from the WUS. The development and used of the SSSP is complicated by two factors:

First, in actual practice, it is difficult to match site conditions, and still find a sufficient number of records from earthquakes with the proper distance and magnitude ranges to develop statistically significant sets of SSSP.

Second, data from several recent ENA earthquakes suggest that EUS earthquakes may be richer in high frequency energy than is typical of earthquakes in the WUS as is illustrated in Figs. 1.1a and 1.1b. Figure 1.1a shows a comparison of the five percent damped relative velocity spectra of the time history of the 3/3/82 magnitude 4.8 New Brunswick earthquake recorded at the Mitchell Lake Road station (hard rock) as compared to the response spectra of the time history from the 3/22/57 Daley City magnitude 5.3 earthquake recorded at Golden Gate Park station (soft weathered rock). The spectral content of the Golden Gate record is typical of the spectral content of WUS records, as can be seen by comparing the spectral content of the Golden Gate record to the SSSP for rock sites developed in Section 6 of this report. Figure 1.1b shows a similar comparison between the spectra from the Golden Gate record and the spectra computed from the time history of the 1/18/82 magnitude 4.8 New Hampshire earthquake recorded at the downstream station at Franklin Falls Dam.

It is observed from Figs. 1.1a and b that the short period spectral content of the two ENA records is much higher than for the WUS record. Several factors may lead to the observed differences:

1. Earthquake source mechanism differences.
2. Effect of local site conditions, e.g., very shallow soil over an unweathered bedrock with a high shear wave velocity (high when compared with WUS).

BEST COPY AVAILABLE

3. The instruments for collecting the strong motion data and the methods used to correct for instrument response introduces errors in the digitized strong motion data.

It is of some interest to note that all ENA records do not appear to exhibit the same enhanced high frequency content as illustrated in Figs. 1.1a and b. Figure 1.2 shows the five percent damped relative velocity spectra from the 6/13/75 magnitude 4.25 earthquake recorded at New Madrid. It can be seen from Fig. 1.2 that the spectral content of the New Madrid record is more similar to WUS records. Note that all three ENA records were obtained within 10 km of the source.

Clearly, because of the large uncertainties involved, no conclusions can be reached on the basis of the above limited comparison. Unfortunately, there is very little additional data available from near source ENA earthquakes with magnitudes greater than 4.

The purpose of the study reported here is principally to develop new sets of SSSP applicable to several categories of site conditions, thus updating previous work. In addition, the methodology is applied to the vertical component of the strong motion.

The approach adopted consists of five parts. In the first part (Section 2) we review some of the work that has been performed to mathematically model source, travel path and the local site conditions that sheds some light on the issues at hand. The results from these studies, along with the modeling studies of Section 4, are used to assist in understanding the comparisons that are made between the spectra from ENA earthquakes and other world-wide data.

In the second part, (Section 3) we point out some of the physical limitations present in the ground motion data due to the data collection technique, including the instruments used in the ground motion data equipment.

The third part, reported in Section 4, consists of a set of analyses performed using simple modeling to better understand the importance/effect of shallow soil layers, weathered rock and deep softer rock columns typical of WUS sites.

In the fourth part, reported in Section 5, we examine the contributions to the uncertainty associated with our SSSP and attempt to determine which factors are the most significant as a guide to the development of criteria to select suites of records to represent a given category.

In the fifth part, reported in Section 6, we present the results of calculations for the updated SSSP for the various site categories considered and examine the sensitivity of the SSSP to the makeup of the sets.

BEST COPY AVAILABLE

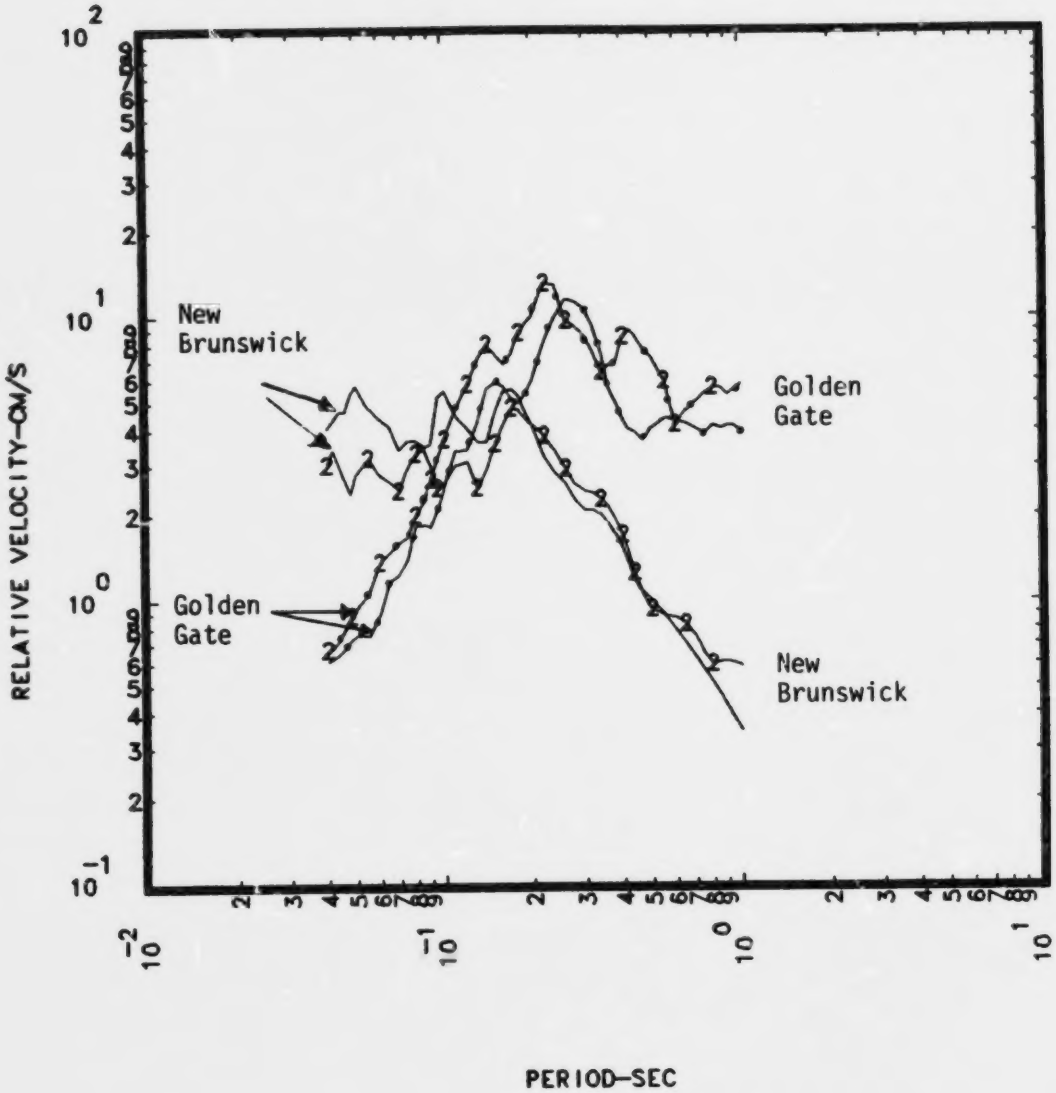

Fig. 1.1a Comparison of the 5% damped relative velocity spectra for both horizontal components for the New Brunswick earthquake recorded at Mitchell Lake Road and the Daley City earthquake recorded at Golden Gate Park.

BEST COPY AVAILABLE

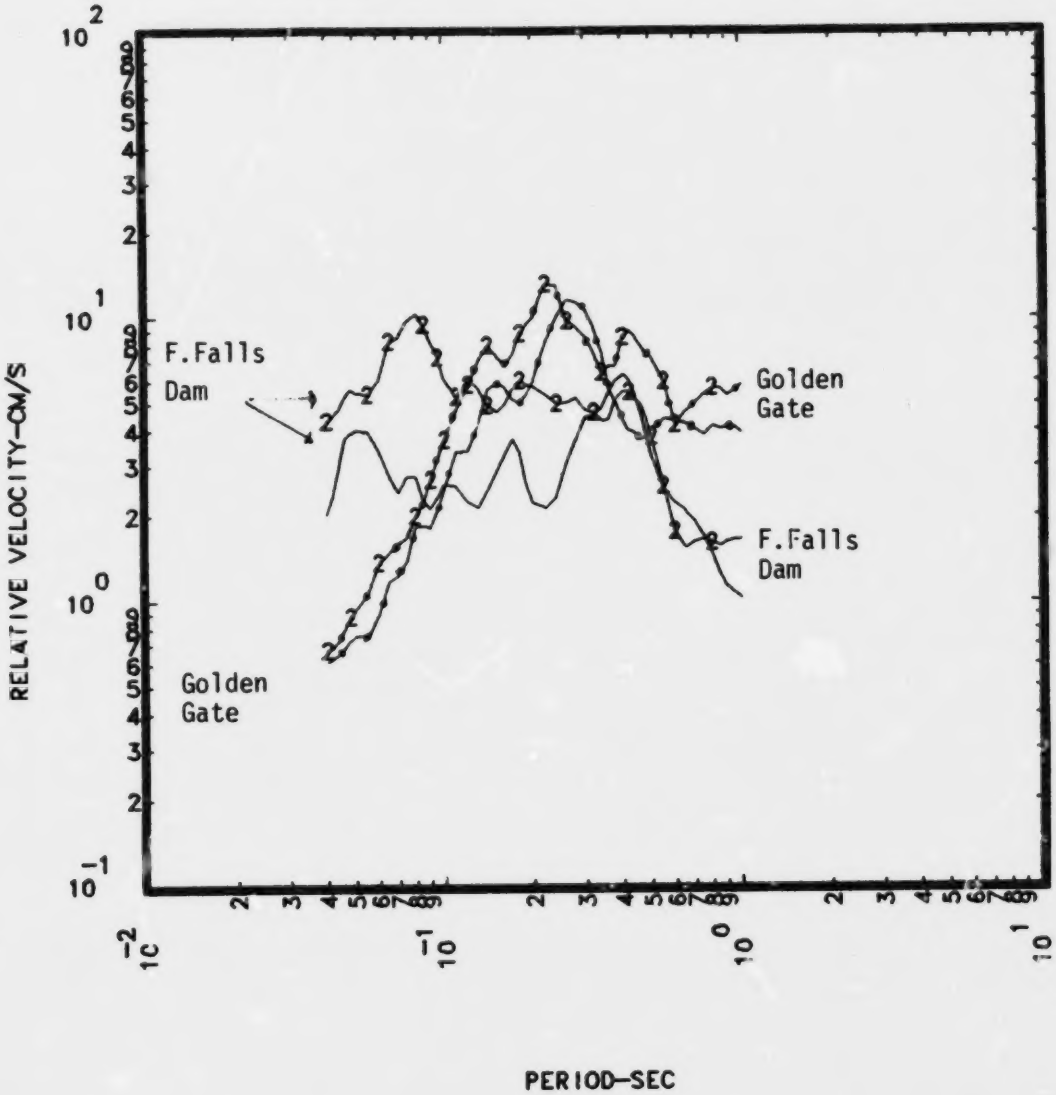

Fig. 1.1b Comparison of the 5% damped relative velocity spectra for both horizontal components for the New Hampshire earthquake recorded at the downstream station at Franklin Falls Dam and the Daley City earthquake recorded at Golden Gate Park.

BEST COPY AVAILABLE

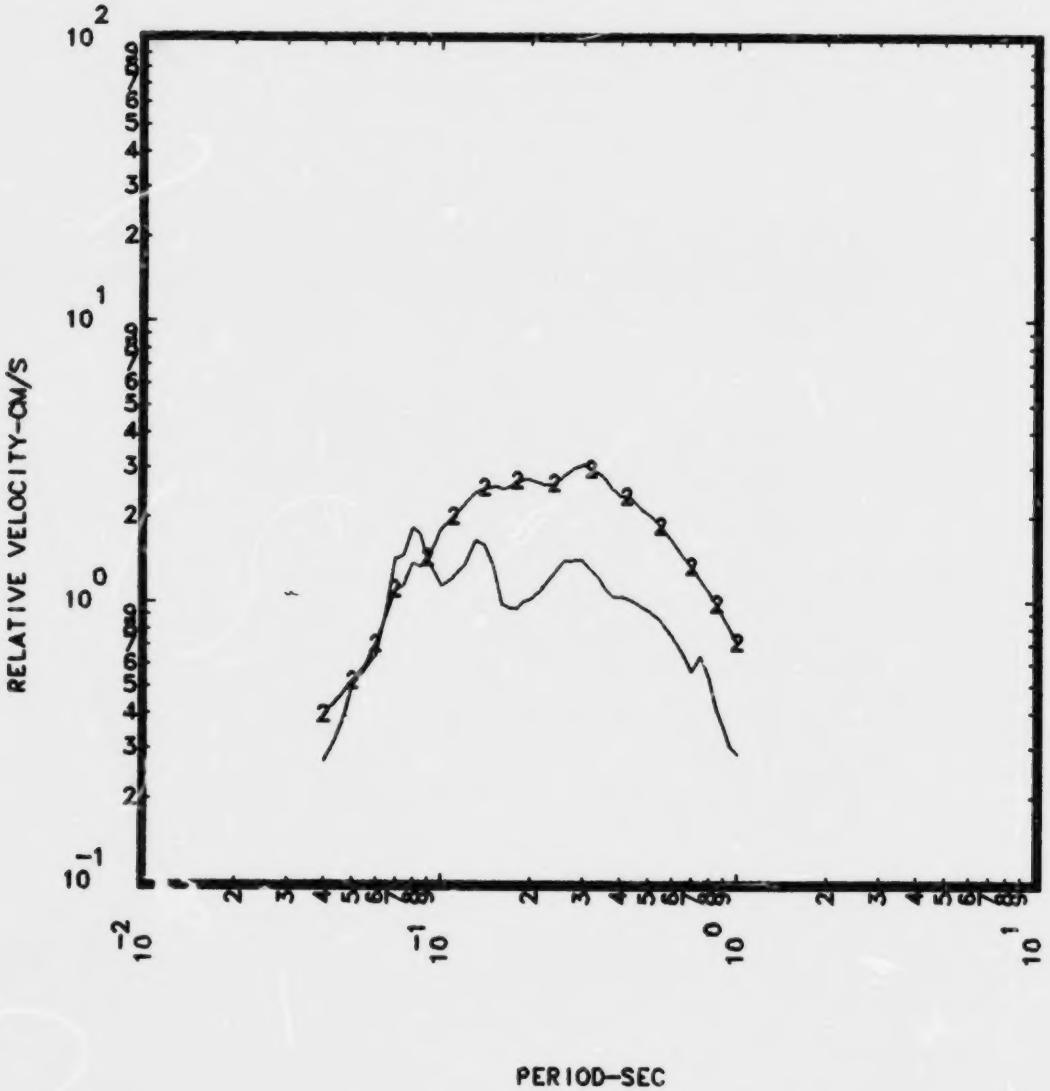

Fig. 1.2 5% damped relative velocity spectra of both horizontal components for the magnitude 4.25 June 13, 1975 earthquake recorded at New Madrid.

BEST COPY AVAILABLE

2. REVIEW OF THEORETICAL-NUMERICAL STUDIES

2.1 Introduction

Since there is insufficient earthquake data available to fully quantify the sensitivity of response spectra to differences in source mechanism, travel path and local site conditions, sensitivity studies based on 3-D numerical modeling procedures have been performed to assess the relative difference in seismic ground motion due to the variation of these three factors, Apsel et al. (1983).

The approach used by Apsel et al. (1983) is based on the calculation of a three-dimensional Green's functions resulting from concentrated point forces buried in a layered viscoelastic half-space. The calculation was performed in the frequency domain with the azimuthal dependence represented by a Fourier series expansion. Time domain results are obtained by a discrete Fast Fourier Transform algorithm. The procedure involves the mathematical characterization of fault slippage at each point on the rupture surface. The ground motion for a distributed source is formulated in terms of integral representations over the rupture surface of temporal convolutions of fault slippage with earthquake ground motion for point sources at each integration point.

The results obtained by the numerical modeling procedure were validated by matching the strong motion recordings of several California earthquakes. In each case, the actual source parameters of recorded earthquakes were used to simulate the source mechanism, i.e. maximum slip velocity, slip displacement (stress drop) and rise time. The quality of the agreement between the calculated and the recorded ground motion was very good.

In the study by Apsel et al. (1983), thousands of three-component time histories were calculated for three different magnitudes of earthquakes, two different fault type, four different soil conditions, seven different distances and all for a variety of rupture depths and rupture configurations. The generalized crustal models representing four site conditions are shown in Table 2.1. Note that the soil properties were only changed in the upper layers, from the ground surface to a depth of 0.5 km. The results of that study are summarized in Sections 2.2 to 2.4. Other studies have concentrated on the effect of the local topography on the strong ground motion. At a site, one such study (Tucker and King 1984), based on empirical data showed the importance of the topographical effect. In Section 2.5, we summarize some of the conclusions reached by Bard and Bouchon (1985) on the effect of valley shapes on the strong ground motion, based on theoretical calculations. These latter results show good agreement with the work of Tucker and King (1984).

2.2 Effect of Rupture Depth on Spectral Shape

The response spectra ratio between shallow and deeper earthquakes for a stiff soil site at different distances for a magnitude 4.5 earthquake are shown in Fig. 2.1. The near field stations show uniformly large maximum acceleration levels as well as high response spectra for shallow sources relative to deep earthquakes. More variation is observed at sites with soft soil. In general, the shallow rupture produces significantly larger near field ground motions.

BEST COPY AVAILABLE

This is directly attributable to the shallow source exciting large amplitudes of surface waves, the deeper source generating smaller surface waves. In addition, the deep earthquake energy is more attenuated by geometric spreading and material damping since the travel path is longer.

2.3 Effect of Rupture Depth and Magnitude on Spectral Values

Under some conditions, a small magnitude shallow earthquake could produce ground motion in excess of those from larger magnitudes, deeper earthquakes. Figure 2.2 shows the comparison between the velocity spectra for 2% damping at site epicentral distance of 5 km for a the stiff soil model for a magnitude 4.5 rupture at 0-2 km, 2-4 km, 4-6 km, and 13-15 km depth and finally a magnitude 5.5 rupture at 10-15 km depth. Figure 2.3 shows the same comparison except for a site epicentral distance of 20 km. It can be seen from these figures that for the same site conditions, the small earthquakes may produce higher energy content at high frequencies than those of stronger earthquakes. However, for the longer periods the stronger earthquake gave higher energy content depending on the site distance and the rupture depth. It is interesting to note that the comparison of these sets of data is consistent with the comparison of some of the ENA data to typical WUS data as illustrated in Figs. 1.1a and b. It is of some interest to note that the depth of the New Brunswick earthquake is estimated to be 4 km and that of the New Hampshire earthquake to be 4-8 km. The depth of the 6/13/75 New Madrid earthquake was estimated to be at least 9 km. Thus it is possible that one factor that is influencing the high frequency content of the recorded ground motion is the shallow depths of the New Brunswick and New Hampshire events. It is of some interest to note that the depth of the earthquake recorded at the Perry Nuclear Power Plant in Ohio was estimated to be 2-7 km. This event produced unusual high frequency energy.

It should be noted that the source model did not change with depth in the Apsel et al. (1983) study. No doubt that this is not generally the case and one might well expect a variation in strength (stress drop) with depth which, of course, would significantly alter the results shown in Figs. 2.1 to 2.3.

As the distance increases to 20 km, the spectra for short periods for small earthquakes may be comparable in shape to those of larger earthquakes. Some spectra are higher and some of them are lower depending on the depth of sources. However, for the soft soil sites the short period spectra for the magnitude 4.5 events are below the magnitude 5.5 spectra at 20 km.

2.4 The Effect of Rupturing to the Surface

One of the most widely accepted tectonic differences between EUS and WUS is the observed depth of earthquake rupture for magnitudes 4 and greater. Typically, earthquakes in the EUS do not rupture to (or even near to) the ground surface in contrast to WUS events which often rupture all the way to (or near to) the ground surface. It has been suggested that surface rupture introduces "breakout phases". The term "breakout phase" has been used by various investigators to describe a high frequency Rayleigh wave generated by surface rupture. The presence of this phase has been predicted on the basis of numerical models of very uniform, smooth rupture on a perfectly planar fault. It had been argued that records which could contain such "breakout phases" should be excluded.

BEST COPY AVAILABLE

In order to study the significance of the "breakout phase" for the far more realistic modeling, it is necessary to compare the ground motions from surface ruptures to those from ruptures that stop just short of the surface. Apsel et al. (1983) investigated this question and concluded that the contributions to strong ground motions from the "breakout phase" are negligible.

2.5 Topography and 1-D versus 3-D analysis Effects.

Bard and Bouchon (1984) investigated the effect of two dimensional resonance of sediment-filled valleys. Depending on the mid-depth (h) to half width (l) of the valley, they calculated maximum spectral peak amplification for various site locations $S = x/l$, where x is the distance of the site from the center of the valley, as shown in Fig. 2.4.

The results of the calculations, shown in Fig. 2.5, show that depending on the site location and the 2-D aspect ration (h/l), there can be a substantial difference between the 1-D case and the 2-D case. However, it also shows that for most cases the 1-D case and the 2-D case predict the same resonant frequencies. Furthermore, the 1-D case is also an acceptable solution for peak spectral amplification when the aspect ratio is near unity for sites located away from the edges and from the center of the valley. The worst case appears to be when the site is located in the middle of the valley.

BEST COPY AVAILABLE

Table 2.1 Generalized Crustal Models in EUS, (Apsel et al. 1983)

Layer Depth (km)	Seismic Velocities α (km/sec)	β (km/sec)	Density ρ gm/cm^3	Material Quality Factors Q_α	Q_β
		Table 1. Hard-Rock Model (EUSGCR1)			
0.0-2.0	5.70	3.30	2.60	620	275
2.0-10.0	6.10	3.50	2.75	910	400
10.0-20.0	6.35	3.65	2.87	1820	800
20.0-40.0	6.60	3.80	3.00	2710	1200
26.0-40.0	6.85	3.95	3.12	3380	1500
40.0-∞	8.15	4.70	3.42	3380	1500
		Table 2. Stiff-Soil Model (EUSGCS1)			
0.0-0.5	3.00	1.70	1.80	175	75
0.5-2.0	5.20	2.90	2.50	480	200
2.0-10.0	6.10	3.50	2.75	910	400
10.0-20.0	6.35	3.65	2.87	1820	800
20.0-26.0	6.60	3.80	3.00	2710	1200
26.0-40.0	6.85	3.95	3.12	3380	1500
40.0-∞	8.15	4.70	3.42	3380	1500
		Table 3. Average-Soil Model (EUSGCS2)			
0.00-0.05	2.00	0.85	1.60	210	50
0.05-0.5	3.00	1.70	1.80	175	75
0.5-2.0	5.20	2.90	2.50	480	200
2.0-10.0	6.10	3.50	2.75	910	400
10.0-20.0	6.35	3.65	2.87	1820	800
20.0-26.0	6.60	3.80	3.00	2710	1200
26.0-40.0	6.85	3.95	3.12	3380	1500
40.0-∞	8.15	4.70	3.42	3380	1500
		Table 4. Soft-Soil Model (EUSGCS3)			
0.00-0.05	0.50	0.20	1.30	19	4
0.05-0.2	1.60	0.50	1.50	92	12
0.2-0.3	2.10	1.20	1.70	92	40
0.3-0.5	3.00	1.70	1.80	175	75
0.5-2.0	5.20	2.90	2.50	480	200
2.0-10.0	6.10	3.50	2.75	910	400
10.0-20.0	6.35	3.65	2.87	1820	800
20.0-26.0	6.60	3.80	3.00	2710	1200
26.0-40.0	6.85	3.95	3.12	3380	1500
40.0-∞	8.15	4.70	3.42	3380	1500

BEST COPY AVAILABLE

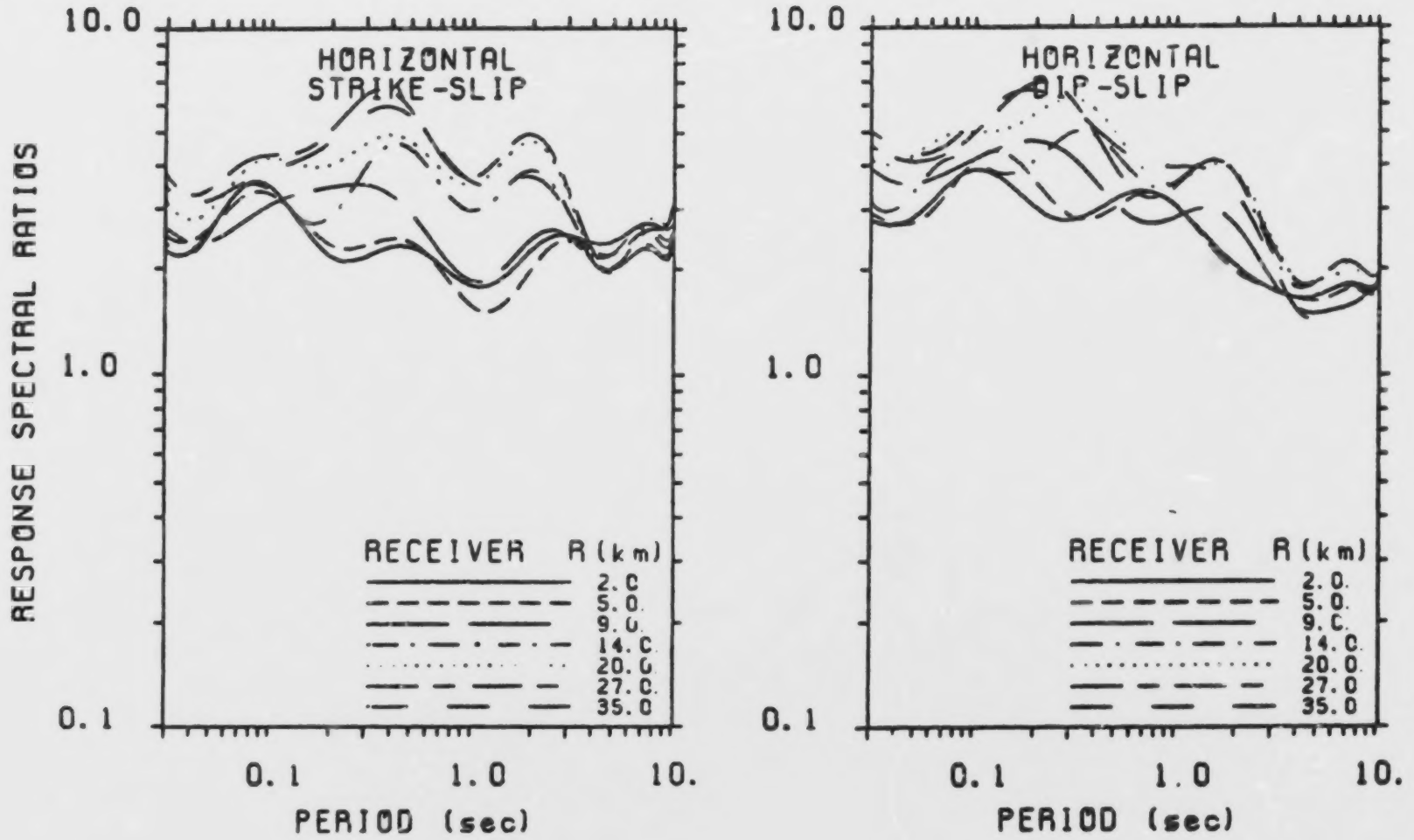

Fig. 2.1 Response spectral ratios for magnitude 4.5 rupture depth study in the stiff soil crustal model for 0-2 km rupture normalized by deeper rupture (4-6 km), (R.J. Apsel et al., 1983)

BEST COPY AVAILABLE

BEST COPY AVAILABLE

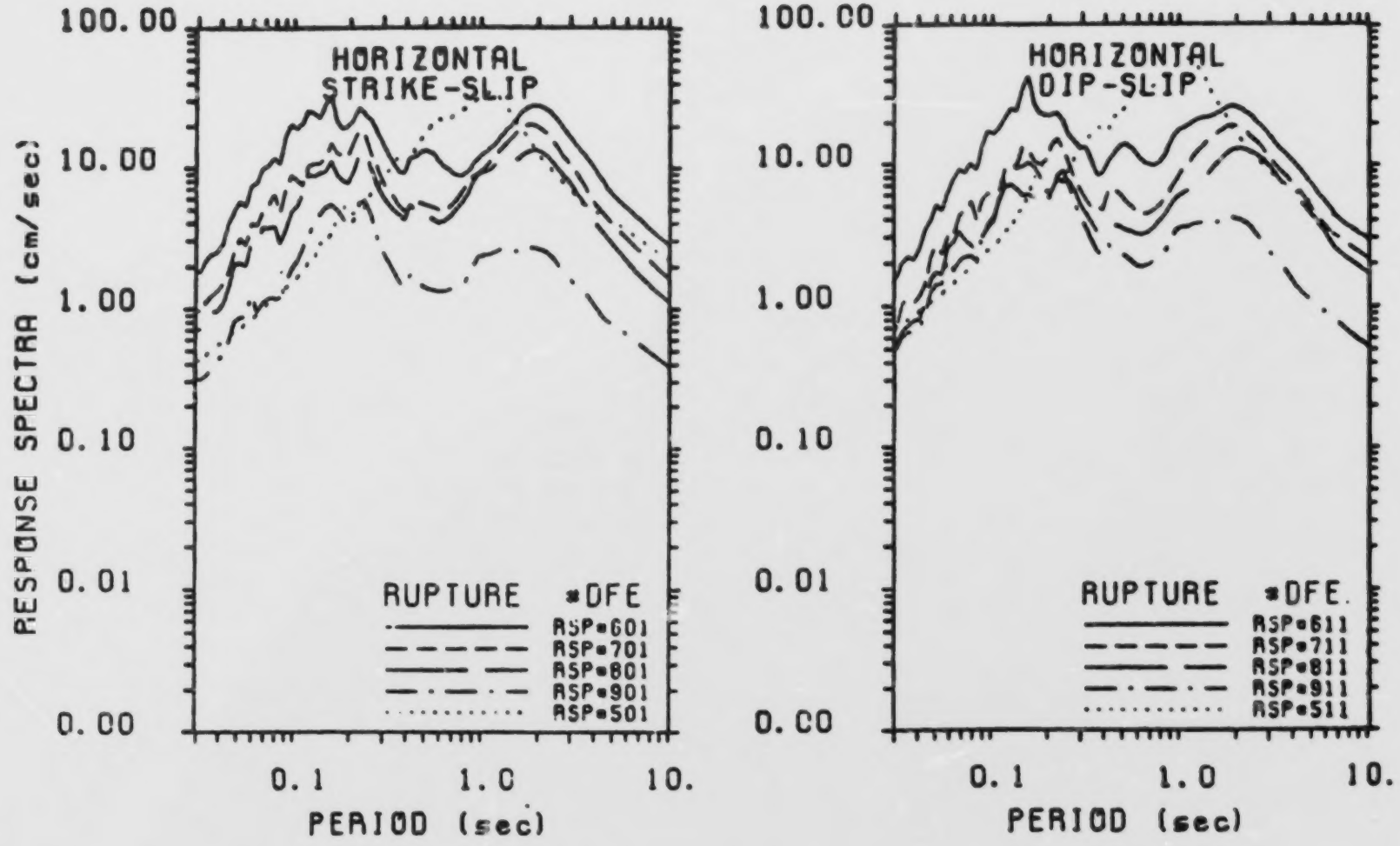

Fig. 2.2 Pseudo-velocity response spectral values (2 percent damping) at site distance of 5 km in the stiff-soil crustal model compared for M4.5 ruptures at 0-2 km (601 and 611), 2-4 km (701 and 711), 4-6 km (801 and 811) and 13-15 km (901 and 911) depths and M5.5 ruptures at 10-15 km depth. (R.J. Apsel et al., 1983)

BEST COPY AVAILABLE

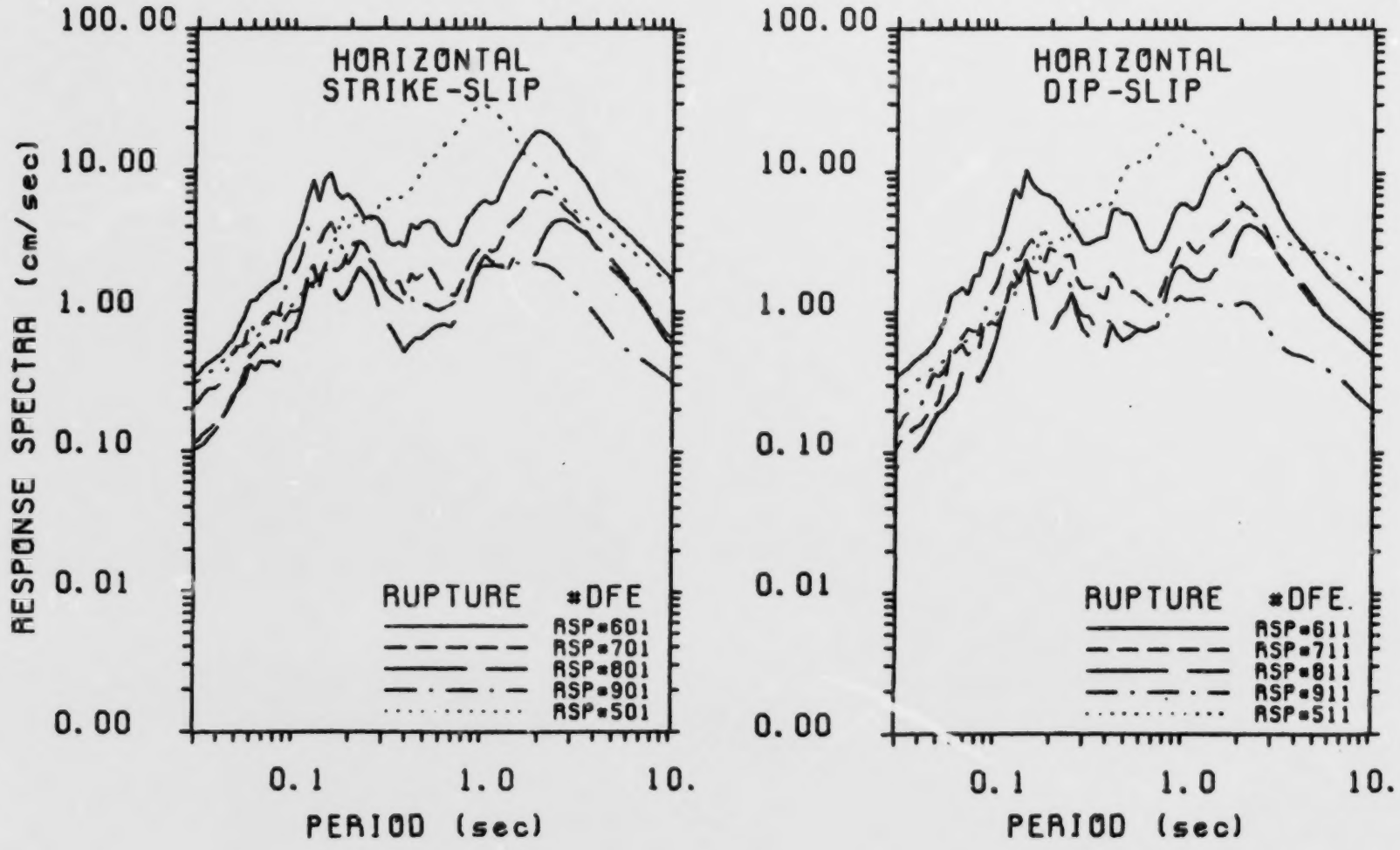

Fig. 2.3 Same as Fig. 2.2 for site distance of 20 km. (R.J. Apsel et al., 1983)

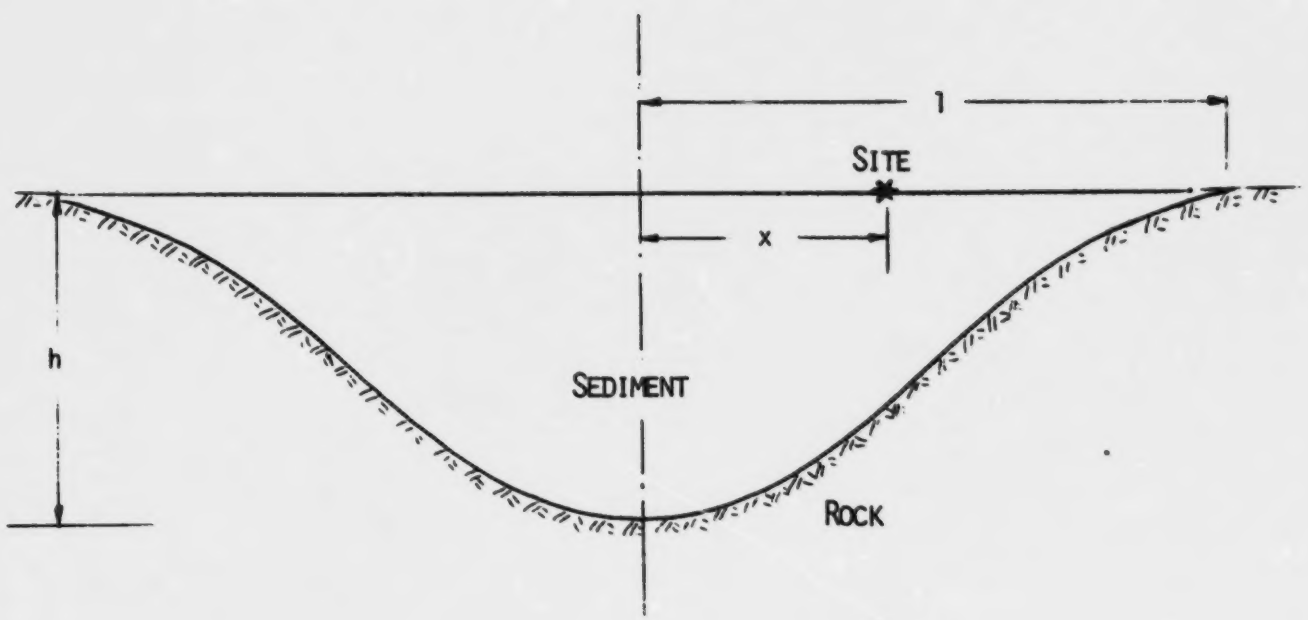

Fig. 2.4 Representation of a sediment-filled valley by a sine-type model, (Bard and Bouchon 1984).

BEST COPY AVAILABLE

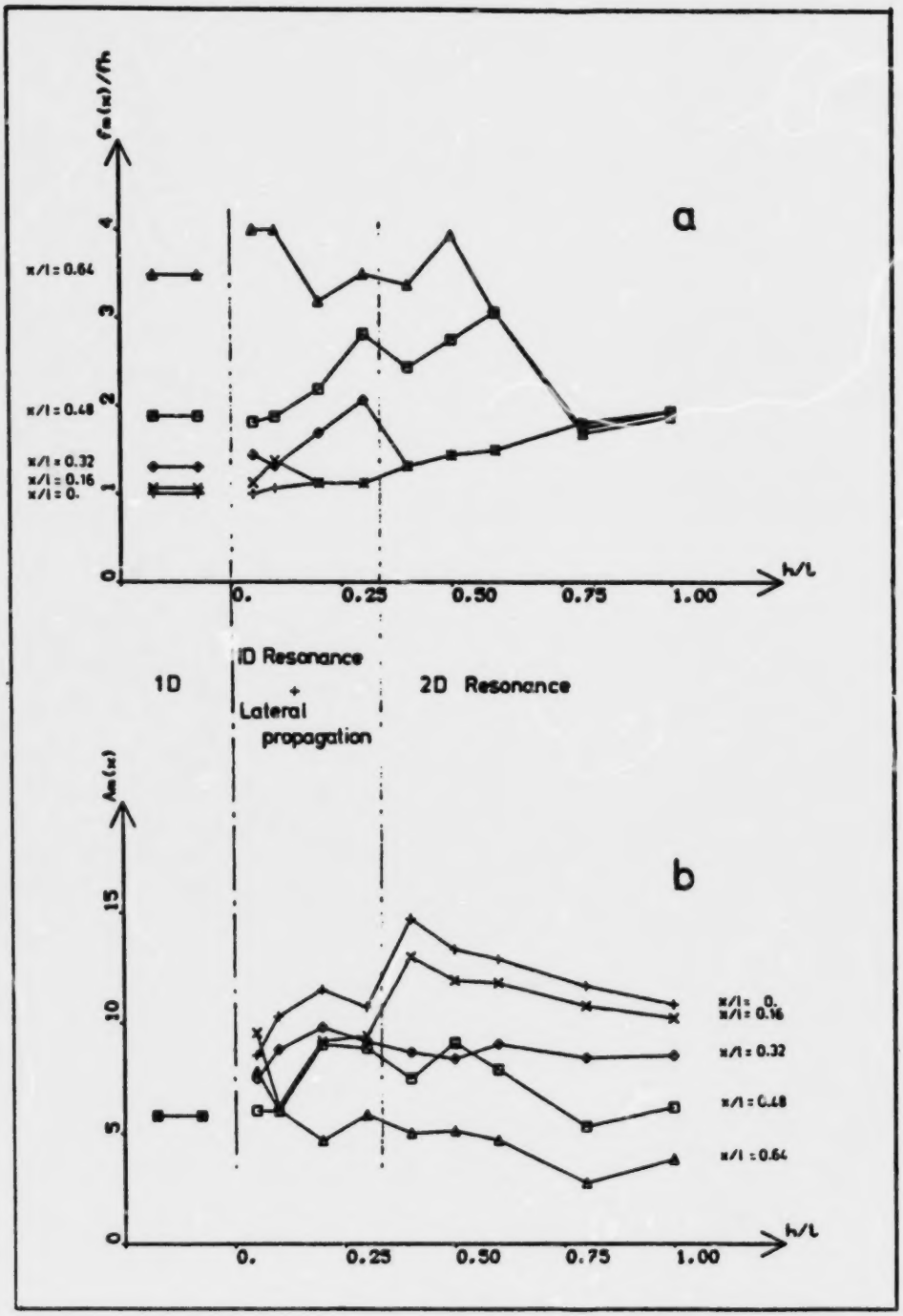

Fig. 2.5 Dependence of the maximum spectral amplification (b) and the corresponding frequency on the shape ratio h/l for five surface sites (from x/l = 0., center, to x/l = 0.64, edge). Both sets of results are compared with the corresponding one-dimensional (1D) values, displayed on the left. The geometrical and mechanical characteristics of the valleys are detailed in the text. (Bard and Bouchon, 1984).

BEST COPY AVAILABLE

3. UNCERTAINTIES IN GROUND MOTION DATA COLLECTION

3.1 Introduction

When using ground motion data in the form of dynamic parameters such as acceleration time histories or velocity time histories, one has to realize that we are in fact using interpretations of the actual physical parameter values. In general, the physical effect is translated into another physical effect which is detected by a sensor, quantified and stored. Thus, the recovery of the original intended parameter involves, in general, multiple mechanical, optical or electrical transformations and finally mathematical manipulations.

This recovery process is complex and uncertainties of different forms and various amounts are introduced along with each manipulation and interpretation.

The purpose of this section is to identify some of the limitations present in the ground motion data set with respect to engineering applications. In the context of this study, the most important limitations in the data sets can be identified as the followings:

1. Some frequency bands in the time histories have been filtered out. It is now recognized, thanks to the data collected recently in the North East, that high frequency motion (greater than 15 to 20 Hz) is present in many small to medium magnitude records.

2. It is not always clear that a record at hand is representative of the entire wave train which was "seen" by the sensor. In particular, some of the older accelerographs triggered by the first P-wave arrival could have missed the largest peak acceleration.

3. The methods of data processing sometimes used by researchers may introduce bias or erroneous estimates of the ground motion (e.g., equal spacing in sampling could miss the highest peak in a record).

4. The dynamic material properties of the site at the sensor location could introduce spurious effects difficult to identify and remove from the records.

3.2 Ground Motion Instruments

It is useful to give some description of the strong motion accelerographs that are in current use and have also been used in the past since they are the first link in the entire chain of data collection. Most of the present records and probably for several more years to come will be from such instruments in spite of the recent developments, in particular with digital instruments. Sander, 1980, and Trifunac and Udwadia (1973) analyzed this problem in detail. The following is a summary review of their studies.

Most accelerograph sensors are still, highly damped single-degree-of-freedom transducers whose relative displacement response is approximately proportional to the ground acceleration. Consequently, it is the relative motion of the

BEST COPY AVAILABLE

mass with respect to the ground that is recorded by the instrument.

Until recently, almost all instruments were of the mechanical-optical-photographic type, as shown in Fig. 3.1 taken from Hudson, 1980. However, some of the Japanese accelerographs are of the moving-coil type (Kurata, et al 1978) while in the U.S. there is now a trend to use force-balance servo accelerometers (Eisenberg, A and McEvilly and Hudson 1980). These latter instruments have a better dynamic range (0.005g-1.0g) and bandwidth (0-100 Hz).

The starting system is one of the most critical components in an accelerograph. It is used to start the recording when the ground motion felt by the instrument crosses a certain threshold level. The choice of the threshold is a critical one since one wants to make sure that the recording will not be triggered by ambient non-seismic vibrations and on the other hand one wants to ensure that the sometimes low portion of a seismic wave train of a large earthquakes is recorded. A major constraint on the starter design is that the delay be a minimum, so that only a minimum amount of ground motion is lost or distorted after the motion first exceeds the threshold level. Very short, impulsive-like, ground motion generated by an earthquake close to the recording site could be such that the maximum acceleration would be so close to the start up time that it could be missed in the recording. There are actually some records of medium size earthquake ground motions being used presently by the earthquake engineering community for which some researcher have suggested that this phenomenon may have occurred. Thus the peak acceleration value for these records analyzed could have been higher than the values presently used. The practical implication could be important when the number of records is small, such as for the ENA.

This is also a major problem with the vertical component and for the suites of vertical SSSP generated in this study. Often much of the initial P-wave train is missed because of the start-up time or trigger problems.

In the long run, however, digital recording instruments with solid state electronics will probably dominate the field of ground motion recording instruments. These instruments now have a memory where enough of the pre-triggering time ground motion is stored so that the entire seismic wave train is recorded. Unfortunately this will only apply to future events and we have to use what we have at the present time.

Table 3.1 shows some of the characteristics of the most commonly used instruments.

3.3 Errors in Digitized Signals

Trifunac, Udwadia and Brady (1973), presented a comprehensive analysis of errors in the digitized signals based on experience with existing instrumentation and processing methods. They identify the various sources of errors and estimate their probable magnitudes, and later summarize the over all effects of the errors at the low and high frequency ends of the spectrum. The following is a summary of the most important errors.

1. Accelerograph related errors.

BEST COPY AVAILABLE

- The transformation of the relative displacement of the transducer into an acceleration can introduce mostly high frequency errors.

- The transducers are assumed to be single-degree-of-freedom systems in performing the transformation. The higher existing modes are neglected, thus introducing high frequency errors. In most accelerographs, the higher modes do not seem to affect instrument behavior below 25 Hz.

- The transverse motion of the recording film or paper in the drive mechanism of the accelerograph introduces errors that vary from instrument to instrument. The magnitude of these errors could be on the order of several millimeters on the recording medium.

- The overlapping and clipping of traces can make an otherwise good record almost unusable for some specific purposes.

- The triggering and starting delays can lead to a missing of the first peaks. Also, the transient from triggering till the motor of the recording mechanism reaches a steady state speed introduces some distortion in the record. For typical starting delays of 0.1 to 0.2 sec this transient is negligible. However in some Japanese SMAC accelerographs the transient is on the order of two seconds (Kurata, Iai and Tsuchida, 1978)

2. Photographic Processing Related Errors

   The main error introduced in the photographic processing appears to be due to the fact that the film is developed in sections, thus introducing discontinuities in the trace which can translate into low frequency errors in the digitized record.

3. Digitizing errors when a digitizing machine is used.

   Random and systematic errors are introduced. The random errors are due to the errors in judgement of the operators and due to parallax and thickness of the cross-hair in the digitizing machine. Systematic errors are long period errors which are negligible in the frequency band of engineering interest. Random errors are nearly normally distributed with zero mean and with a standard deviation equal to approximately one digital point.

BEST COPY AVAILABLE

TABLE 3.1
SUMMARY OF INSTRUMENT CHARACTERISTICS

Instrument	Accelerograph Sensitivity cm/g	Full Scale g	Recording Medium	Recording Duration	Trigger Threshold level (g)	Starter Component Direction
USGS Standard	5.5 - 19.7	1	6.12 inch photo paper	1.25 min	-	H
AR-240	5 - 7.5	1	12 inch photo paper	7 sec after LSM	-	H
RFT-250	1.9	1	70 mm perforated	5 sec after LSM	-	H
RMT-280	+ 200 Hz FM dev. 1 +	1 1	1/4 inch perf .film	after LSM	-	H
SMA-1	1.9	1	70 mm film	at least 10 sec.after LSM	0.005 - 0.05	V
SMAC-A	4	1	Waxed paper	3 min	0.01 -(0.005)	V
SMAC-B (B2)	4 (8)	1 (.5)	Waxed paper	3 min	0.01 -(0.005)	V
SMAC-C (C2)	4 (8)	1(0.5)	Waxed paper	3 min	0.01 -(0.005)	V
SMAC-D	1	.5	35 mm scratch film	1.5 min	0.005	V
SMAC-E (E2)	.5 (1)	1 (0.5)	35 mm scratch film	1.5 min	0.01 -(0.005)	V
DC (DC3C)	8 (4)	0.5(0.1)	smoked paper (waxed paper	3 (1,2,3) min	0.01	V
SMAC-Q	.5	1	35 mm scratch film	1.5 min	0.01	V
MO-2	1.5 Horz. 2.2 Vert.	1	35 mm un-perf. film	47, 70 sec	0.01	V
VAR	1.6	1	Photo paper	1 min		

KEY: LSM - ____ Strong Motion
V - Vertical
H - Horizontal

BEST COPY AVAILABLE

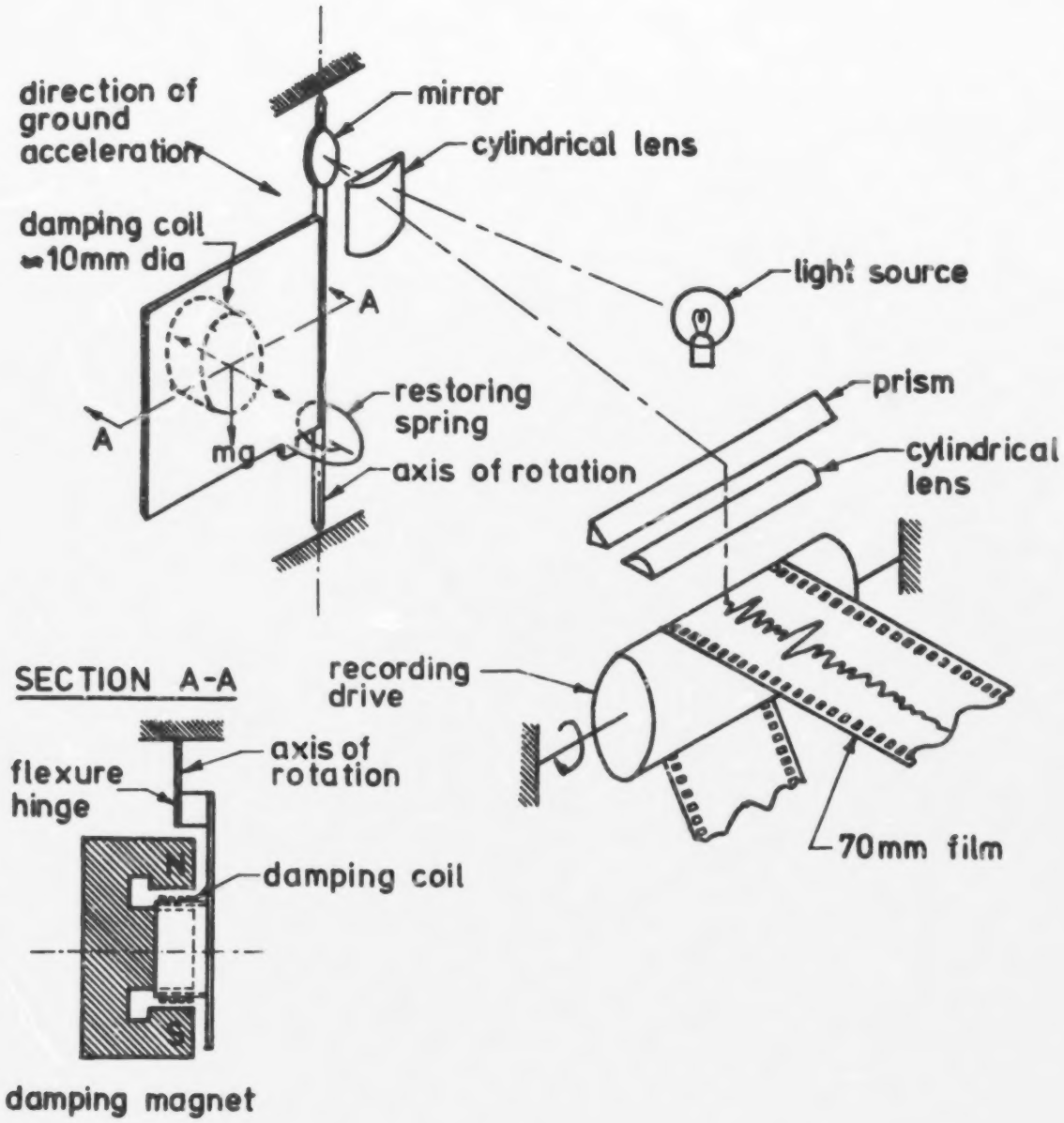

Fig. 3.1 Schematic Diagram of Mechanical-Optical Photographic Strong-Motion Accelerograph (from Hudson, 1980)

BEST COPY AVAILABLE

4. EFFECT OF SHALLOW SOIL, WEATHERED BEDROCK, TRAVEL PATH AND MAGNITUDE ON GROUND MOTION

4.1 Introduction

The response spectra from ENA earthquakes, especially the New Hampshire and New Brunswick earthquakes, generally show higher spectral amplitudes in the high frequency ranges than those of earthquakes in the WUS. This fact may be due to the differences in source mechanism, in the attenuation of high frequency waves over the travel path, or in the local site conditions. It is our objective to assess the relative importance of these factors based on the available data. To sort out the site effects from the source and the travel path effects, we performed site response calculations using simple models for the sites where the New Hampshire and New Brunswick earthquakes were recorded. After the site effect was removed, the average response spectra were compared to the response spectra of a set of strong earthquake ground motions recorded on hard rock in the western U.S. To make this comparison meaningful, the distribution of magnitudes and distances in both data sets should be similar. However, because the size of the data set of strong motions recorded on hard rock is too small, we used a data set of motions recorded on moderated to soft rock. We assessed the effect of earthquake magnitude on frequency content from these comparisons.

A simple rock model was used to assess the effect of the Q factor on attenuation of the high frequency waves. Finally, we investigated the effect of weathered bedrock on site responses. This was done by modeling three typical rock sites in the western U.S. and performing site response calculations using a set of recorded and calculated rock motions from the New Hampshire and New Brunswick earthquakes.

4.2. Effect of Shallow Soil Layers for ENA Earthquake Records

The records available from the New Hampshire and the New Brunswick earthquakes were used to study the characteristics of their frequency contents. The records located at the crest of the dams were not included in the analysis. Table 4.1 lists the records used in this study. Most of the sites listed in Table 4.1 consist of very shallow soil layers having thicknesses less than 25 feet generally overlying a competent hard rock. This type of site condition was not considered in the Seismic Characterization of the EUS project (Bernreuter et al. 1985) since it was assumed that the top layers are routinely removed in the construction of Nuclear Power Plants (NPP). The soil type consists of boulder fill, alluvium and marine deposits (glacial till) with shear wave velocities ranging between 700 fps and 1,500 fps. The underlying bedrocks have a compressional wave velocity around 15,000 fps and a shear wave velocity in the ranges of 6,500 to 9,000 fps.

Simple models for the soil columns at each site were developed for site response calculations. The site response was calculated by assuming one-dimensional vertically propagating SH waves. Sites were modeled as a system of horizontal layer and a viscoelastic material model for each layer was assumed. The input motion consisted of both horizontal components of recorded motions at each site. The effect of having a very shallow soil site was removed by calculating the motion at an hypothetical rock outcrop. Because a

BEST COPY AVAILABLE

one dimensional model was used, the P-waves and S-waves are assumed completely decoupled and each horizontal component produces its own SH wave propagation. The vertical component produces the P-wave propagation. The hypothetical rock outcrop motion at each site was calculated using the SHAKE program (Schnabel et al. 1972).

The set of records identified in Table 4.1 can be separated into two groups. One group (set 1) consists of the records with epicenter distances less than 10 km and the other group (set 2) of records with epicenter distances of about 60 km. The distant records (set 2) show a maximum ground acceleration of less than 0.04g and the other set of data (set 1), consisting of the near field records, has the strongest ground motion. Figure 4.1 shows the upper and lower envelope, 50th and 84th percentiles 5% damping velocity response spectra at the hypothetical rock-outcrop calculated from the records in set 1. Figure 4.2 shows the 50th and 84th percentile 5% damping acceleration response spectra for the same set of estimated rock-outcrop motions. Figure 4.3 shows the medians of velocity spectra for the recorded motion on the very shallow soil and the estimated rock motion. It can be seen from this figure that the average response at very shallow sites is between 1.5 to two times higher than at the corresponding rock outcrop. The highest amplification occurs in the frequency range of 14 Hz to 28 Hz.

To increase the size of the data set, four more distant records at the Union Village Dam were added to the first set of data (set 1). The calculation procedure described above was applied to the soil models at these record sites. However, after performing the analysis we normalized the response spectra to alleviate the problem of having drastically different peak acceleration values between the records at Union Village Dam and the records of set 1. In these calculations the corresponding hypothetical rock outcrop motions were normalized to 1g peak acceleration. Then the normalized spectra were used in the statistical analysis. The 50th and 84th percentile 5% damping response spectra were calculated and plotted for comparison. These comparisons for velocity and acceleration 5% damping response spectra are shown in Figs. 4.4 and 4.5 respectively. The spectral values for shallow soil motions are higher than those of rock motion by a factor of 1.1 to 1.3 for the periods range of 0.04 to 0.15 seconds . Thus, we can conclude that the site effect does not provide for a drastic change in the shape of the response spectra. This fact implies that the unusually high level of energy in the high frequencies of the records of ENA as compared to typical WUS records must be attributed to the source mechanism of ENA earthquakes, the shallow depth of these events and/or to the travel path (i.e. the properties of rock media which governs the Q factors) rather than to the local site effects. As noted in Section 2.3, the somewhat deeper CUS earthquakes do not show unusually high levels of energy in the high frequencies.

4.3 Effect of Weathered Bedrock on Recorded Motion

The characteristics of the typical rocks in the western U.S. may be different from those in the east. Furthermore, the top layers of the rock column can have a wide spectrum of levels of weatherization, especially in the last tens of feet near the ground surface. The purpose of this section is to investigate the impact of the weathered rocks on the recorded motion. Site

BEST COPY AVAILABLE

response analyses were performed on three typical models representing various degrees of weathered conditions for three different rock types. Three site profiles and site properties were taken from the published literature. They are briefly described as follows:

a. CIT Seismological Laboratory: (Shannon and Wilson 1980a)
The site conditions were reported as weathered granitic rock. Based on the field geological survey at the site, the shear wave velocity is 2,670 fps down to 35 feet depth and is 4,210 fps from 35 feet to 50 feet deep, as shown in Figure 4.6.

b. Golden Gate Park: (Shannon and Wilson 1980b, USGS-1978)
The accelerographic station at this site is located on a knoll which is underlain by thin, alternating beds of radiolarian chert and shale. Below a few feet of weathered rock, the formation consists of hard - brittle chert as well as moderately-hard and brittle shale. The bedrock is part of the Franciscan basement complex that underlies the sediments throughout San Francisco. The shear wave velocities, shown in Fig. 4.6, were based on in-situ measurements of seismic velocities as published in USGS, 1978.

c. Diablo Canyon Nuclear Power Plant (DCPP) Site: (FSAR)
The DCPP site schematically consists of various thickness bedded sandy mud stone and fine grain sandstone. The shear wave velocity, published in the FSAR, is shown in Fig. 4.6. The average damping ratios are in the ranges of 2 to 5% of critical. The variation of dynamic rock properties with shear strains are shown in Figs. 4.7 and 4.8.

Using the same one dimensional (1-D) propagation model described in section 4.2, each computed or actual rock outcrop motion at the sites from the Set 1 ENA earthquakes was propagated through each of the three site profiles. The response at the surface of each site was calculated and these results were compared to those of the input motion.

Figure 4.9 shows the comparison of the 50th and 84th percentiles velocity spectra for the recorded input motions (outcrop recorded motions from ENA earthquakes) and the calibrated output motions which consist of the corresponding responses using the CIT seismological lab site profile. The overall effect of this weathered rock site is similar to the very shallow site in spite of the much higher shear wave velocity at the CIT site (about 2,700 fps).

Figure 4.10 shows the comparison of the 50th and 84th percentile velocity spectra for the Golden Gate site. An even greater effect than when using the CIT site profile is found at this site. This is similar to the effect found with the site category II described in Bernreuter, et al (1985), i.e., intermediate thickness soil site. The shear wave velocity is so low that the site does not actually behave as a rock site. A large amplification is seen in the intermediate frequency ranges from 4 to 15 Hz where a maximum amplification of 3 to 4 is found around 8Hz. Figure 4.11 shows similar comparisons for the Diablo Canyon Nuclear Power Plant site. The degree of

BEST COPY AVAILABLE

amplifications is relatively smaller than that of the other two sites as the depth of weathered rock column is relatively small. However, the three "rock" columns considered here amplified the high frequency accelerations by approximately the same amount, i.e., 1.6 to 1.9 times.

The above comparisons indicate that a relatively shallow layer of weathering generally acts to amplify the ground motion, much as a shallow soil column.

4.4 Effect of Traveling Path

In Section 4.3 we examined the effect of a shallow layer of weathering. Typically in the WUS much deeper layers of softer (lower shear wave velocity-lower Q value) rocks exist than in the EUS. During an earthquake, the seismic waves travel through a number of geologic formations and undergo multiple reflections, refraction and dispersions. Due to the substantial difference in subsurface and surface conditions from site to site and due to the lack of appropriate data, it is difficult to assess the effect of travel path using an empirical approach. However, the effect the of material energy absorption factor along the wave propagation path can be investigated theoretically by numerical modeling techniques. Three-dimensional numerical modeling techniques simulate the source mechanism and wave propagation process. Calculation is performed using a layered half-space site model. The motion is attenuated by geometrical spreading and by the material damping (or Q factor). To perform an analysis on a 3-D model requires a considerable amount of effort. On the other hand, the effect of the Q factor and the stiffness of rock media on the seismic response to earthquake waves can be easily analysed by using the simpler 1-D model.

The 1-D model for the CIT seismological laboratory site used in Section 4.3 has been extended for the purpose of this investigation. As shown in Fig. 4.6, the CIT site consists of 35 feet of weathered granite rock with shear wave velocity of 2,670 fps and 15 feet of moderate weathered rock with shear wave velocity of 4,210 fps. The Q factors for these two layers were estimated at about 20 and 25, respectively. Underneath the weathered rock, a hypothetical rock formation of 4,000 ft thickness is assumed to be overlying a half-space of bedrock with a shear wave velocity of 8,000 fps and a Q factor of 100. Sensitivity studies were performed for the variation of stiffness and Q factor in the 4,000 ft rock formation. Two cases of analysis were performed and the results were compared:

1. In the first case, the shear wave velocity of the rock formation is fixed at 7,000 fps while the Q factor changes from 100 (case 1a) to 50 (case 1b) and then to 25 (case 1c). The corresponding damping ratio are 0.5%, 1.0% and 2%. This case will demonstrate the sensitivity of the Q-factor in the response calculation for a competent hard rock.

2. Then, in the second analysis (case 2), the shear wave velocity was changed to 4,500 fps while the Q factor was also reduced to 50. By comparing case 1a and case 2, we investigate the same kind of material property differences between the eastern and western U.S.

BEST COPY AVAILABLE

It is generally recognized by seismologists that the attenuation in the EUS is lower than in the west (e.g., Singh and Hermann 1983, Aki 1980, Bollinger, 1975, Nuttli 1973a and 1973b). The relatively low Q values chosen for this analysis are meant to simulate the upper portion of the weathered rock layer.

The recorded rock motion at the Mitchell Lake Road station from the 1982 New Brunswick earthquake was used as input motion for the adjacent rock outcrop. The response motion was calculated at the ground surface of the site. The 5% damping spectral accelerations for each case are shown in Figs. 4.12 and 4.13.

It can be seen from Fig. 4.12 that the spectral acceleration of 0.78 g for the case of Q= 100 is reduced to 0.4 g for the case of Q= 25 at a frequency of 50 Hz. The effect of the variation of Q on low frequency waves, say for wave less than 10 Hz, is not significant. In Fig. 4.13, the combined effect of rock stiffness and Q on site response is very significant. The peak at 50 Hz for the case of shear wave velocity 7,000 fps and Q= 100 almost disappears when these parameters are reduced to 4,500 fps and 50 respectively. The combined effect of a stronger material and higher Q factor is not important for frequencies less than approximately 10 Hz. Since most of WUS accelerograph sites are located on sites underlain by moderate to soft weathered rock with about half the Q value of EUS sites, the high frequency content is more likely to be damped out when the waves are traveling from the source to the site.

4.5. Effect of Earthquake Magnitudes

To study the effect of earthquake magnitude on the frequency content of the recorded motions, two groups of earthquake data have been selected: one group with magnitudes greater than 5.4 and one group, comparable to ENA records, with magnitude less than 4.9. Ideally, both groups of data should have been recorded on hard rock within the epicenter distance less than 10 km. However, due to the data limitation, the selection of the first group of data was restricted to the hard rock motion records only, while the second group is based on comparable magnitudes but also on rock sites, even if they are not on hard rock.

The strong motion earthquake records used for the first group are listed in Table 4.2. Since two of the acceleration levels are much higher than those of the other peak motions, the response spectra were normalized to 1g peak ground acceleration. The comparison between this group and the ENA group is shown in Figs. 4.14 and 4.15. It can be seen that the normalized spectral shapes are significantly different in frequency content when we compare recorded motions from strong earthquakes and weak earthquakes. As both groups of records were selected on hard rock sites, the main differences can be considered to be generated by differences source diffences, in travel path, azimuth, and topography. The strong motion from the WUS group shows much higher energy level for the seismic waves with period larger than 2 seconds. The wave amplitudes in this frequency range do not appear to be affected by the differences in Q factor. It seems that the frequency content is greatly influenced by source parameters such as the size, the type, depth and source mechanism of the earthquake.

BEST COPY AVAILABLE

Owing to the considerable difference in magnitudes between the selected WUS group and ENA group, we also selected a group consisting of the Oroville and Ancona earthquakes. Table 4.3 lists the data used for this group. The magnitude value and distances of the recordings in this group are comparable with those of the ENA group. The comparison of the velocity and the acceleration spectra are shown in Figs. 4.16 and 4.17. It can be seen that the energy content of the Oroville-Ancona group is also larger than those of ENA group for periods greater than 0.05 seconds (frequencies lower than 20 Hz). For the frequencies higher than 20 Hz, the situation is reversed; the spectrum for the Oroville-Ancona group is smaller than that of the ENA group. However, the median spectrum for the Oroville-Ancona group is smaller than that of the WUS group. The larger the earthquake magnitude, the higher the spectral amplitudes in long period waves for the epicenter distance within 25 km. The normalized spectra were also overplotted in Figs. 4.18 and 4.19. Because the size in earthquakes and distances of the ENA group and Oroville-Ancona group are similar, we can theorize that the factors attributed to the difference in high frequency could well be due to the difference in attenuation (Q factor) and stiffness of the rock media, as we demonstrated in the last section. The other factors that could also affect the frequency content of the recorded motions are possibly the wave content of the motion, the earthquake rupture shallowness, the structure of the layered rock formation and topography around the site. When seismic waves travel through a layered formation, multiple reflection or refraction take place and converge into a new type of wave. When seismic waves reach a site with complicated topography, the multiple chaotic reverberations take place and create more chaotic amplification. All of these factors can substantially alter the recorded motion at the sites. In most earthquake engineering studies the travel path effect is not differentiated from the source mechanism effect or the local site effects. It is very difficult to separate the relative importance of each factor based on empirical analysis of the limited data available.

4.6. Conclusions

Based on the comparison of empirical data, the analysis of simple models and the review of literature we conclude that:

1. The effect of very shallow soil layers and weathered rock surface is important on the frequency content of recorded motions. These types of sites can profoundly amplify or de-amplify some narrow bands of frequency ranges depending on the thickness of the soil/rock layers and the layers properties.

2. The travel path effect includes the effect of multiple reflections, refraction, conversion, dispersion and reverberation of the seismic waves propagated from the sources to the sites. There is not sufficient data to do reliable empirical analyses. Based on our 1-D analysis, we found that the combined effects of stiffness and attenuation (Q factor) can significantly reduce the high frequency energy content of a recorded motion. As shown in the summary of our review on 3-D analysis, the travel path effect, which basically reflects the Q factor and reflection

BEST COPY AVAILABLE

for 3-D wave propagation, is important. The major effect is attenuating the amplitude of high frequency waves.

3. Based on our empirical analysis of the ENA earthquake data and the WUS data, we found that a significant parameter governing the frequency content is earthquake magnitude. The spectral content of larger earthquakes and smaller earthquakes is significantly different. In general, larger earthquakes appear to generally produce higher energy content in the intermediate and low frequency ranges. The results from theoretical computations shown in our review are consistent with the empirical data.

4. The difference in high frequency energy content between the ENA group and the Oroville-Ancona group appears to be due to the difference in combined stiffness and attenuation (Q factor) of the rock media and to the difference in depth of the earthquake sources. The theoretical results, show that shallow earthquakes will give a higher energy content for the same distance.

BEST COPY AVAILABLE

BEST COPY AVAILABLE

Table 4.1 ENA Earthquake Records Used For This Study

EQK.	Date	Site Name	Comp (Deg)	Dist. (km)	Mag. m_b	Recorded Accel. (g)	Site Condition	Estimated Accel. Rock Outcrop (g)
NH	1/19/82	F. F. Dam Rt. Abut	45	8	4.7	.294	Boulder fill, 10 ft.	.186
NH	1/19/82	F. F. Dam Rt. Abut	315	8	4.7	.550	Boulder fill, 10 ft.	.393
NH	1/19/82	F. F. Dam D. Stream	225	8	4.7	.144	Alluvium, 100 ft. WT at 20 ft.	.147
NH	1/19/82	F. F. Dam D. Stream	135	8	4.7	.386	Alluvium, 100 ft. WT at 20 ft.	.338
NH	1/19/82	U. V. Dam Lt. Abut	245	60	4.7	.0097	Boulder fill, 7 ft.	.0055
NH	1/19/82	U. V. Dam D. Stream	155	60	4.7	.0069	Boulder fill, 7 ft.	.0037
NH	1/19/82	U. V. Dam D. Stream	245	60	4.7	.0378	Moraine, 30 ft.	.0344
NH	1/19/82	U. V. Dam D. Stream	155	60	4.7	.0230	Moraine, 30 ft.	.0191
NBW	3/31/82	Homles Lake	18	6	4.8	.181	Alluvium, 16 ft.	.084
NBW	3/31/82	Homles Lake	288	6	4.8	.347	Alluvium, 16 ft.	.307
NBW	3/31/82	Mitchell Lake Rd	118	4	4.8	.152	Bedrock	.152
NBW	3/31/82	Mitchell Lake Rd	28	4	4.8	.236	Bedrock	.236
NBW	3/31/82	Loggie Lodge	189	6	4.8	.298	Alluvium, 16 ft.	.214
NBW	3/31/82	Loggie Lodge	99	6	4.8	.575	Alluvium, 16 ft.	.465
NBW	5/6/82	Loggie Lodge	245	7	4.0	.149	Alluvium, 16 ft.	.084
NBW	3/31/82	Indian Brook	321	3	4.8	.425	Alluvium, 16 ft.	.281
NBW	3/31/82	Indian Brook	231	3	4.8	.413	Alluvium, 16 ft.	.272

Table 4.2 WUS Earthquake Motions Recorded on Hard Rock

Earthquake	Date	Station	Mag M_s	Mag m_b	Dist. (km)	Max. Accel. (g)	Site Condition
San Fernando	2/9/71	Pacoima Dam	6.6	6.6	3.2	1.115	Hard Rock
San Fernando (Aftershock)		Pacoima Dam		5.4	12	1.113	Hard Rock
San Fernando	2/9/71	Griffith Park Obs.	6.6	6.2	16.9	.177	Hard Rock
San Fernando	2/9/71	CIT Seisim Lab.	6.6	6.2	18.4	.1886	Hard Rock
San Fernando	2/9/71	Lake Hughes #4	6.6	6.2	24.9	.172	Hard Rock
Imperial Valley	10/15/79	Cerro Prieto, Mexico	6.9	5.7	15.7	.165	Hard Rock
Imperial Valley	10/15/79	Superstition Mt.	6.9	5.7	24.5	.189	Hard Rock

BEST COPY AVAILABLE

BEST COPY AVAILABLE

Table 4.3 Earthquakes with Compatible Magnitude and Distance as Compared to ENA Earthquakes

EQK	Station	Date	Mag.	Distance (km)	Depth	Max. Accel. (g)	Site Condition
Oroville	CDM#6	8/8/75	4.9	6	9.2	.109	Rock
Oroville	CDM#8	9/27/75	4.6	11.	12.0	.155	Rock
Oroville	CMD#6	8/16/75	4.6	4.5	9.4	.107	Rock
Oroville	CMD#6	9/26/75	4.0	5.5	9.7	.100	Rock
Oroville	CMD#8	8/16/75	4.3	6.5	9.4	.007	Rock
ANCONA	ROCCA	6/14/72	4.7	6		.415	Rock
ANCONA	ROCCA	6/14/72	4.7	6		.528	Rock
ANCONA	ROCCA	6/21/72	4.7	6		.188	Rock

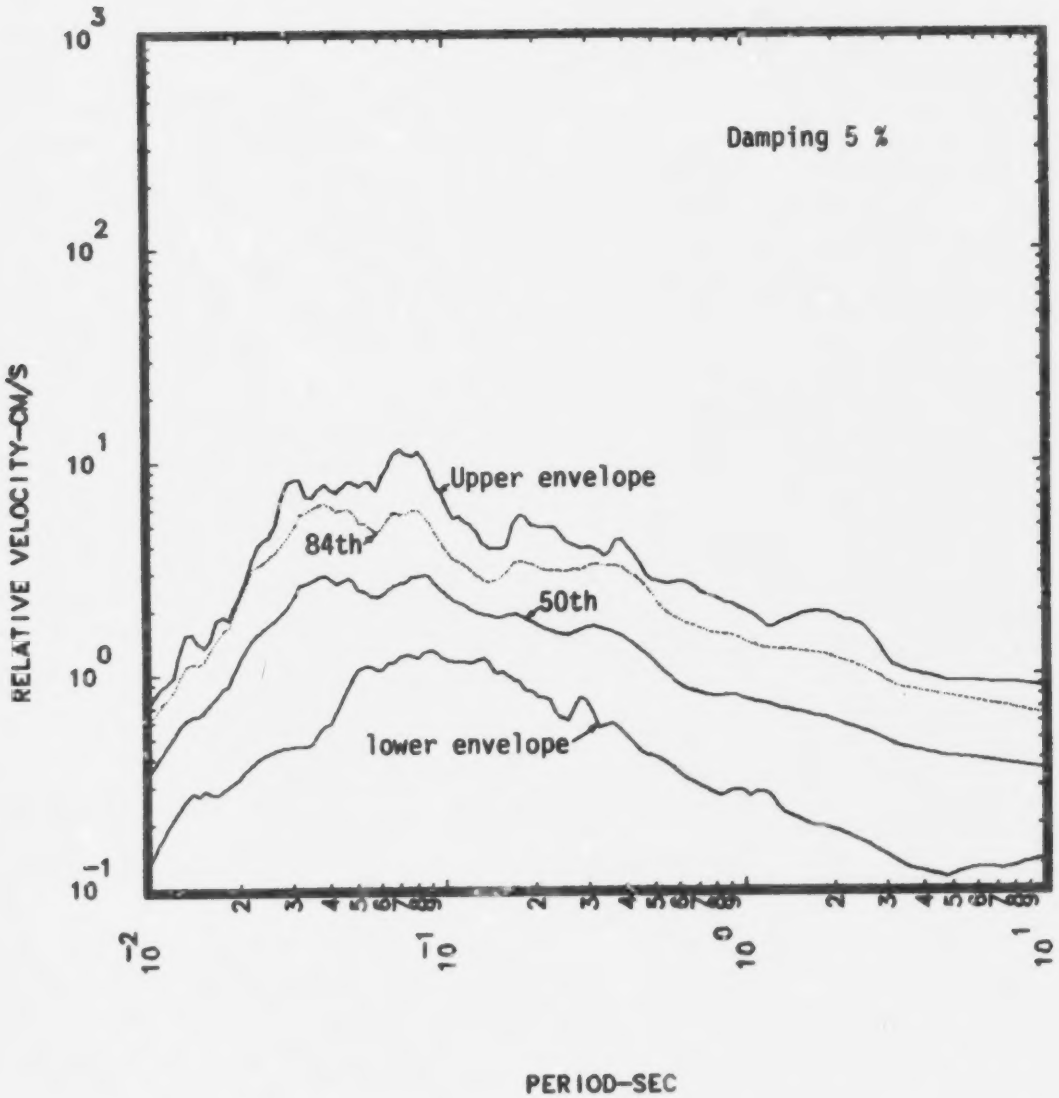

Fig. 4.1 The envelope, 50th and 84th percentile relative velocity spectra for estimated rock-outcrop motions from the corresponding ENA earthquake motions recorded on shallow soil sites.

BEST COPY AVAILABLE

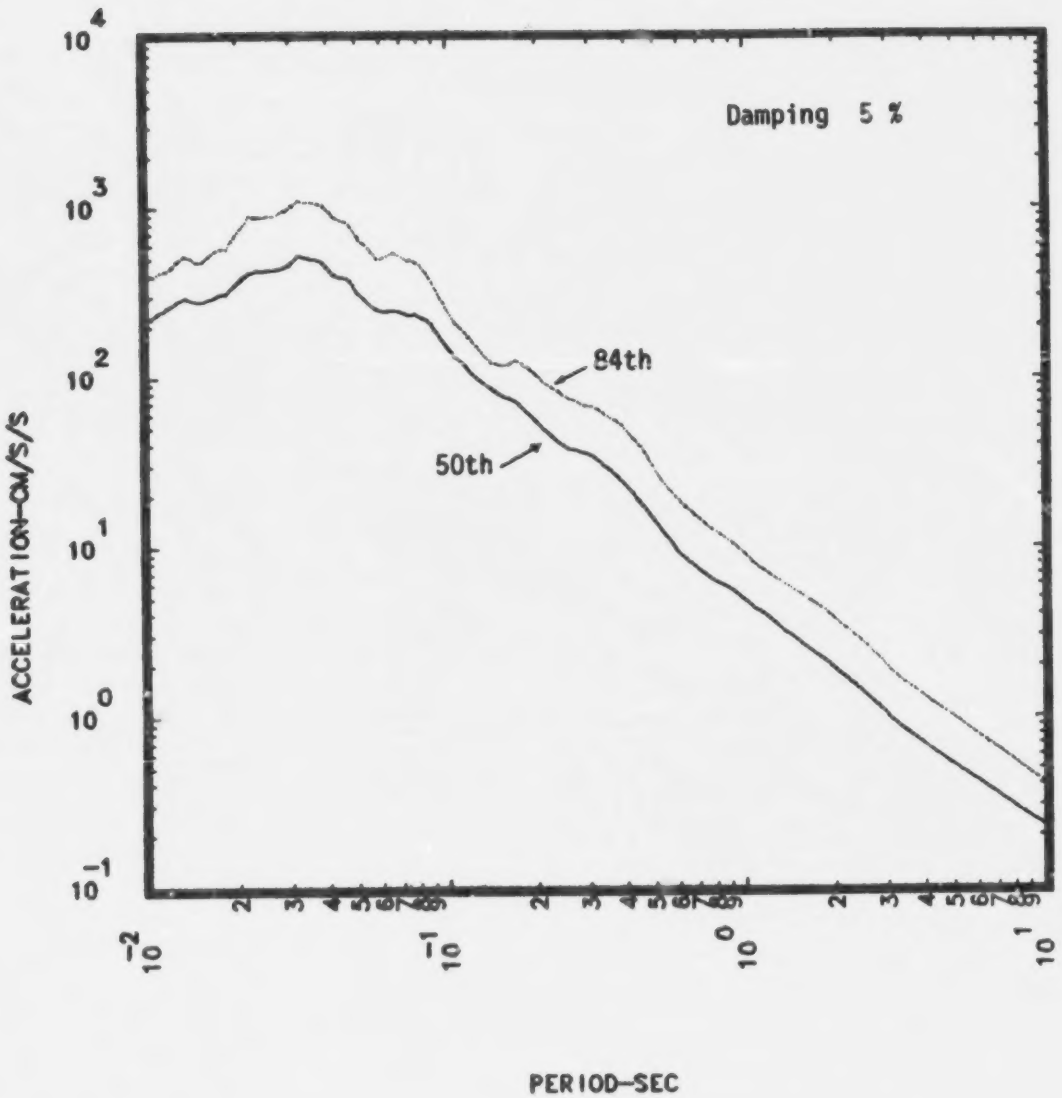

Fig. 4.2 The envelope, 50th and 84th percentile acceleration spectra for estimated rock-outcrop motions from the corresponding ENA earthquake motions recorded on shallow soil sites.

BEST COPY AVAILABLE

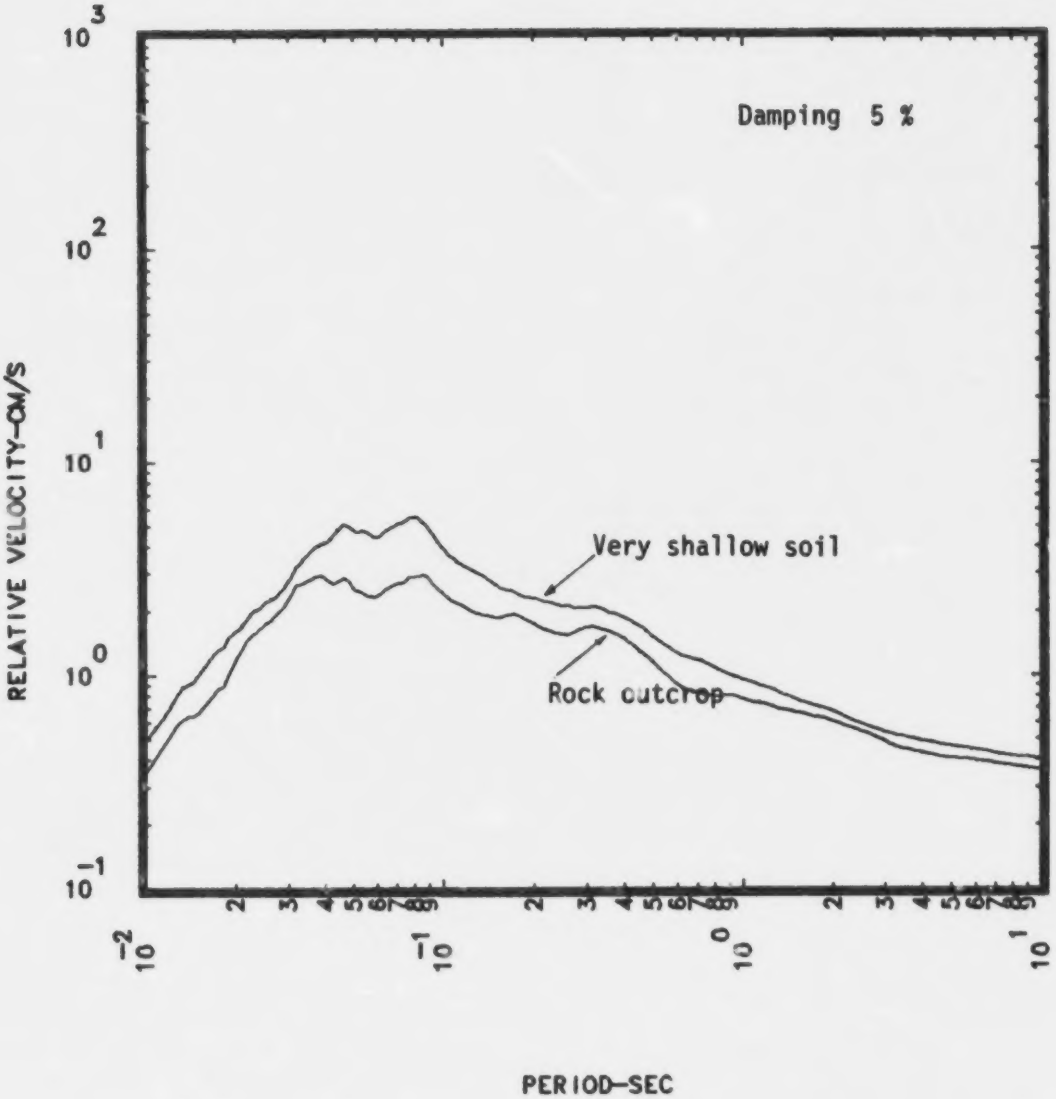

Fig. 4.3 Comparison of 50th percentile (medians) 5% damped relative velocity response spectra between the recorded motions at very shallow soil sites and the corresponding rock outcrop motions.

BEST COPY AVAILABLE

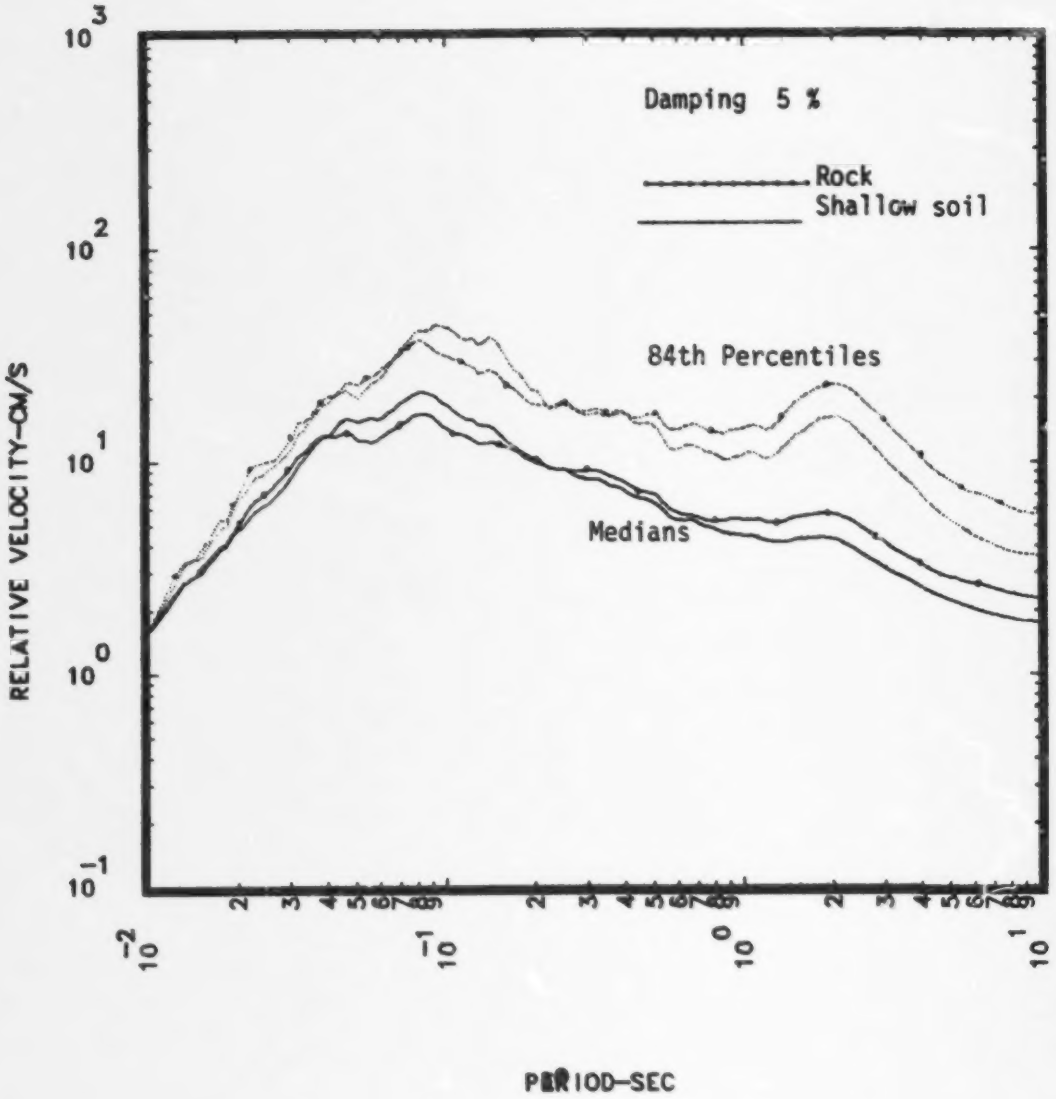

Fig. 4.4 Comparison of 50th and 84th percentile normalized velocity spectra between the recorded motions at shallow site and the corresponding rock outcrop motions.

BEST COPY AVAILABLE

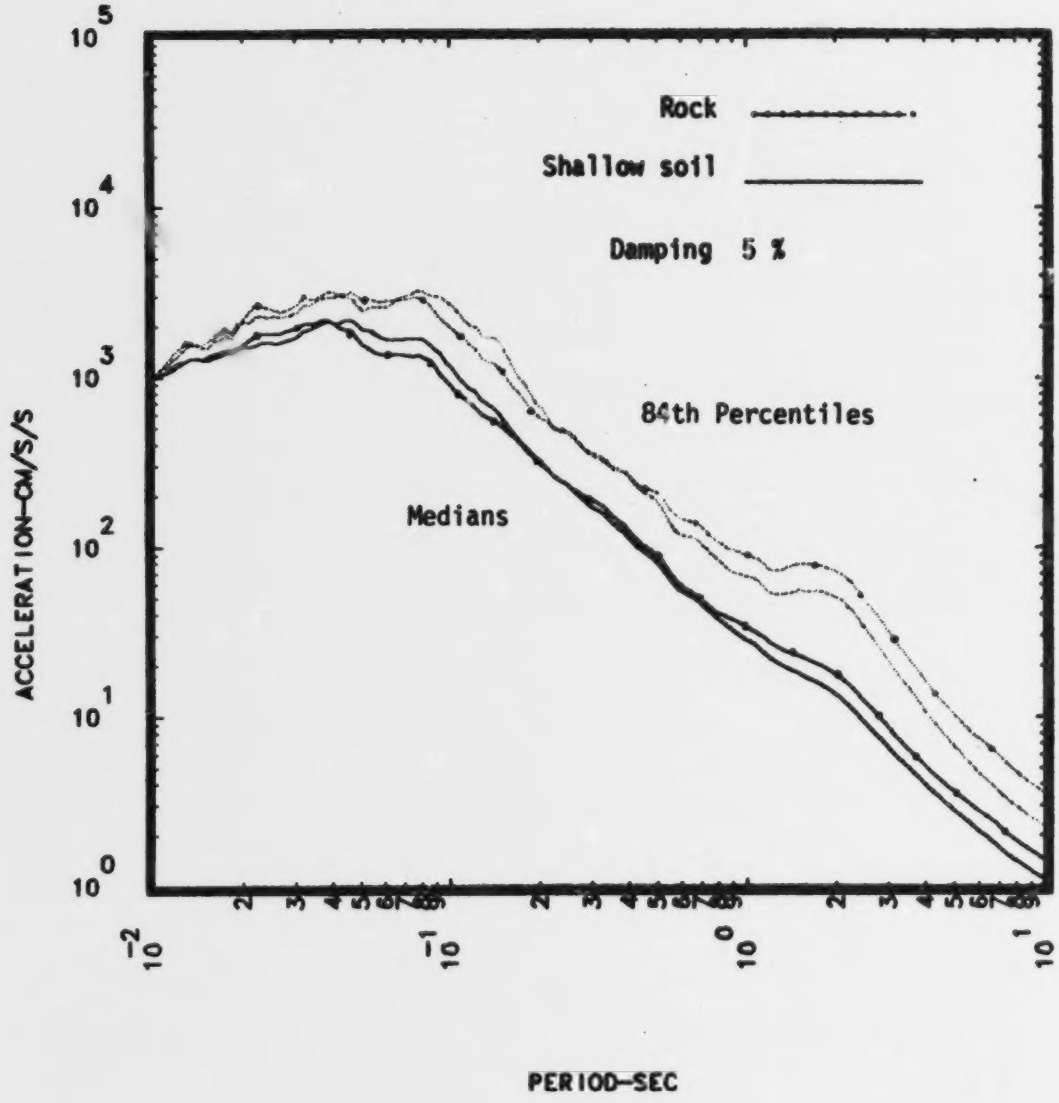

Fig. 4.5 Comparison of 50th 84th percentile normalized acceleration spectra between the recorded motions at shallow sites and the corresponding rock outcrop motions.

BEST COPY AVAILABLE

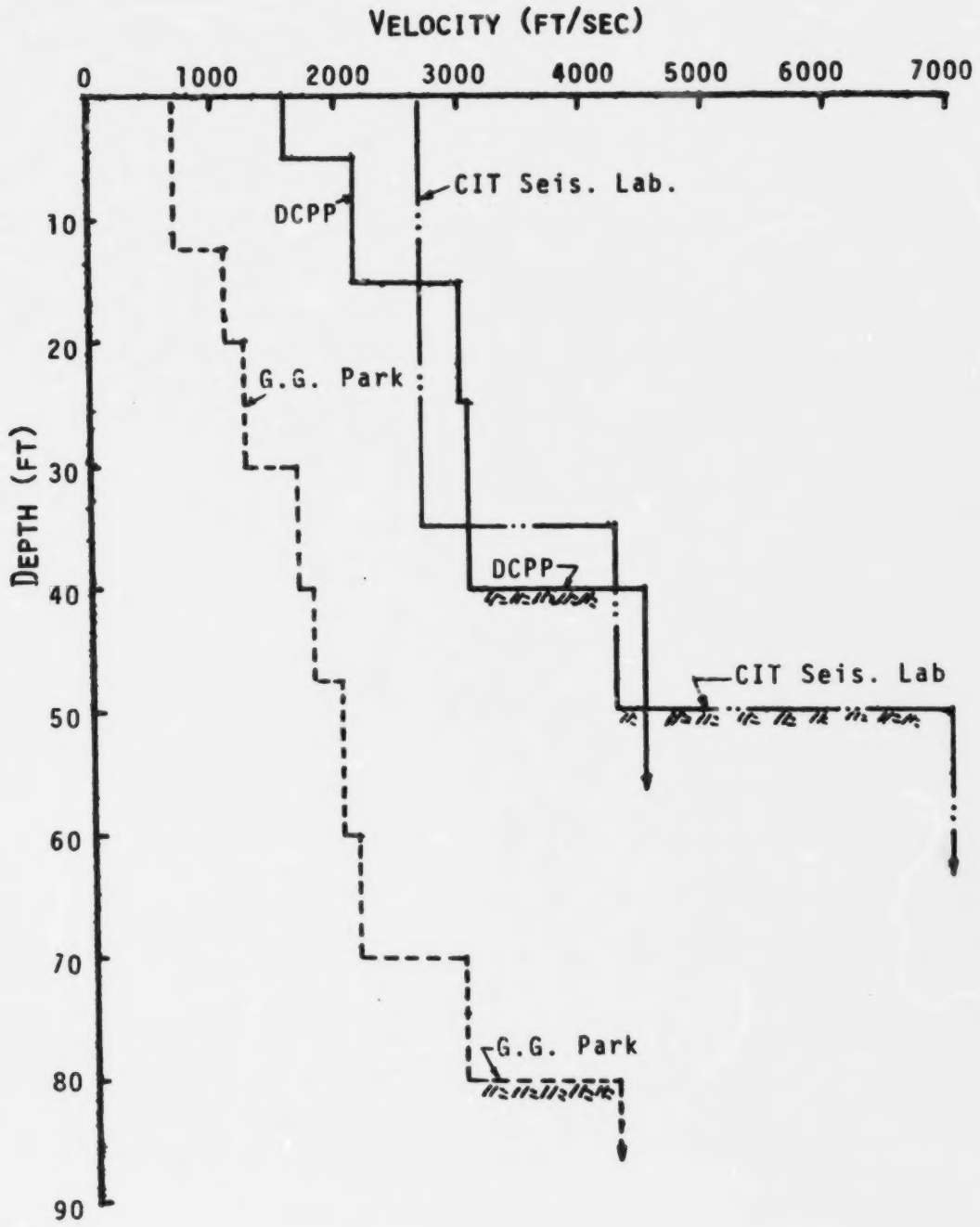

Fig. 4.6 The velocity profiles of three weathered rock sites.

BEST COPY AVAILABLE

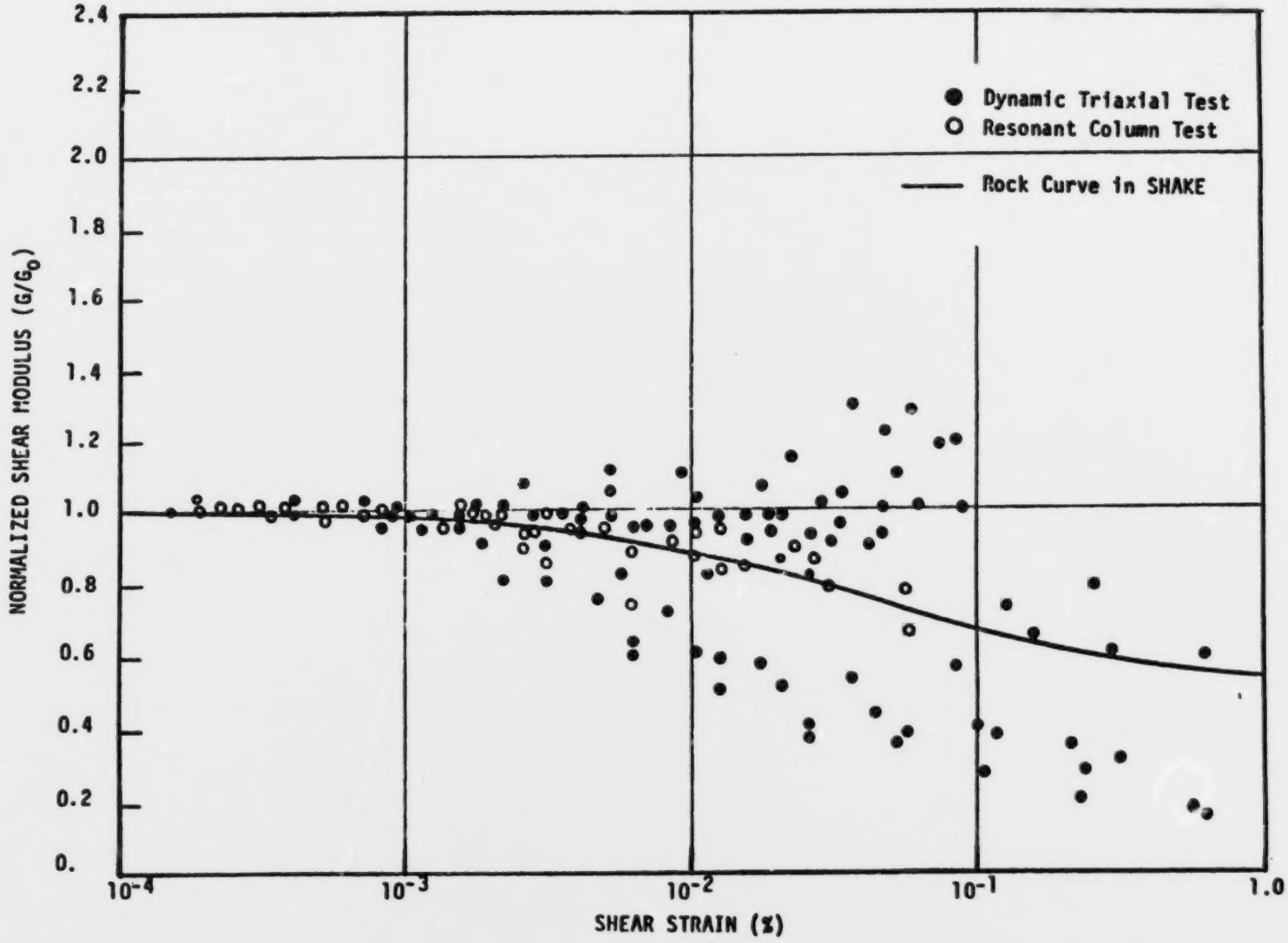

Fig. 4.7 Variation of shear modulus with shear strain for rocks at the DCPP site based on 1977 laboratory test data.

BEST COPY AVAILABLE

BEST COPY AVAILABLE

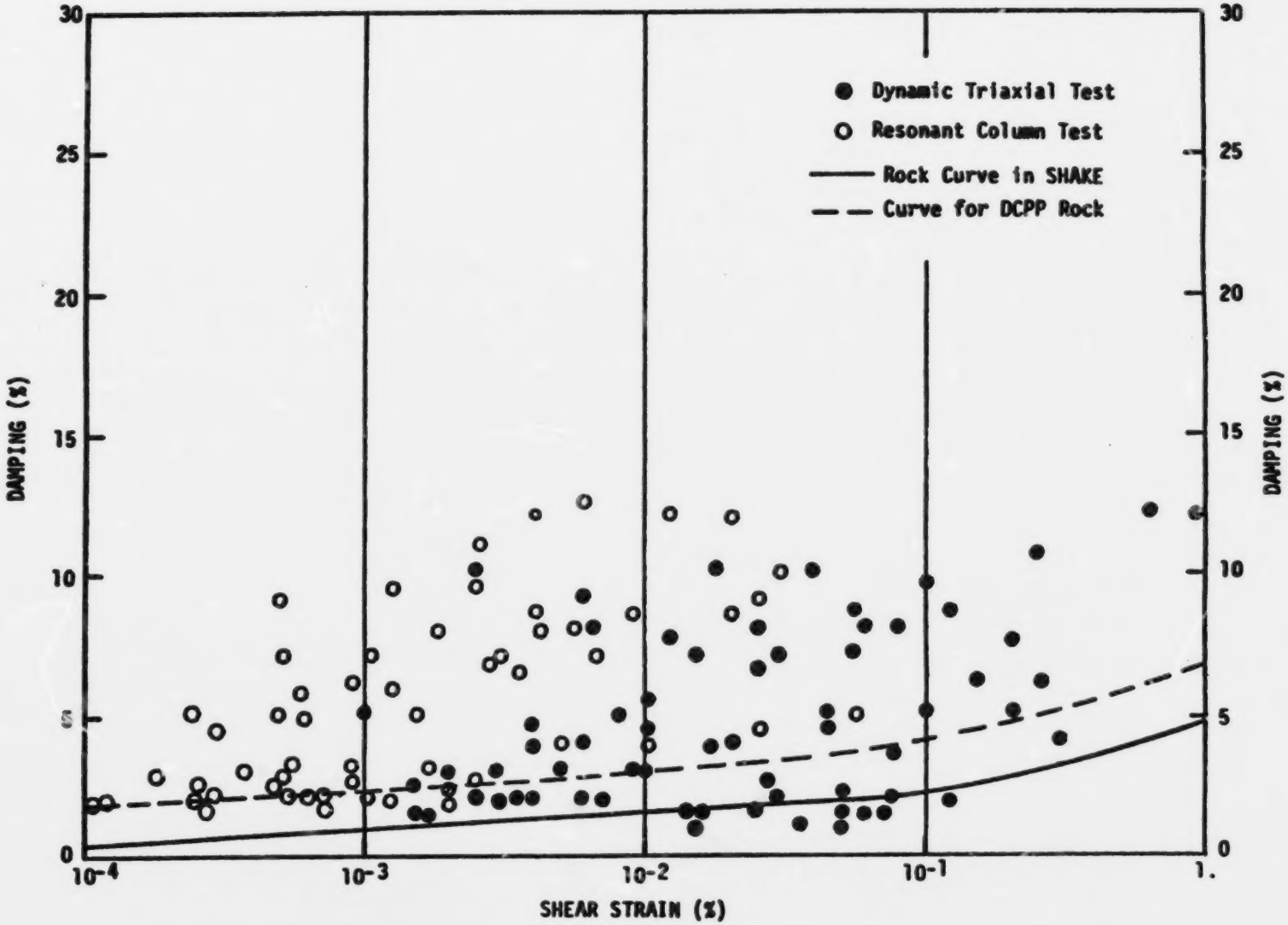

Fig. 4.8 Variation of damping ratio with shear strain for rocks at the DCPP site based on 1977 laboratory test data.

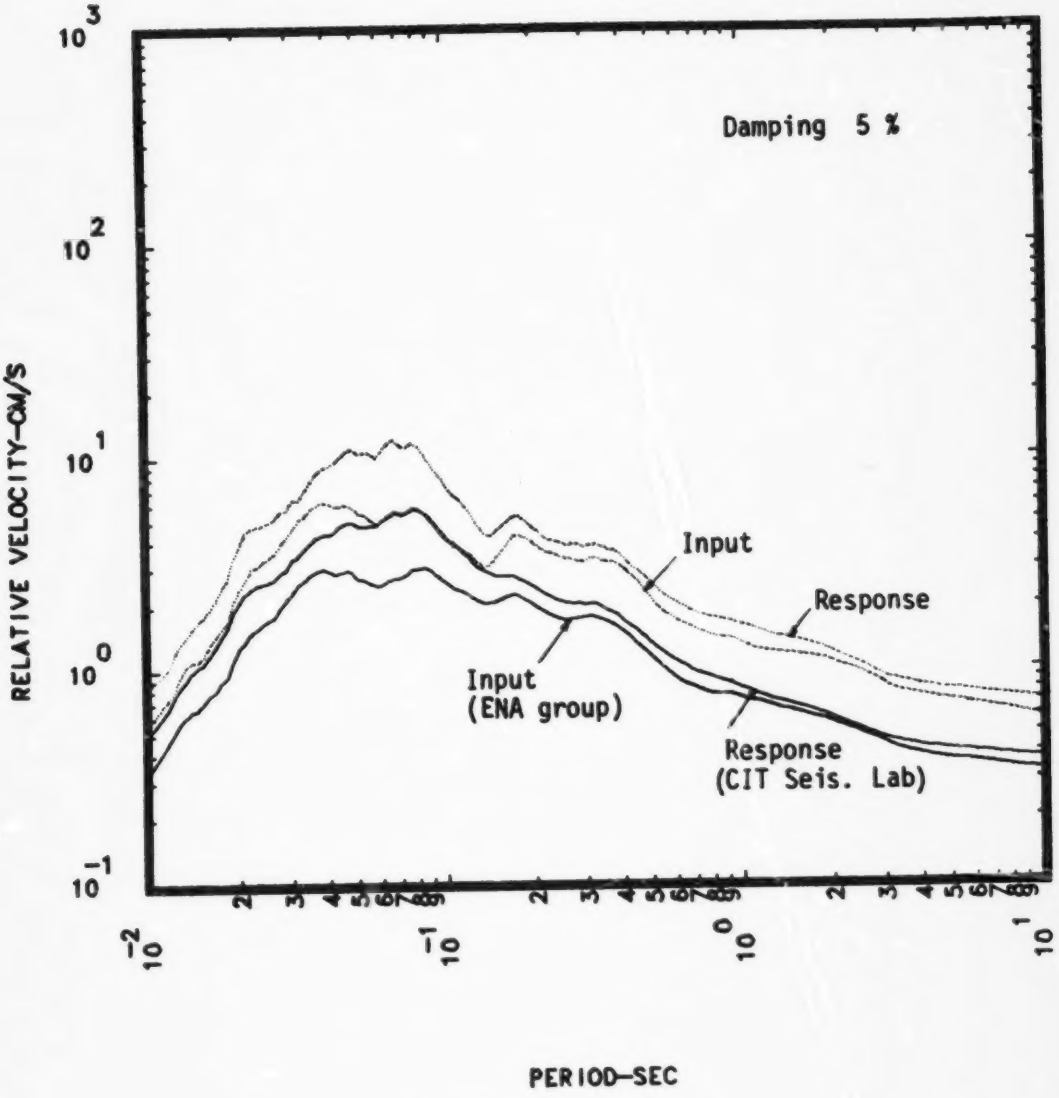

Fig. 4.9 Comparison of median and 84th percentile spectra between the group of input motions and the group of output responses at the CIT Seismological Lab site.

BEST COPY AVAILABLE

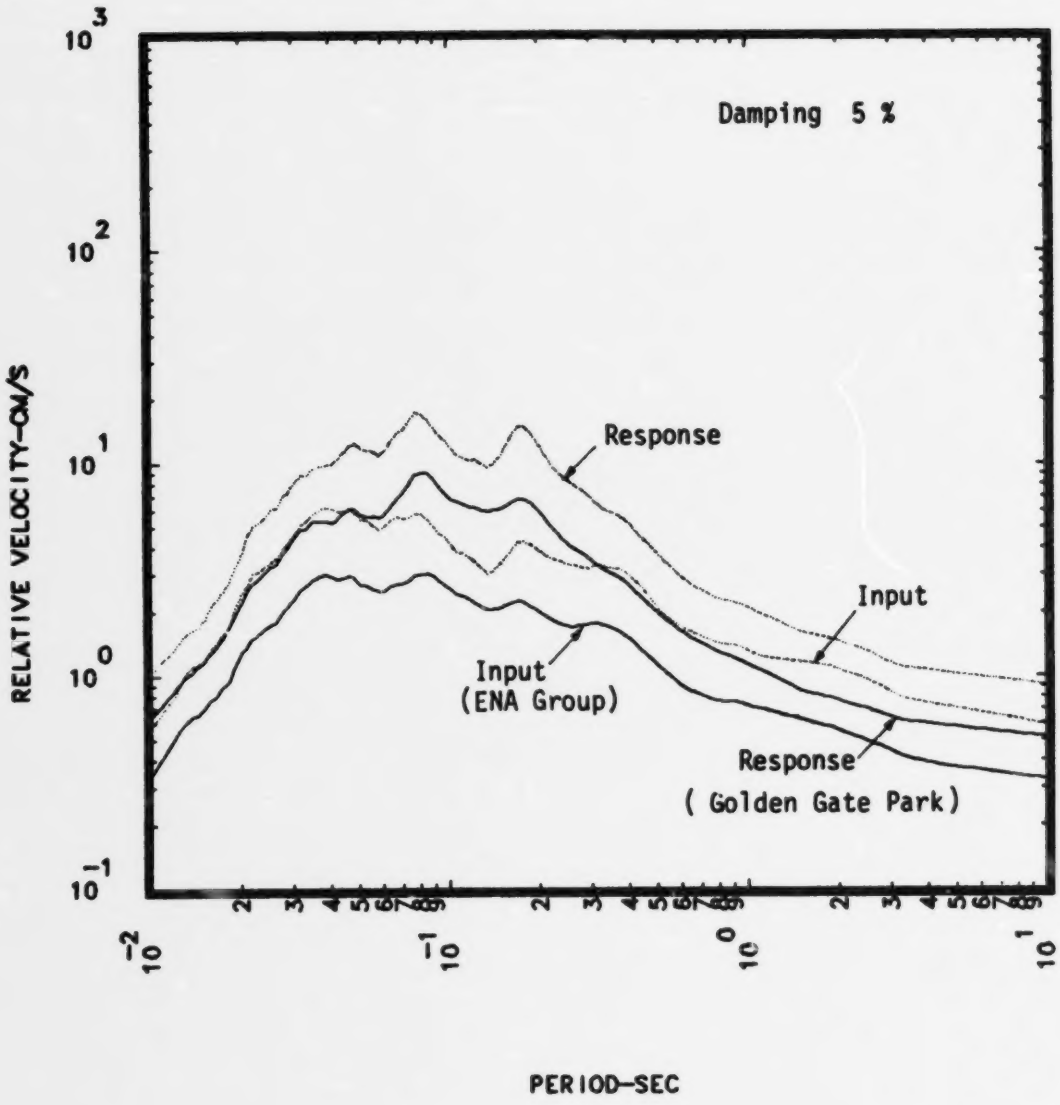

Fig. 4.10 Comparison of median and 84th percentile spectra between the group of input motions and the group of output responses at the Golden Gate park.

BEST COPY AVAILABLE

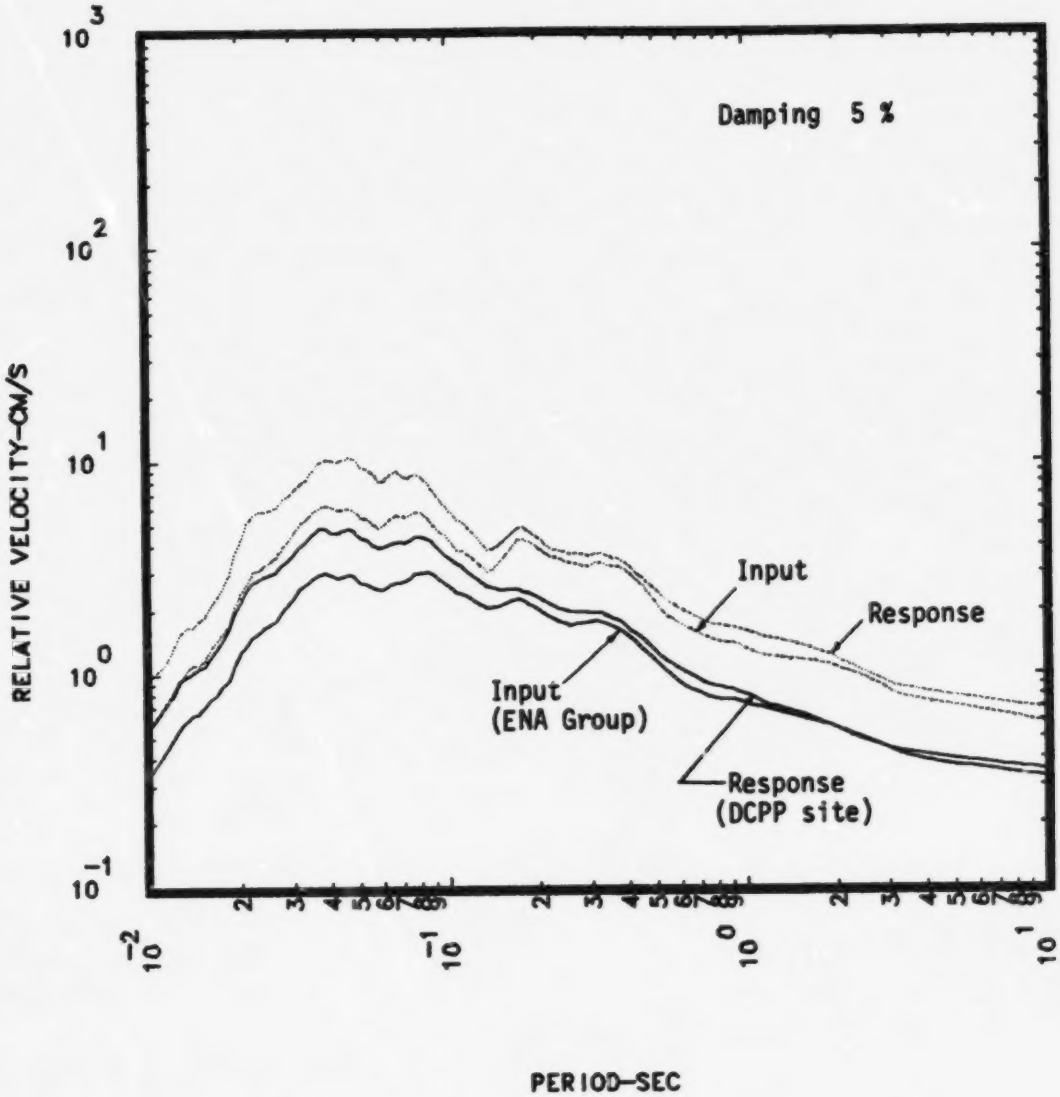

Fig. 4.11 Comparison of the 50th and the 80th percentile spectra between the group of input motions and the group of output responses at the Diablo Canyon Power Plant site.

BEST COPY AVAILABLE

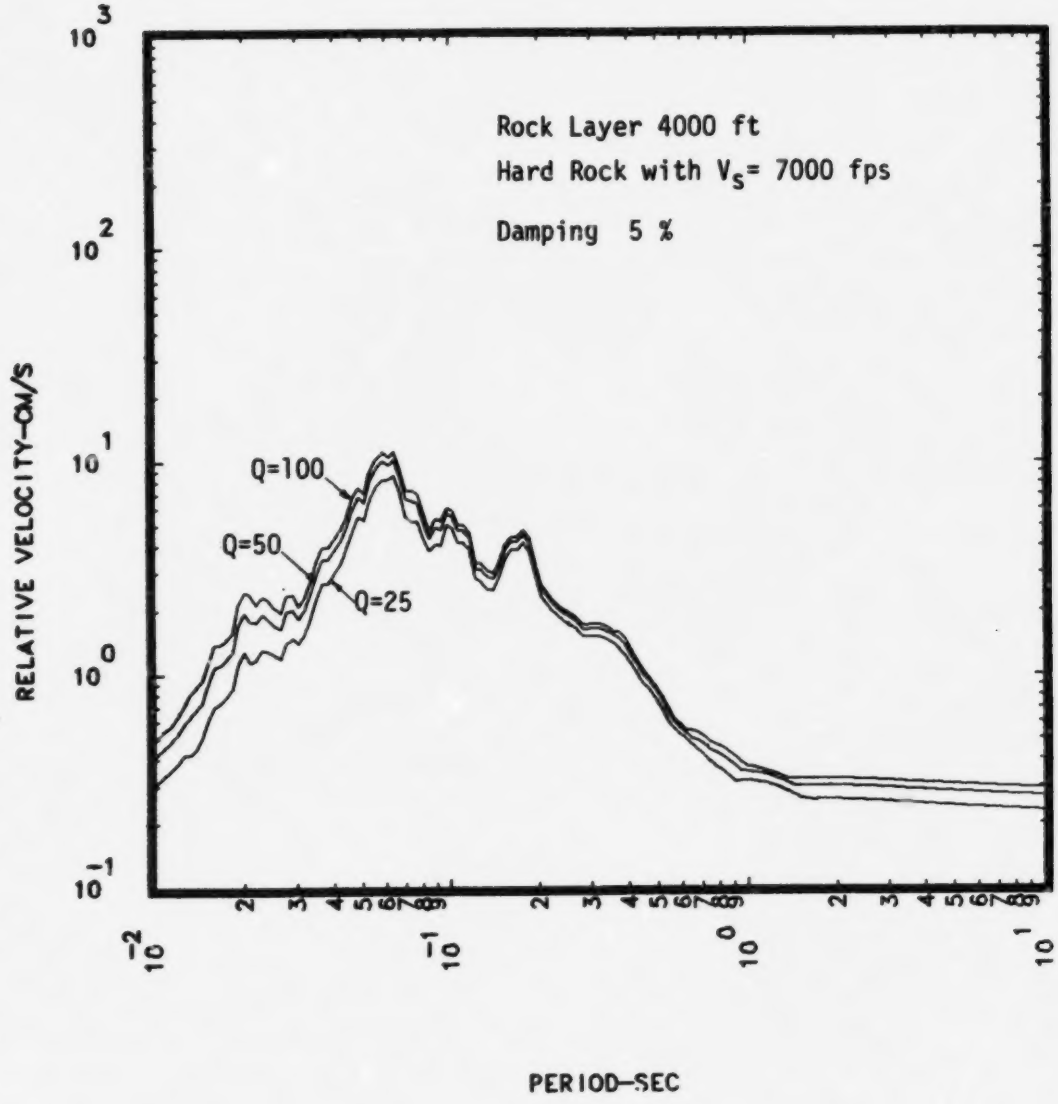

Fig. 4.12 The effect of material energy absorption factor Q, on the response of one dimensional wave propagation through a hard rock medium.

BEST COPY AVAILABLE

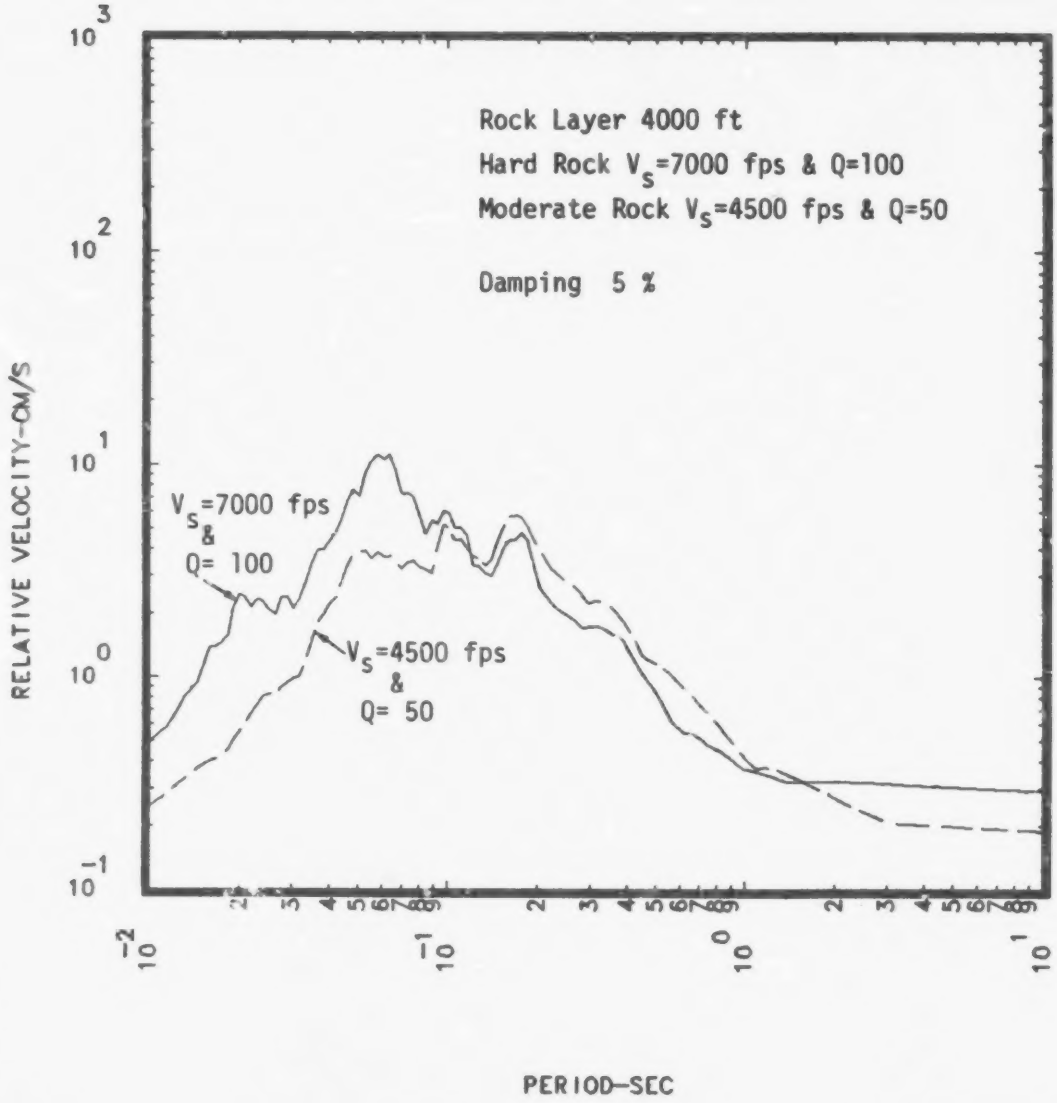
Rock Layer 4000 ft
Hard Rock V_S=7000 fps & Q=100
Moderate Rock V_S=4500 fps & Q=50
Damping 5 %
V_S=7000 fps & Q= 100
V_S=4500 fps & Q= 50
RELATIVE VELOCITY-CM/S
PERIOD-SEC

Fig. 4.13 The combined effect of material stiffness and energy absorption factor on the response of 1-D wave propagation through rock media.

BEST COPY AVAILABLE

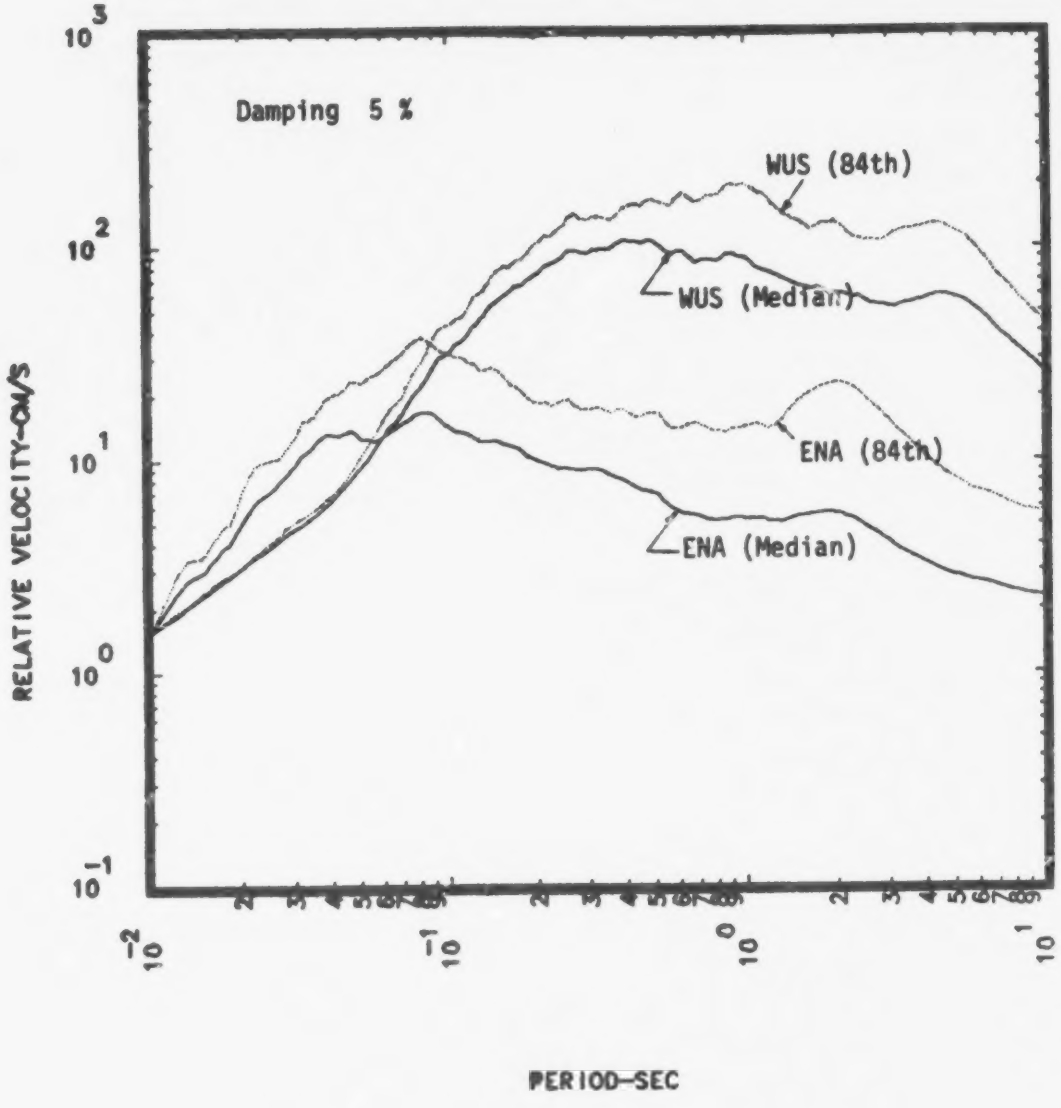

Fig. 4.14 Comparison of the median and 84th percentile normalized velocity spectra between motions from the strong WUS earthquake group and the smaller ENA earthquake group, both groups of earthquake data were recorded on hard rock.

BEST COPY AVAILABLE

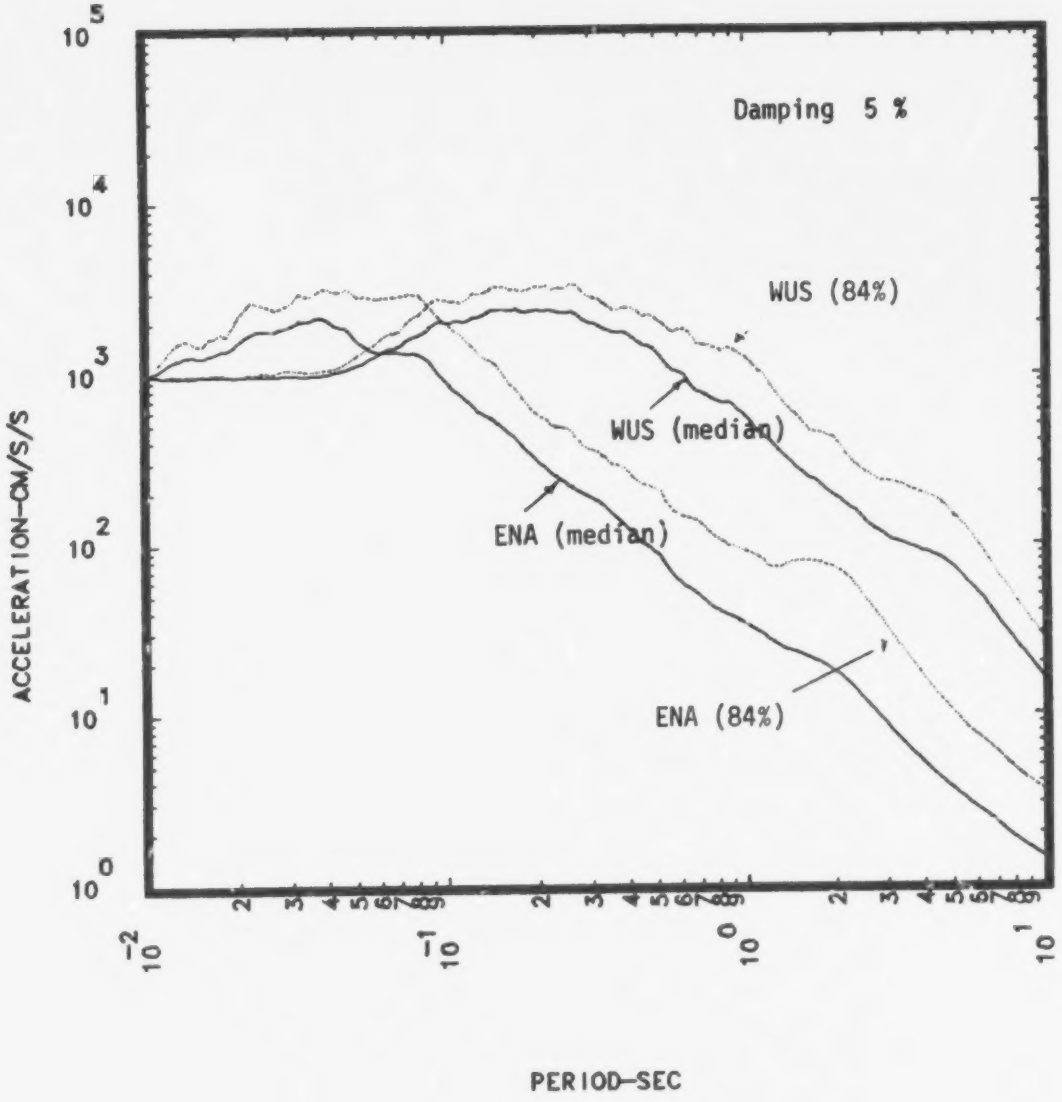

Fig. 4.15 Comparison of the median and 84th percentile normalized acceleration spectra between motions from the strong WUS earthquake group and the smaller ENA earthquake group, both groups of earthquake data were recorded on hard rock.

BEST COPY AVAILABLE

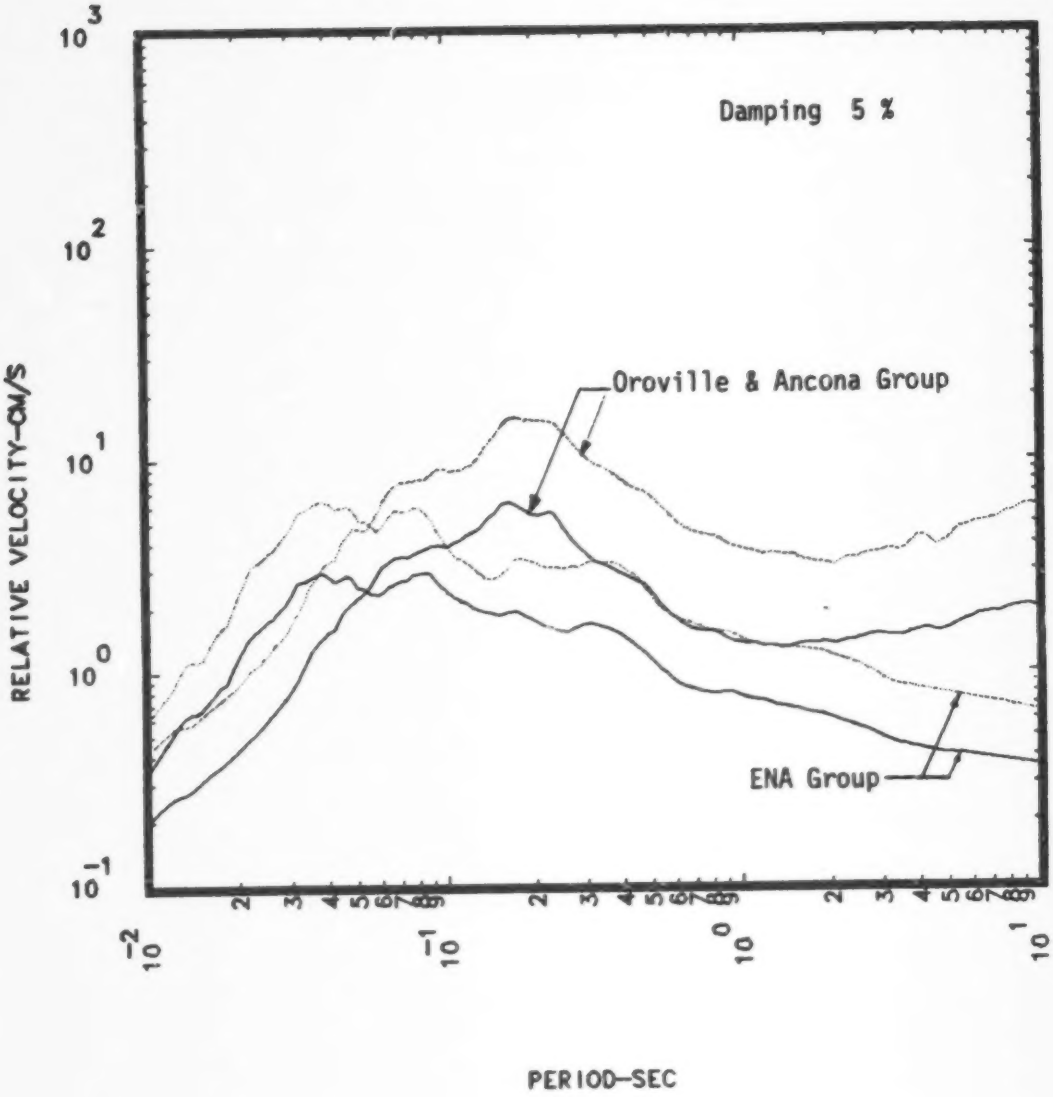

Fig. 4.16 Comparison of the 50th and the 84th percentile velocity spectra between motions from the ENA group and the combined Oroville & Ancona group.

BEST COPY AVAILABLE

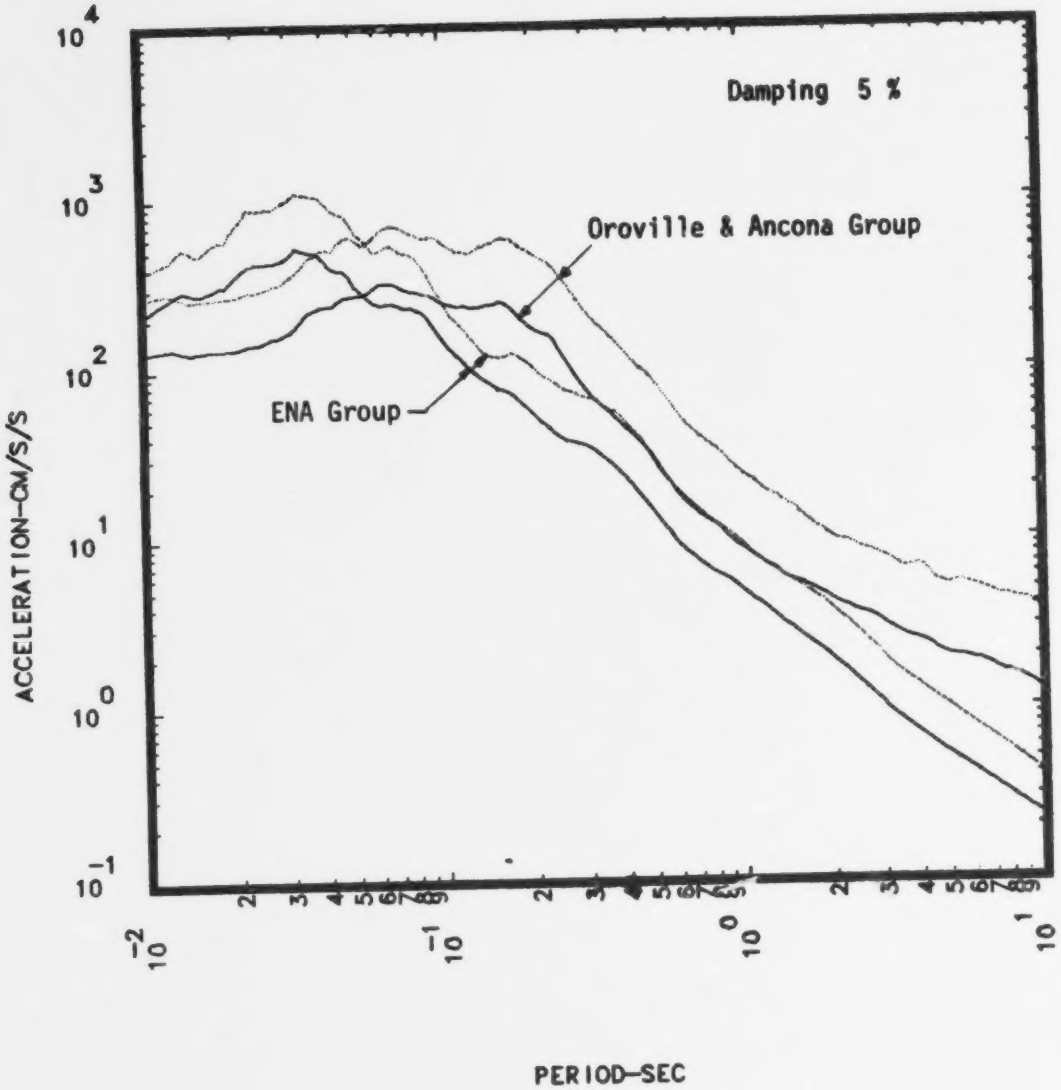

Fig. 4.17 Comparison of the 50th and the 84th percentile acceleration spectra between motions from the ENA group and the combined Oroville & Ancona group.

BEST COPY AVAILABLE

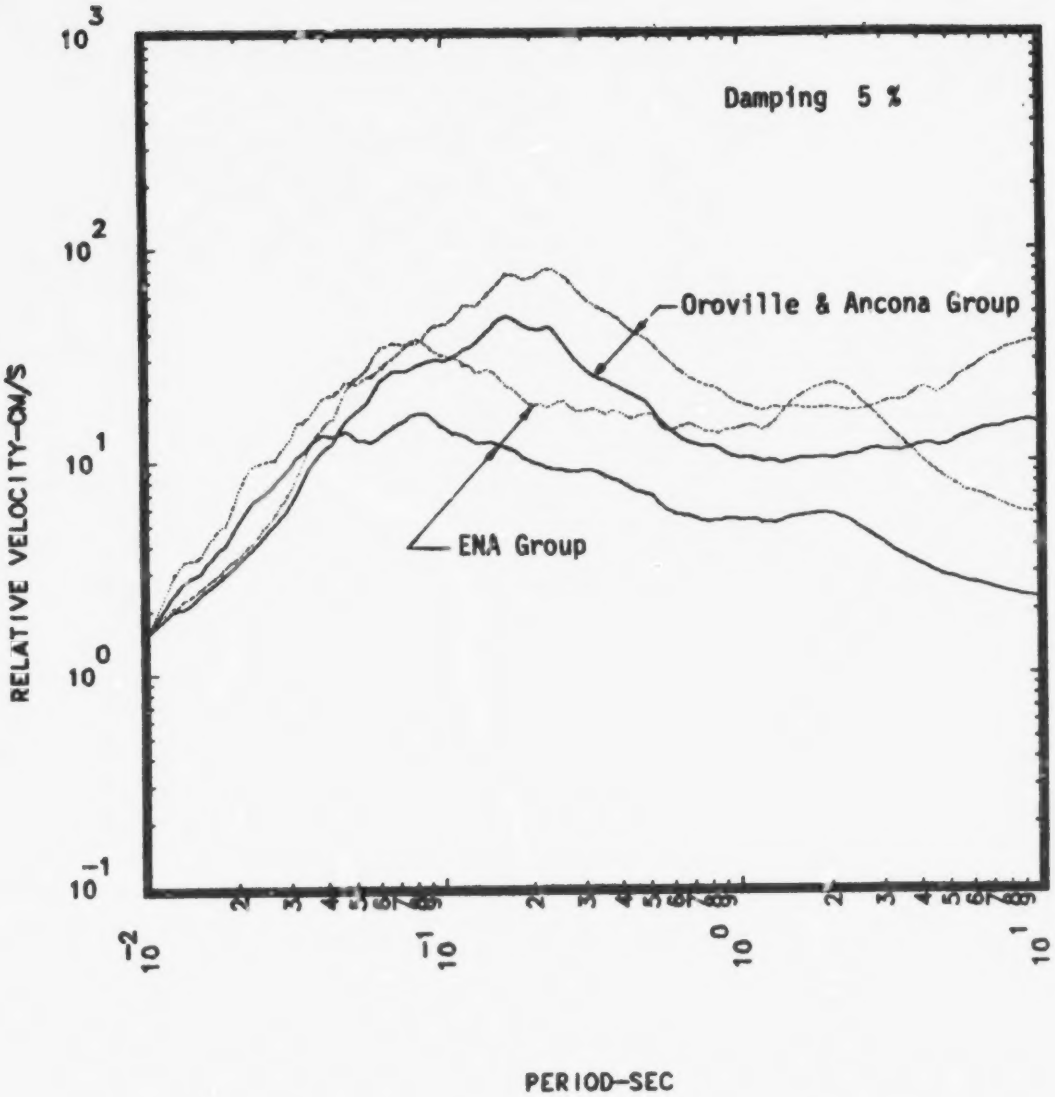

Fig. 4.18 Comparison of the 50th and the 84th percentile normalized velocity spectra between motions from the ENA group and the combined Oroville & Ancona group.

BEST COPY AVAILABLE

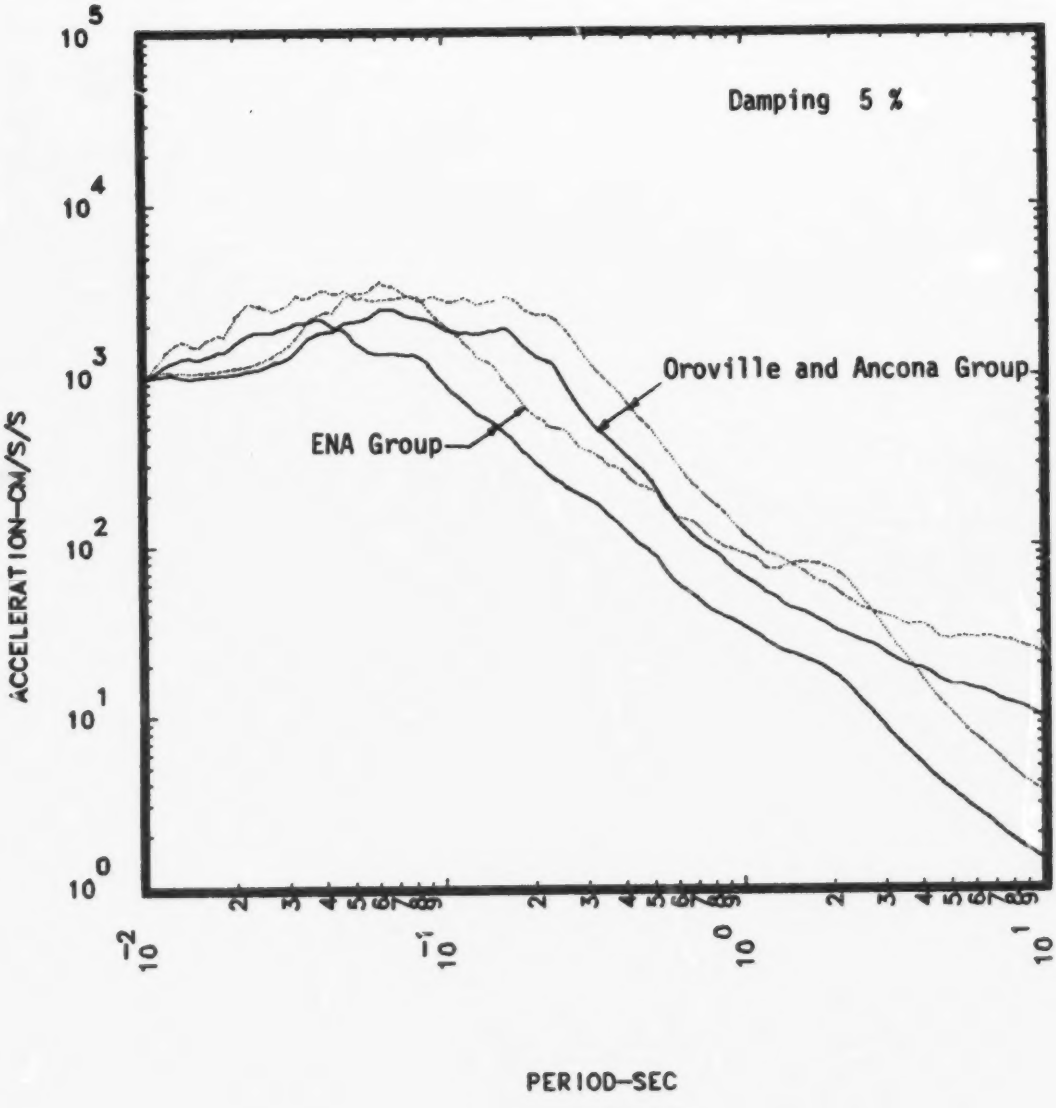

Fig. 4.19 Comparison of the 50th and the 84th percentile normalized acceleration spectra between motions from the ENA group and the combined Oroville & Ancona group.

BEST COPY AVAILABLE

5. UNCERTAINTIES IN GROUND MOTION PREDICTION AND CRITERIA FOR SELECTION OF THE DATA SET

5.1 Introduction

It is generally agreed that there is considerable uncertainty in estimates of ground motion at a site from any postulated earthquake. There are a number of sources contributing to the uncertainty which can be lumped into three major categories:

1) Uncertainties due to "source effects", e.g., fault geometry, and the rupture physics, etc. which varies from earthquake to earthquake.

2) Uncertainties introduced because the travel path from the fault to the site varies from earthquake to earthquake and site to site. We also include the relative geometry of the site relative to fault (radiation pattern) effects in this category.

3) Uncertainties introduced by the local site geology. Although technically part of the travel path, it is worthwhile to single out the last few hundred meters of travel path. Also lumped into this category are recording building/pad effects.

There are several generic approaches that can be used to estimate the ground motion at any given site from some postulated earthquake:

1) Detailed numerical-theoretical modeling of the fault geometry, rupture physics, travel path and site geology.

2) Empirical approach using regression analysis techniques applied to "appropriate" data sets to obtain relations between the expected ground motion and the parameters of the postulated earthquake, e.g., magnitude, distance away, etc.

3) Use of empirical/theoretical models, e.g., the random vibration (Stochastic) approach.

The use of any one of these techniques is plagued by our lack of understanding of the relative significance of each of the three main categories of uncertainties.

More specifically, in this section we want to examine how these uncertainties impact the estimations made by the SSSP approach and, in general, attempt to shed some light on the relative importance of each of the main sources of uncertainties.

5.2 Site Specific Spectra Approach

The SSSP approach was suggested by Bernreuter (1979a). It is a variation on the "regression analysis" approach.

BEST COPY AVAILABLE

The regression analysis approach, typically, attempts to fit to some appropriate data set a model of the form:

$$\log y = C_1 + C_2 M + C_3 \log (\text{distance metric}) + C_5 (\text{distance metric}) + C_6 (\text{site type parameter}) + E \qquad (5.1)$$

where: y = ground motion parameter of interest, e.g., peak acceleration, spectral acceleration at some frequencies, etc.
C_i = constants to be determined from the regression analysis.
E = error term, with zero mean and standard deviation σ

If indeed one had a large unbiased data set, then the problem would be simple. But, we do not have such a data set, although for some areas it is improving rapidly. Unfortunately, nuclear facilities are located in the Eastern United States (EUS) where the data set is still very limited.

The SSSP approach was developed as an attempt to overcome the lack of data in the EUS. The assumption is made that, on the average, major differences between the ground motion observed from typical EUS earthquakes and the ground motion from earthquakes of the same "magnitude" recorded elsewhere are primarily due to attenuation (travel path) and local site effects differences. The travel path differences can be minimized by selecting a suite of records of the appropriate magnitude range recorded "near" the epicenter or rupture surface. The local effects can be minimized by the use of records recorded on similar site conditions. The estimated SSSP is obtained by averaging all of the response spectra computed from the selected suite of ground motion recordings. In most applications of the SSSP approach it has been assumed that the distribution of spectral amplitudes at any period is lognormally distributed. This assumption is also made in this paper. Generally, the 1-sigma spectrum resulting from the averaging process is used. Under the lognormal assumption it becomes the 84th percentile spectrum.

In selecting the suite of records a number of questions arise:

- What is the appropriate magnitude range to use?
- What is the appropriate distance range to use?
- What distribution on distance is appropriate?
- What is the minimum number of earthquakes and travel paths that must be in the data set?
- How "similar" must the recording sites be to the site at which the prediction is to be made?

The answers to some of these questions are, of course, regulatory issues, e.g., what earthquake is the selected suite of earthquakes attempting to model? In all cases, the answers depend on our understanding of the relative contribution to the uncertainty from the three major categories of sources of uncertainty. For example, if all earthquakes of the same magnitude M had basically the same source properties, then one would only need a few earthquakes to capture the potential variation in ground motion observed at a site from earthquakes of magnitude M.

COPY AVAILABLE

The U.S. Nuclear Regulatory Commission (NRC) practice, (Kimball, 1983, Reiter and Jackson, 1983), has been to utilize acceleration time histories from a suite of earthquakes whose magnitudes are within ± 0.5 magnitude units of the target. For EUS sites, the safe-shutdown-earthquake (SSE) is defined in terms of Modified Mercalli (MM) epicentral intensity, in most cases either MM VII or MM VIII. NRC has generally assumed that a M_L = 5.3 earthquake models a MM VII and a M_L = 5.8 models a MM VIII earthquake.

In terms of the target distance, NRC has generally utilized acceleration time histories recorded within 25 km of the source with the average distance being 15 km. No clear criteria have been developed to define "similar" site conditions. Generally, there is little data which can be used to define the site conditions at most accelerograph sites. This lack of data makes it difficult to select records recorded at sites with "similar" site conditions. Thus one of the major objectives of this study is to attempt to determine a measure of what "similar" might entail.

5.3 Model for the Uncertainty

A typical example of the uncertainty resulting from an application of the site specific spectra approach is illustrated on Fig. 5.1a which shows an overplot of all of the spectra selected to define the site specific spectra for a deep soil site in the EUS. F this case, the SSE was specified as M VII. As noted in Section 5.2 it is assumed that the spectral values at period are lognormally distributed. Figure 5.1b shows the resultant median and 84th percentile spectra for the set of spectra shown on Fig. 5.1a. The uncertainty, under the assumption of the lognormal distribution, is measured by the size of σ_T, the standard deviation of the assumed lognormal distribution. It is seen from Figs. 5.1a, and 5.1b that the uncertainty is large. Considering this large uncertainty in the SSSP estimate for the SSE at a typical deep soil site in the EUS, one might ask if it is due primarily to factors which are indeed uncertain such as: the physics of the rupture process of the earthquake; it's possible location relative to the site; it's magnitude; or is it primarily due to the fact that data recorded at too diverse a set of sites was used.

To address this question we need to better understand the relative contribution of each of the categories of uncertainties defined in Section 5.1.

The total uncertainty σ_T can be approximated by the relation:

$$\sigma_T^2 = \sigma_S^2 + \sigma_{TP}^2 + \sigma_{LS}^2 + \sigma_M^2 + \sigma_R^2 \qquad (5.2)$$

where σ_S= Contribution to the uncertainty in the observed spectra due to variations in source properties between earthquakes of the same magnitude.

σ_{TP}= Contribution to the uncertainty in the observed spectra due to travel path and seismic radiation pattern variations.

BEST COPY AVAILABLE

σ_{LS} = Contribution to the uncertainty in the observed spectra due to the fact that the records were obtained at different sites and in different buildings.

σ_M = Contribution to the uncertainty in the observed spectra because a range of magnitudes was used.

σ_R = contribution to the uncertainty because a range of distances (geometric spreading) was used.

In a typical regression analysis type of approach, the distances R and magnitude, M, are included as independent variables, and are generally not assumed to have known values. Thus in this case σ_M and σ_R are implicitly assumed to be equal to zero. However, in the case of the SSSP type of analysis proposed in this study the distance R and magnitude M are not considered to be independent variables. Rather they are only assumed to belong to a range of distance values and a range of magnitude values, the M and R range being independent. In this case, σ_M and σ_R may not be insignificant and deserve some careful considerations.

Unfortunately, it is very difficult to study the relative contribution of each of the component σ's to σ_T. Ideally, one would like to isolate each factor, e.g., fix the site and travel path and examine the recorded ground motions from a wide variety of earthquakes. Clearly, this is not possible. The best that can be expected is a series of nearby earthquakes. To study travel path, one would like to fix the source and site and vary the location of the earthquakes. If all earthquakes were truly similar then this would be possible, but this is clearly not the case. If one knows σ and σ_{TP}, then one could estimate σ_{LS} by using data at fixed sites at which a number of earthquakes have been recorded and data at various sites recorded for the same earthquake. These questions have been addressed to some extent by Bernreuter (1979 a and b), McCann and Boore (1983) and McCann (1983). McCann (1983) and McCann and Boore (1983) used data from the 1971 San Fernando earthquake recorded at several nearby subsets of locations to study σ_{TP} and σ_{LS}. It is difficult to draw firm conclusions because only one earthquake is involved and unfortunately a wide variety of buildings/depths of instrumentation are involved, although the building type and depth of the recording instrument were explicitly accounted for.

5.4 Uncertainty Introduced by the Travel Path

Because of the difficulty of fixing the travel path, it is worthwhile to first examine how much variation in the observed ground motion at a fixed site from a source with fixed parameters is introduced by changes in the travel path. Because this variation can be considerable (as will be shown in the next section), the data we propose to use to address this issue consists of the ground motion recorded from large underground nuclear explosions (UNE).

Figure 5.2 shows the 5 percent damped relative velocity spectra obtained from data recorded from 5 UNE at the Nevada Test Site (NTS). These 5 events each had a yield greater than 100 kilotons and within $\pm$ 5 kilotons of each other.

COPY AVAILABLE

The distance between the UNE and the recording station (station 10) was 55 ± 2 km. All of these UNE were located in Pahute Mesa area of NTS within a few kilometers of each other. It is observed from Fig. 5.2 that there is considerable variation between the spectra from event to event.

Figure 5.3 shows the envelope, median and 1-Sigma spectra based on the spectra for the five UNE shown in Fig. 5.2. As noted in Section 5.3 the computation is made assuming that the distribution is lognormal. The uncertainty as measured by standard deviation of the natural log of S_v ($\sigma_{\ell n S_v}$) varies with the period with an average value of about 0.2. It is observed that there is as much as a factor of two difference between the computed median and the maximum observed value. It should be noted that if only the radial component is used the spread is somewhat reduced to a factor of 1.6. These results indicate that very minor variations in the travel path can result in considerable uncertainty in the observed ground motion at a site. There is some additional data, discussed in Section 5.6, which sheds additional light on the question of just how much variation in the observed ground motion at a site is due to only variations in travel path.

5.5 Uncertainty Introduced by the Source

The question we would like to address in this section is: assuming that one could fix the site and travel path, what is the variability in the observed ground motion at a fixed site from all possible earthquake source mechanisms for earthquakes of magnitude M? Note that this variablility could well be a function of M.

It is useful to first examine simple theoretical models and the little available data to address this issue.

Typically, to the first order, Brunes' model (1970) is used to represent the source spectrum of an earthquake. Brunes' model relates a few fundamental parameters of the earthquake to the Fourier amplitude spectrum of the displacement. The source function that would be observed at a distance R from the source in a half-space, (i.e., no complexity of layering transmission path, etc.) is:

$$FS_d(R,\omega) = \frac{K\Delta\sigma}{Rf_o} \frac{1}{\omega^2 + f_o^2} \tag{5.3}$$

where

$\Delta\sigma$ = Stress drop (source parameter)
f_o = Corner frequency (related to the rupture area)
R = Distance
K = constant

Using this simple model and a few other assumptions, Thatcher and Hanks (1973) showed that the local magnitude M_L of an earthquake is related to the parameters of Brunes' model of an earthquake by the relation

$$M_L = \log\Delta\sigma - 3/2 \log f_o + C \tag{5.4}$$

BEST AVAILABLE

Thatcher and Hanks (1973) showed that this relation fits the data. Using Eqs. (5.3) and (5.4), it is relatively easy to show that

$$FS_a(R,\omega) = \frac{K f_o^{1/2} \, 10^{M_L}}{R} \cdot \frac{\omega^2}{\omega^2 + f_o^2} \qquad (5.5)$$

where FS_a = Fourier spectrum of the acceleration

There is a close relationship between FS_a and the undamped relative velocity spectrum of interest in structural analysis. Eq. (5.5) shows that for a given magnitude we can expect the level of FS_a to vary as $\sqrt{f_o}$ for frequencies greater than f_o, and as $f_o^{-3/2}$ for frequencies much less than f_o. Thatcher and Hanks (1973) provide measured data which suggest that f_o varies by about an order of magnitude for earthquakes in the range of 4.5 to 6.5. Thus, we would expect at a minimum up to a factor of 3 difference between the maximum and minimum levels of FS_a for the range of engineering frequencies of interest. If one thinks in terms of the SSSP approach, all of these earthquakes would be averaged together relative to the median prediction, we might expect that our uncertainty as measured by Sigma ($\ln FS_a$) would be in the range of 0.4 - 0.5 or a factor of 1.5 or so uncertainty.

Figure 5.4 shows the 5 percent damped relative velocity spectra (both horizontal components) for two earthquakes of approximately the same magnitude (M_L = 4.6) and within a few kilometers of each other, at approximately the same depth computed from records obtained at the Oroville Airport. It is observed that the relative level of the high frequency (short period) spectral amplitudes differ by about a factor of 3. Figure 5.5 shows a similar comparison for two M_L = 3.6 earthquakes based on records obtained at the Brawley airport. Although the two earthquakes recorded at Brawley were relatively close together, they are so close to the recording station that the radiation pattern could be a factor in the observed differences between the spectra. Once again the variation between the two earthquakes is about a factor of 3 or more.

Naturally, as the earthquakes become larger, there is a strong possibility that a larger number of "barriers" become involved. Thus, we might well expect to see a wider variation in the observed ground motion at a fixed site for larger earthquakes.

5.6 Uncertainty Introduced by the Site

In this section we want to examine how much uncertainty is introduced into our ground motion estimates from mixing data recorded at a number of different sites. If the site is fixed, then $\sigma_{LS} = 0$, and

$$(\sigma_T)^2_{\text{fixed site}} = \sigma_S^2 + \sigma_{TP}^2 + (\sigma_M^2 + \sigma_R^2) \qquad (5.6)$$

then, we can estimate σ_{LS} from

AVAILABLE

$$\sigma_{LS}^2 = \sigma_T^2 - (\sigma_T^2)_{\text{fixed site}} \qquad (5.7)$$

To do this, one needs to have recorded ground motion data at a number of sites that have experienced repeated earthquakes. The problem is that there are only a few sites which have ground motion data from a number of earthquakes. Some data sets from UNE having limited effects from travel path and source can also be very useful. Then, smaller data sets can be used to estimate the reduction in uncertainty achieved by fixing the site relative to a fixed source and travel path.

In addition to the reduction in the uncertainty in our predictions (at a fixed site), we would expect that the median prediction might depend on the actual conditions at any given site. Finally, we might expect the predicted spectrum to have more "character", i.e., have local maximums and minimums relative to a general data set.

As noted, ground motion recorded from UNE can shed considerable light on this question. Lynch (1971) used data recorded at thirteen stations from fourteen UNE to study this problem. Source and travel path variations for each site were minimized by restricting the data to only UNE located on Pahute Mesa. The level of ground motion was low so that the nonlinear effects in the soil at the sites should be small. The sites were located from 52 to 170 km from Pahute Mesa. Lynch (1971) analyzed this data using a covariance analysis that explicitly included each site rather than a typical regression analysis. Briefly, covariance analysis relates a component of spectrum SV at period i recorded at K stations to the yield of events detonated in a restricted area. The statistical model has the form

$$SV_{ik} = A_{ik} W^{Bi} \qquad (5.8)$$

$i = 1, 2, \ldots,$ No. of Periods

$k = 1, 2, \ldots, K$

and $w =$ yield

The analysis determines for each component at each period, i, a yield scaling exponent B_i, the standard deviation of the estimate σ_i, and K sets of amplitude coefficients A_{ik}. The amplitude coefficients A_{ik} implicitly reflect the average distance from the event area to the recording station, local station amplification and any factor associated with the transmission path. The parameter σ_i reflects the variance due to neglected source parameters, transmission path factors for each station and differential changes in the average distance to each recording station.

A plot of $\exp(\sigma_i)$ obtained from Eq. (5.8) using the restricted Pahute Mesa data set and $\exp(\sigma_i)$ obtained from a general regression, Lynch (1969), of the form

$$SV = A W^{B_1} R^{B_2} \qquad (5.9)$$

is shown in Fig. 5.6. Figure 5.6 shows the amount of reduction in the uncertainty when the data is restricted to a fixed site.

BEST COPY AVAILABLE

The data set used by Lynch (1969) was somewhat different than the data set used by Lynch (1971); however, in both cases, the data were restricted to Pahute Mesa UNE. Thus, the reduction in uncertainty can be primarily attributed to fixing the site conditions as source and travel path variations are about the same. It is very interesting to note from Fig. 5.6 that the uncertainty associated with the model described by equation 5.9 is much larger than generally associated with typical earthquake data sets. This is surprising because we have what appears to be a rather homogenous data set compared to the typical earthquake data sets. However, a closer look at the make up of the stations involved indicates that a relatively large percentage of them are of near-by pairs exhibiting wide variations in response (as illustrated in Fig. 5.7 for one pair of stations, one station being located on a rock outcrop and one located on a nearby soil deposit.)

Lynch and Williams (1972) performed a covariance analysis on data obtained from 22 UNE located at Yucca Flat. Figure 5.8 compares the computed $\exp(\sigma_i)$ of the Yucca Flat data set to the $\exp(\sigma_i)$ of the Pahute Mesa data set. It is seen that they are very similar.

The values of the $\exp(\sigma_i)$ shown in Fig. 5.8 primarily measure the varability introduced by modest changes in travel path as source and site effects have been held constant. From Fig. 5.8 it is seen that σ_i varies slightly as a function of the period. It can reasonably be approximated by a constant value of 0.4. This value of σ_i is larger than the value of $\sigma_{\ln Sv}$ observed in Section 5.4. This is not surprising because the variations in the travel paths of the data used in Section 5.4 were smaller than the variations in the travel paths for the data used by Lynch.

Note, however, that both data sets represent rather limited variations in travel paths. Thus for earthquakes we could expect that the uncertainty introduced by travel path alone could be much larger. In addition, the increase in the variability introduced by the radiation patterns of the earthquakes could also be very significant.

If a given site has experienced a number of earthquakes for which records of the ground motion are available, then it is possible to determine if the site generally amplifies ground motion relative to typical correlations such as those developed by McGuire (1978) and Joyner and Boore (1981). It is also possible to determine if the data at a given site are less dispersed than the more general data set for a number of sites. The difficulty is to assess the role that site response factors play relative to source and travel path factors. Source and travel path variations are extremely important. It is difficult to account directly for these factors other than by the simple approach of grouping the available data so that these factors are minimized.

The El Centro and Ferndale sites have the most complete data sets. Both of these sites are deep soil sites, although the overall soil depth is greater at El Centro than at Ferndale, and the soil is somewhat stiffer at Ferndale than at the El Centro site.

Bernreuter (1979b) used the data recorded at these two sites to compare the peak acceleration to the mean predicted by typical correlations among peak accelerations, site type, earthquake magnitude, and distance. For his

AVAILABLE

comparison, he used the correlation developed by McGuire (1978) as representative. For soil sites, McGuire determined that

$$a = \frac{24.5 \exp [0.89M]}{R^{1.17}} \; ; \; \sigma_{\ell na} = .62 \; , \qquad (5.10)$$

where

M = Local Richter magnitude
R = Distance from energy release
σ = Standard deviation

Figure 5.9 shows a comparison of the recorded accelerations at the El Centro and Ferndale sites normalized by exp 0.89M as a function of R. Also shown, is the median normalized line given by Eq. 5.10 and the ± one-sigma lines. It is evident from this figure that consistently higher-than-average peak accelerations are recorded at the Ferndale site during the earthquakes. The El Centro site appears to have average acceleration.

In order to quantify the dispersion of the data, separate regression analyses were performed for the data at the El Centro and Ferndale sites. The results of these analyses are:

$$\ell n(a) = 4.82 + 0.52M - 0.83 \; \ell n(r) \qquad (5.11)$$
$$\sigma_{\ell na} = 0.39$$

for Ferndale, and

$$\ell n(a) = 4.12 + 0.53 = 0.85 \; \ell n(r) \qquad (5.12)$$
$$\ell_{na} = 0.67$$

for El Centro.

There is significantly less scatter to the data at the Ferndale site than to the data at the El Centro site. The data at El Centro have about the same standard deviation as the more general data used by McGuire, which included eight El Centro records and nine Ferndale records. Although the distances R for the Ferndale events are less certain than for El Centro events, no systematic error appears to exist, and it is unlikely that the errors are large enough to significantly change the conclusion reached above.

We also examined the Oroville data set. We performed a regression analysis on the data in Seekins and Hanks (1978) and used the resulting relation to normalize the recorded peak accelerations. Figure 5.10 shows the ratio between the measured and estimated peak acceleration as a function of distance. In Fig. 5.10 the ratios for the Johnson Ranch data are denoted by the symbol J and the ratios for the Oroville Airport data by the symbol A. The ± one- sigma limits are also shown. It is seen that the observed peak acceleration recorded at the Johnson Ranch site is consistently high (6 out of 8 data points above the +one- sigma limit) and the observed peak acceleration recorded at the Oroville Airport is consistently low (9 out of 11 data points

below the median. However, there is a much greater spread in the airport data than in the ranch data.

We also examined how the error term might be reduced by going from the general data set to a fixed site and we examined (for the fixed site cases) those sites at which eight or more earthquakes were recorded. We obtained

$\sigma_{\ell na}$ = 0.60 General data set
0.42 Johnson Ranch Station
0.26 Station 5
0.61 Station 1
0.36 EBH Station
0.7 Airport

These results are in reasonable agreement with the results for the Ferndale, and El Centro data. There is considerable scatter to the data making it difficult to estimate σ_{LS} . The "stiffer sites" (Ferndale, Johnson Ranch, Station 5, EBH) show lower $\sigma_{\ell na}$ value than deep and than softer stations (El Centro and Station 1).

To estimate σ_{LS} we need σ_T for fixed sites. We approximated this by defining a site category for each site for the Oroville data set and used the model

$$\ln a = C_1 + \Sigma CS_i S_i + C_2 M + C_3 \ln R \qquad (5.13$$

where

C_i and CS_i are constants to be determined by a regression analysis

S_i are site categories, S_i is one if the data point was obtained at site i and is zero otherwise

R = hypocentral distance

M = local magnitude

Our fit to the data resulted in a σ_T= 0.52 for "fixed sites". Using σ_T = 0.60 from our general fit to the data without site categories we estimate that

$$\sigma_{LS}^2 = \sigma_T^2 - (\sigma_T)^2_{\text{(fixed site)}} = (.60)^2 - (.52)^2 \qquad (5.14)$$

$$\sigma_{LS} = 0.30$$

McCann and Boore (1983) and McCann (1983) attempted to sort out the various contributions to the uncertainty in the prediction of ground motions using data from the San Fernando Earthquake. McCann (1983) concluded that local site effects contributes about 30% of the uncertainty, i.e. $(\sigma_{\ell na})_{LS}$ = 0.23 based on a few sites. This result is consistent with our results.

AVAILABLE

5.7 Uncertainties Introduced by the Range for M and R Used

In a typical regression analysis approach both the magnitude and distance variations are explicitly accounted for. This is not the case in the SSSP approach where a range of distances and magnitude are included. In fact it should be noted that one of the important features of the SSSP approach is to include the potential uncertainties in magnitude and location of the SSE in the predicted spectrum. However, if the uncertainty introduced by the range for M and R are much larger than the uncertainties introduced by the other sources of uncertainty, then it would seem necessary to rethink the ranges for M and R used. Recall from Section 5.2 that the "target" is typically an earthquake of M_L = 5.3 (for MM VII SSE) and M_L = 5.8 (for MM VIII SSE) with an average distance of 15 km.

A simple estimate of the uncertainty introduced in our estimate of the ground motion using the SSSP approach can be obtained by using the results of typical regression analysis of data sets. e.g., Joyner and Boore (1981) found that

$$\log_{10} a = C_1 + 0.25M - \log_{10} r - 0.0026r \qquad (5.15)$$

$$\text{where } r^2 = d^2 + 53$$

The term -.0026r is relatively unimportant for the distance range out to 25 km. Thus the potential multiplicative error, E^* in the actual value of the acceleration at the high frequency end of the estimated spectra obtained by use of the SSSP approach for distances (d) of 0 to 25 km with an average distance of 15 km is of the order

$$0.64 < E^* < 2.3$$

That is, the spectra from the most distant earthquake used will be about a factor of 0.6 smaller than the "target" and the very near fault data might be a factor of 2 larger than the target. These variations are of the same order or on the average smaller as the uncertainties introduced by the other sources of uncertainty.

The maximum potential uncertainty introduced by the range in magnitudes used ($\pm$ 0.5 units) is on the order of $10^{(.125)}$ or a factor of 1.3. Clearly the actual uncertainty introduced by the distribution of earthquake magnitudes used is less than the other uncertainties.

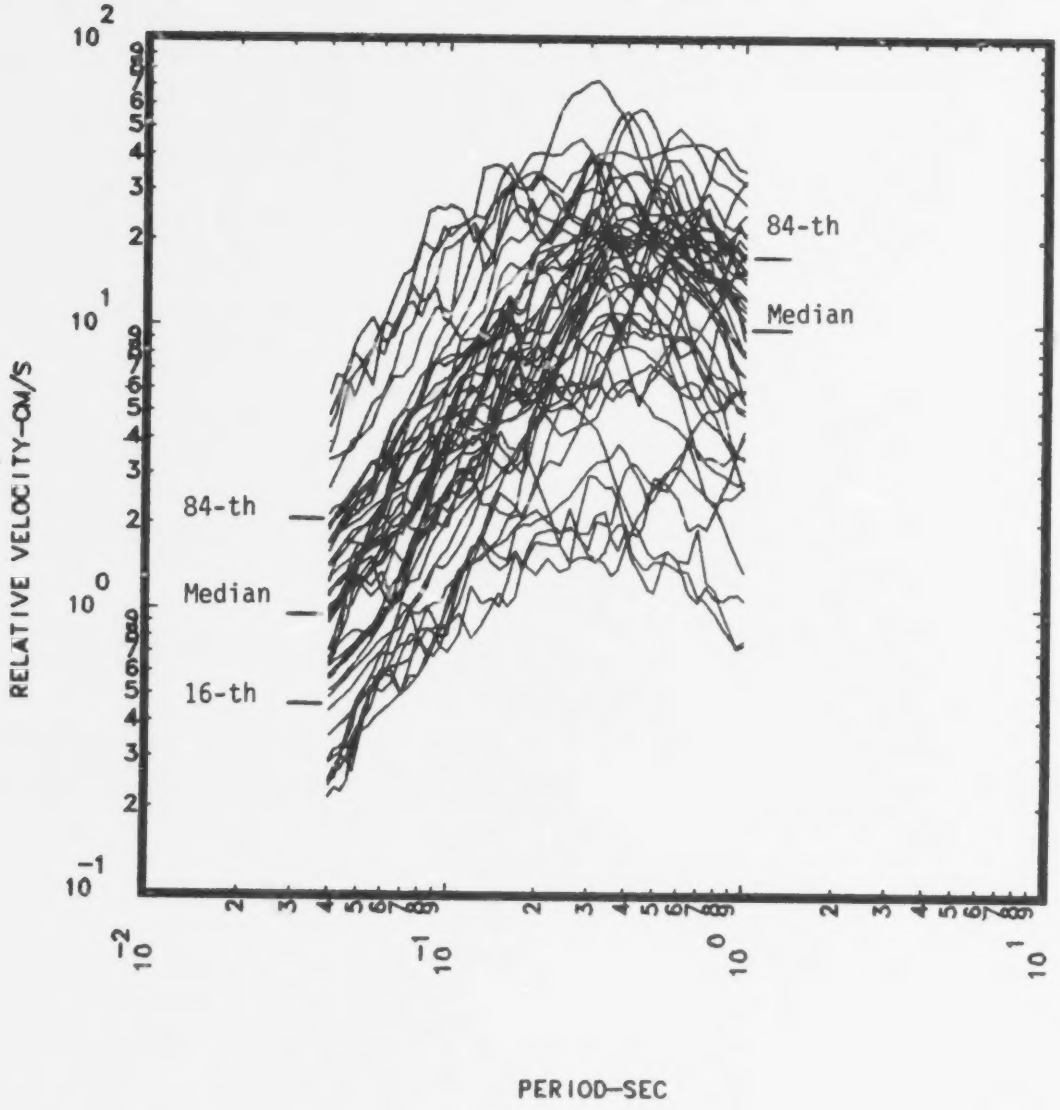

Fig. 5.1.a Over plot of all of the suite of spectra selected to define the SSSP for a deep soil site having a SSE of MMVII.

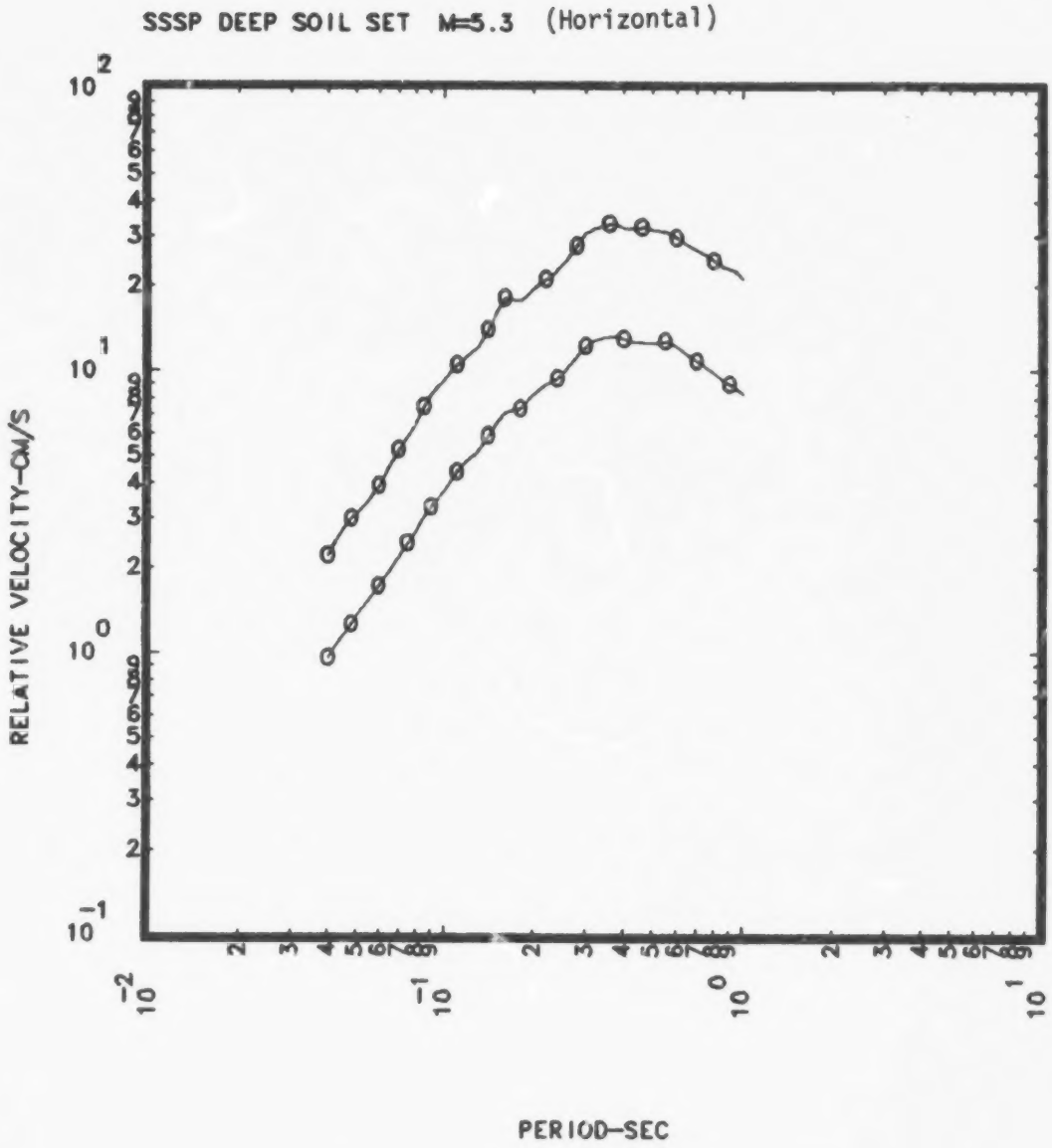

Fig. 5.1b The Median and 84th percentile spectra of the suite of records shown in Fig. 5.1a.

COPY AVAILABLE

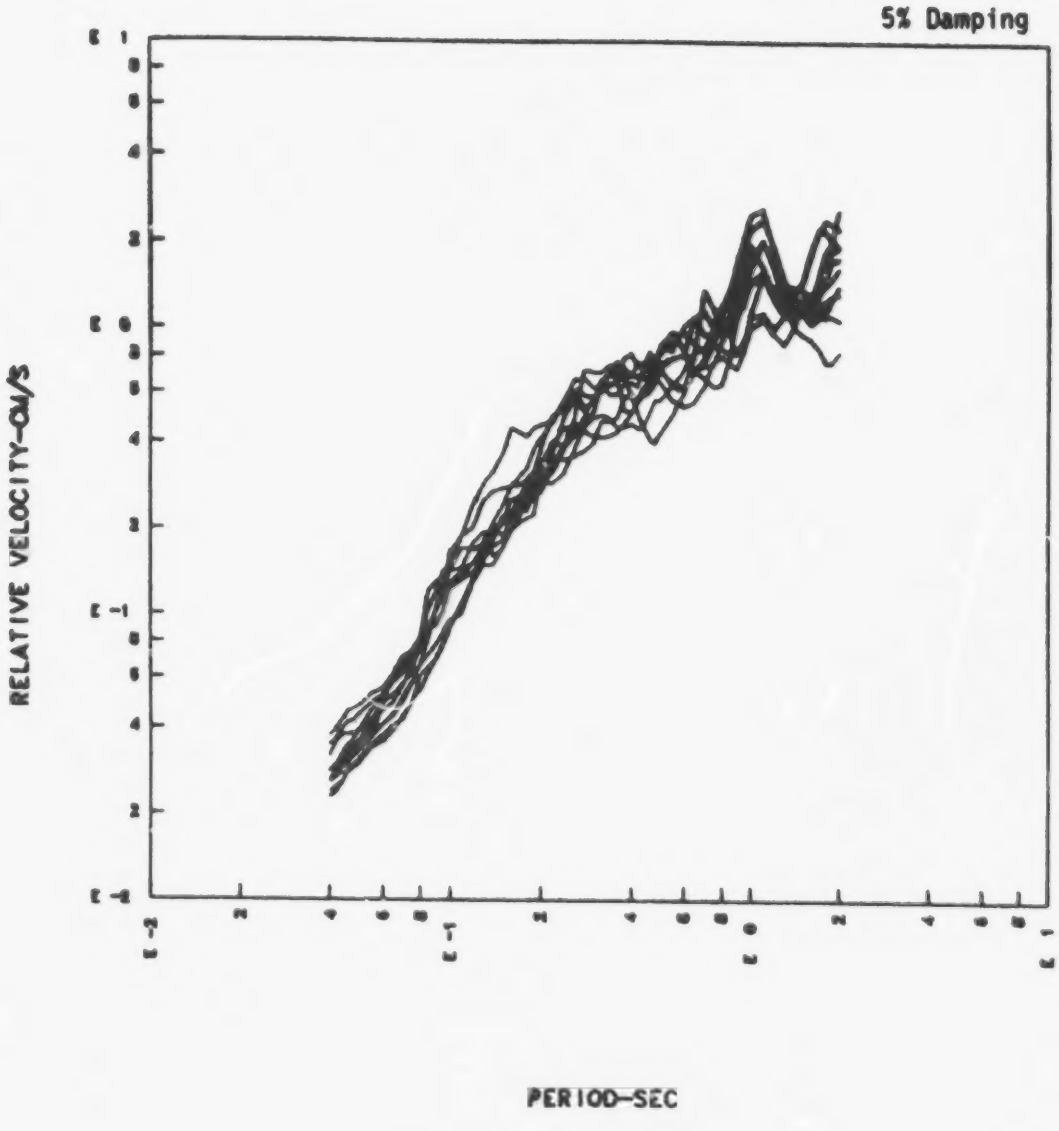

Fig. 5.2 Over plot of both radial and tangential components of 5 UNE recorded at a single deep soil station. These 5 UNE all had a yield of ± 5 kilotons of each other at a distance of 55 ± 2 km from the recording station.

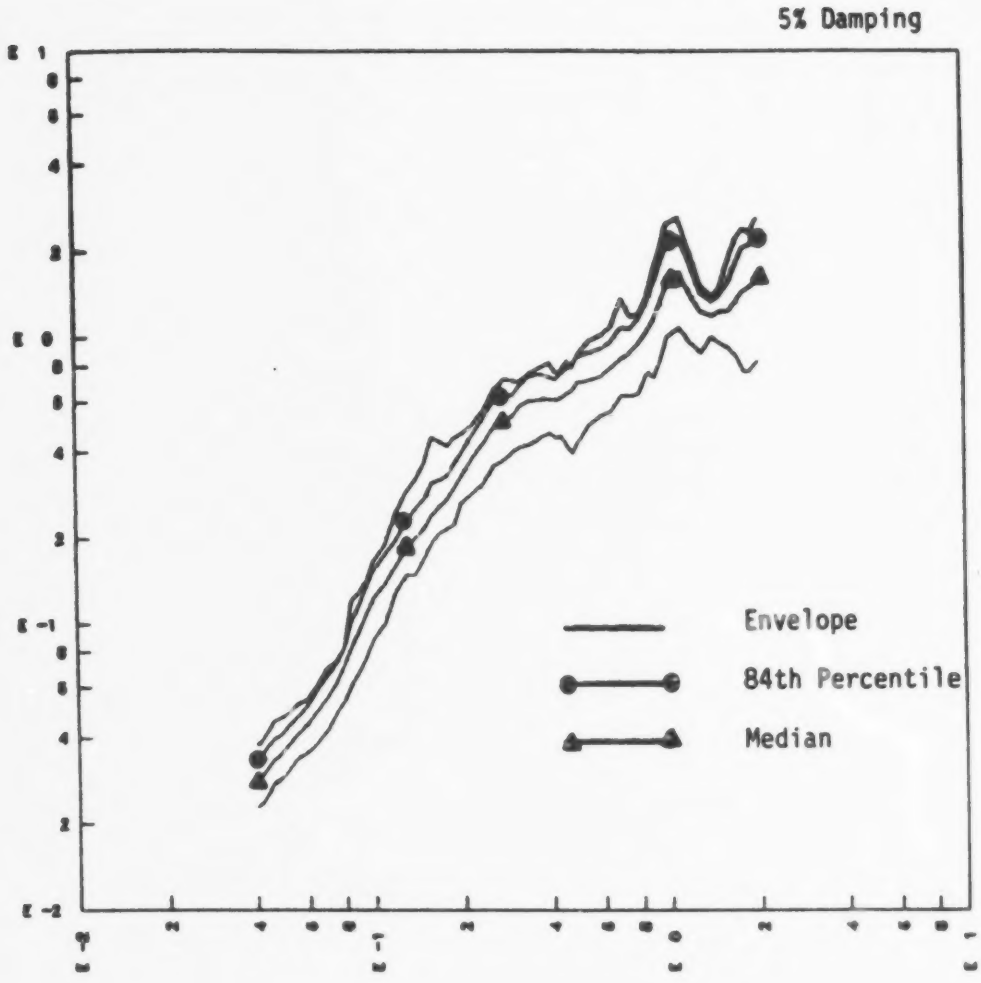

Fig. 5.3 The envelope, median and 84th percentile spectra of the suite of spectra shown in Fig. 5.2

BEST COPY AVAILABLE

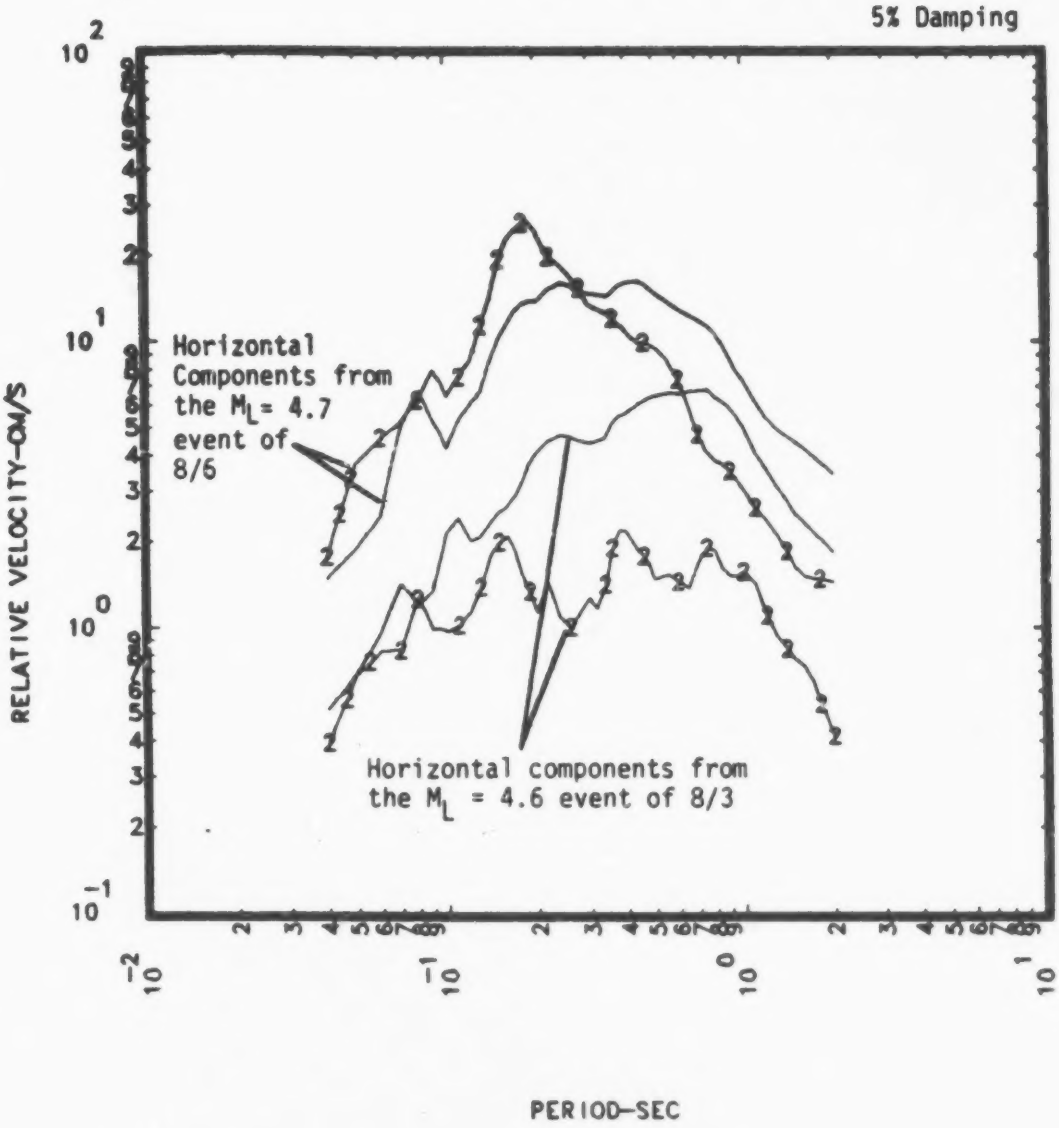
5% Damping
RELATIVE VELOCITY-CM/S
PERIOD-SEC
Horizontal Components from the M_L = 4.7 event of 8/6
Horizontal components from the M_L = 4.6 event of 8/3

Fig. 5.4 Comparison of the spectra from two earthquakes located within a few kilometers of each other with similar M_L and recorded at the Oroville Airport.

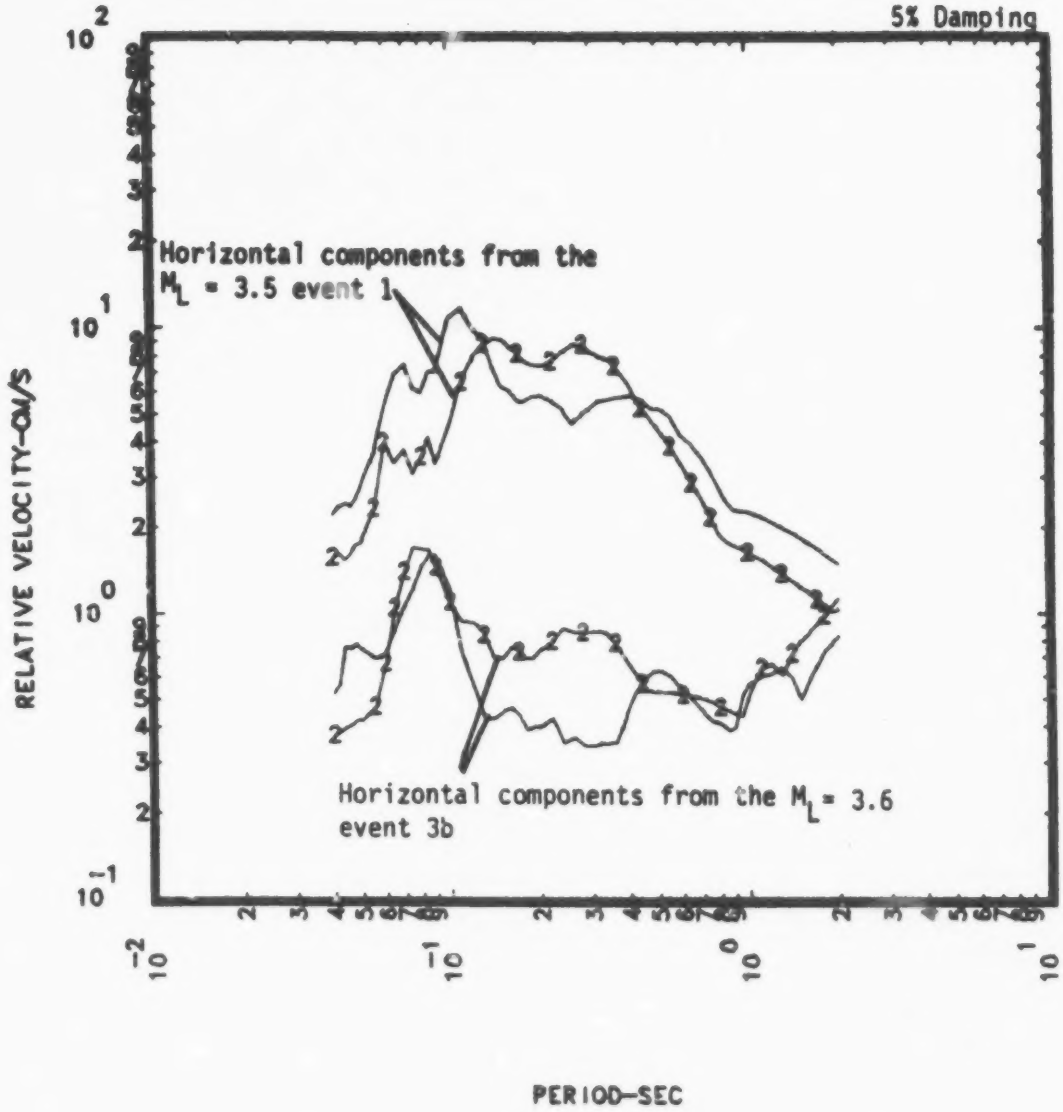

Fig. 5.5 Comparison of the spectra from two earthquakes located within a few kilometers of each other with similar magnitudes and recorded at the Brawley Airport. Event numbers and magnitudes from Johnson and Hanks (1976).

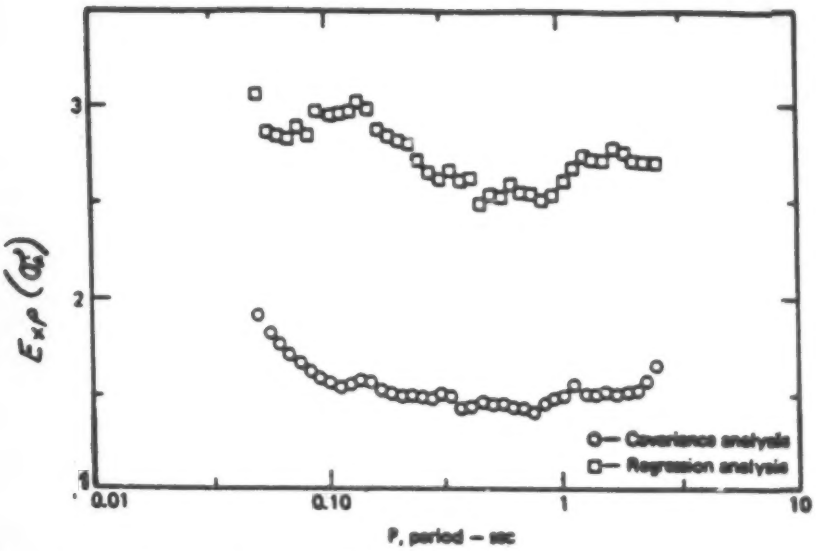

Fig. 5.6 Comparison of Exp (σ_i) obtained from a covariance analysis accounting for each site to that obtained by Lynch (1969) which does not include site factors.

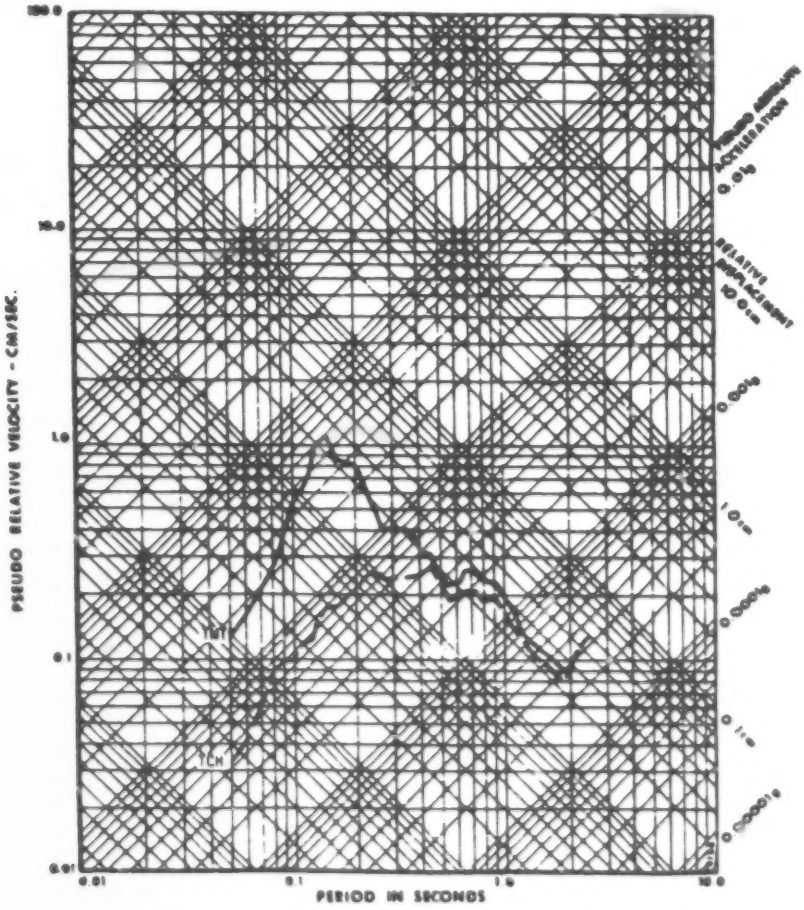

Fig. 5.7 Comparison of the radial component of the spectra from two nearby stations TMT (Tonopah motel, shallow alluvium) and TCH (Tonopah church, rock).

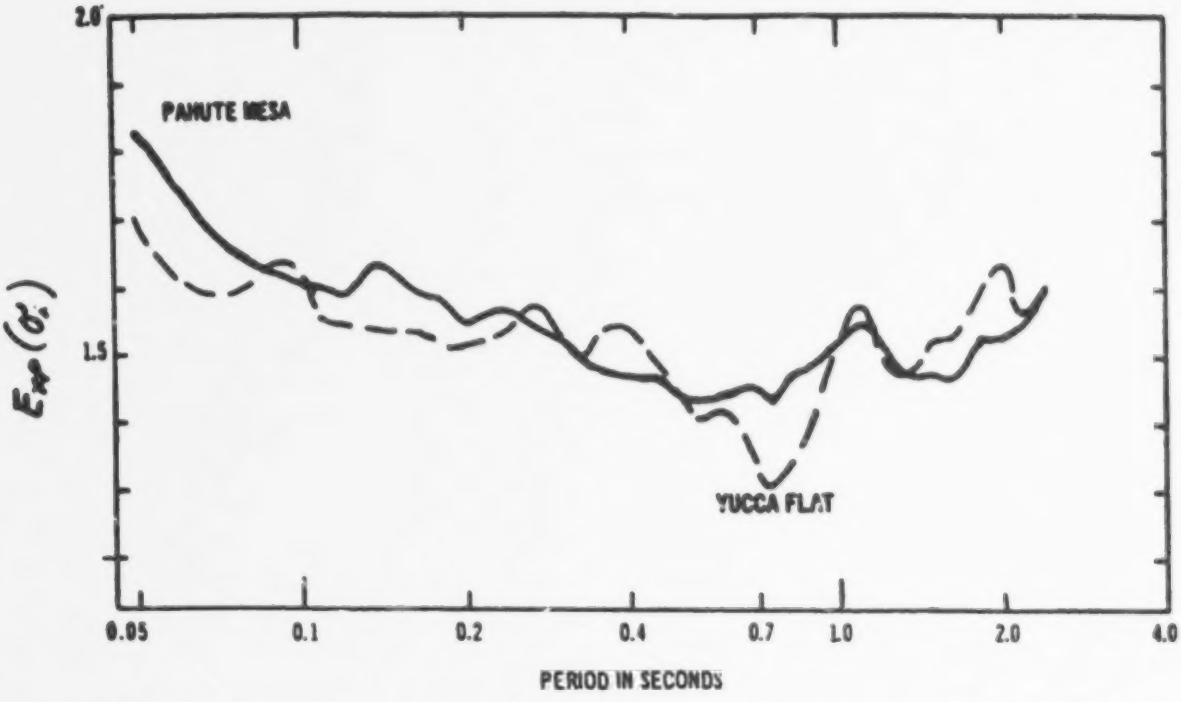

Fig. 5.8 Comparison of Exp ($^{\sigma}$i) for the covariance analysis for Pahute Mesa UNE (Fig. 6.1) to that for Yucca Flat UNE.

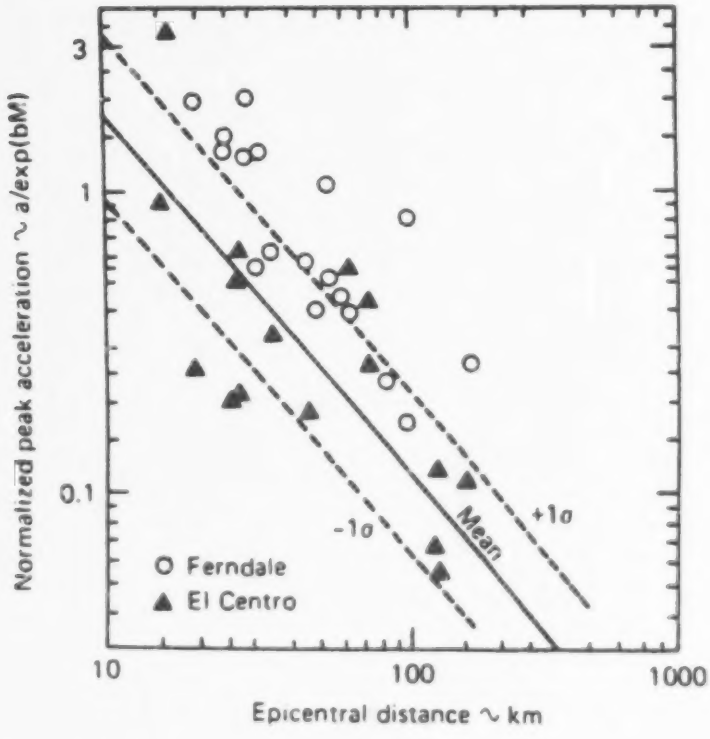

Fig. 5.9 Normalized peak accelerations recorded at El Centro and Ferndale sites compared with McGuire's (1978) correlation.

COPY AVAILABLE

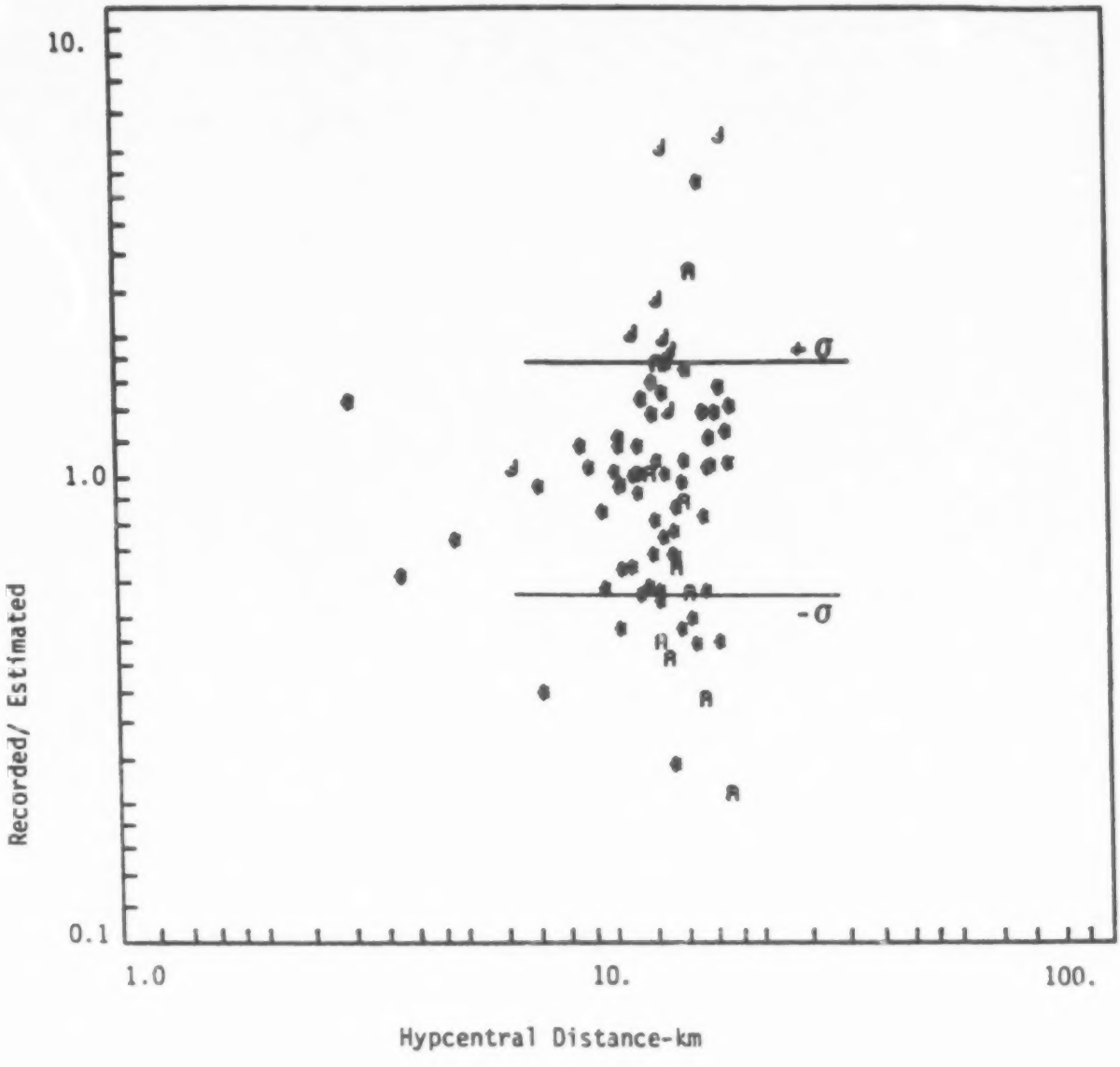

Fig. 5.10 Normalized peak horizontal acceleration for the Oroville data set. The data for Johnson Ranch are denoted by J and for the Oroville Airport by A. The data from the other stations are denoted by *.

AVAILABLE

6. DEVELOPMENT OF SITE SPECIFIC SPECTRA FOR ENA

6.1 Criteria for Selecting Records

In order to develop SSSP for a given site for a particular SSE, it is necessary to have criteria to select the suite of records to use to generate the SSSP. These criteria must address the questions raised in Section 5, namely:

- What is the appropriate magnitude range to use?
- What is the appropriate distance range to use?
- What distribution on distance is appropriate?
- What is the minimum number of earthquakes and travel paths that must be in the data set?
- How "similar" must the recording sites be to the site at which the prediction is to be made?

We noted in Section 5 that questions such as the magnitude range, distance range and average distance are basically regulatory issues. However, it is important that the chosen ranges are not so large as to significantly increase the uncertainty.

The NRC practice, (Kimball 1983, Reiter and Jackson 1983,) has been to utilize acceleration histories from a suite of earthquakes whose magnitudes are within $\pm$ 0.5 magnitude units of the target. For ENA sites, the safe-shutdown-earthquake (SSE) is generally defined in terms of Modified Mercalli (MM) epicentral intensity, in most cases either MM VII or MM VIII. NRC has generally assumed that a M_L = 5.3 earthquake models a MM VII and a M_L = 5.8 models a MM VIII earthquake.

In terms of the target distance, NRC has generally utilized acceleration time histories recorded within 25 km of the source with the average distance being 15 km.

In Sections 2 to 5 we have attempted to determine what the most significant parameters are and to estimate the contribution to the overall uncertainty from each of the three major categories of the sources of uncertainty defined in Section 5.

It can be concluded from the discussion in Section 2 that the focal depth of an earthquake is an important parameter. However, there are so few records available, that it is not possible to include a depth criterion in the selection of records for the development of SSSP for different SSE and site categories.

We also concluded in Section 2 that it does not appear to be significant if a particular rupture process breaks through to the surface.

Two instrumentation factors that emerge from Section 3 as being significant are the startup/trigger problem and the signal to noise problem. Ideally, it would be best to only use data from records for which the entire signal (both P and S wave trains) has been recorded. Unfortunately, there are very few complete records. We have generally only selected records which are relatively complete, i.e., have the entire S wave train. In a few cases,

BEST COPY AVAILABLE

e.g., the Mitchell Lake Road station data, we have included late start records which do not contain the entire S wave train. As the maximum horizontal motion is generally in the S wave train, this poses no problem. The same is not true for the vertical component. If the maximum motion is in the first arrival, then it is generally missed. Thus, there is no way of estimating how good the vertical SSSP are.

We have cut the SSSP off at a period of one second even though the signal to noise ratio for records from earthquakes with magnitude less than 5 is generally large. Conversely the spectra are not valid for periods less than 0.04 seconds because the signal to noise ratio becomes too low beyond these short periods. Thus, we have used 0.04 seconds as the short period cutoff.

The results of Sections 4 and 5 allow us to address the questions raised above. The results of Section 4 suggest that one should not use too large of a magnitude range to select the suite of records used to develop the SSSP for a given case. The results of Section 5 indicate that the uncertainty introduced by the range for magnitude ($\pm$ 0.5 units) used in the past by NRC is not large compared to the other uncertainties.

The choice of the appropriate distance range and distribution is a regulatory choice of the location of the SSE relative to the site. The results of Section 5 suggest that NRC's current practice does not introduce uncertainties larger than the uncertainties from source and travel path variations. In fact, the results of Section 5 indicate that we need as many sources and travel paths as possible. We can also conclude, based on the results of Section 5, that if the one-sigma SSSP is not more than a factor of 2 larger than the median SSSP, then the suite of records/earthquakes represented is too small relative to the number of source types and/or travel paths. This indicates that care is required not to use too many records from a single event.

In the application of the SSSP approach the local site's geology must be treated differently than the other categories of uncertainties because the estimate is for a fixed site and hence, unlike the other parameters, the local geology is not a random variable. Thus we have two conflicting problems in the selection of data. First, because of the fixed nature of the site, we would like to limit our data selection to very similar site conditions. However, our results also show that we can expect large variations in the observed ground motion at any fixed site because of the uncertainties introduced by source and travel path effects. This means that we need a large sample to be sure that we have adequately defined the estimated median and 84th percentile spectra. In general, such a sample can only be obtained by relaxing the criteria used to determine if a site is "similar" to the target site because at many accelerograph sites we only have very limited information about the parameters needed to determine if the accelerograph site matches the site for which the prediction is to be made. Unfortunately, the results of Sections 4 and 5 indicate that the local site effect is a very important factor which strongly suggests that a category system for classification of sites is needed. It is possible to develop such a system and to estimate what the error is in using it, as compared to getting an "exact" match. This task has been completed in a modified (but applicable) form in Bernreuter et al.

BEST COPY AVAILABLE

(1985). Before we describe the applicable results from Bernreuter et al. (1985), it is useful to note that too few records fit even very simple criteria to make it possible to populate a very elaborate category system of site classification. It is then of some interest to estimate the potential errors that might be introduced by use of too broad a criterion of what constitutes a similar site.

6.2 Potential Errors Introduced by Site Classification Schemes

In this section we want to examine the errors that any practical criteria we might select to say site A is similar to site B might introduce. Small number of strong motions records available that pass the magnitude and distance criteria, coupled with a general lack of knowledge about detailed site conditions at most accelerograph sites, means any useful criteria for site similarity must be very simple.

A first step towards such a criteria was taken in Bernreuter et al. (1985) where eight categories were defined based on soil type, depth and bedrock shear wave velocity.

In order to define site categories, site data for more than 60 nuclear power plants sites throughout the United States were reviewed. Such site data includes geologic profile (layering and depth to rock), soil parameters (soil type, shear wave velocity, compressional wave velocity, density, shear modulus and damping ratio at high strain levels) and bedrock properties (shear wave velocity, compression wave velocity and density). Like most site classification systems, soil depth to the bedrock and soil type are the primary site parameters used to define site categories. Based on their review of the available data from FSARs and PSARs of U.S. nuclear plants sites, they defined the following categories based on the range of the thickness of the soils above bedrock and primary soil type:

Site Class I: Rock Sites. This category includes sites with exposed bedrock including plutonic, igneous, metamorphic, crystalline and sedimentary rock. Sites where the thickness of the soil is less than 25 feet are also assumed to fall in this category and the surface material is neglected as it is generally removed. The mean shear wave velocity from 60 sites is about 6200 fps with a coefficient of variation (COV) of 40%.

Site Class II: Intermediate thickness soil sites. This category includes sites having soil layering thickness ranging from 25 to 300 ft over bedrock. Based on the samples distribution of available sites, we further classify this site class into six subclasses, three till-like (T1,T2, T3) and three sand-like (S1,S2, and S3).

(T1,S1): Soil deposit of 25 to 80 ft over rock. The mean shear wave velocity for each site is calculated by weighted sublayer sites, the mean shear wave velocity is 1500 fps with a COV of 40%. The mean thickness is 48 ft with a COV of 30%. The mean and COV of bedrock shear wave velocity are 6000 fps and 30% respectively.

BEST COPY AVAILABLE

(T2,S2): Soil thickness of 80 to 180 ft over rock. The mean and the COV of sites are 1550 fps and 40% respectively. The mean soil thickness is about 120 ft with a COV of 40% and the shear wave velocity of the bedrock is 6400 pfs with a COV of 40%.

(T3,S3): For soil depth of 180 to 300 ft over rock. Only four sites fell into this category. The mean shear wave velocities of soil and rock are 2000 fps and 9350 fps respectively. The mean soil thickness is 250 ft. No COVs were computed due to insufficient site data available to us at this time.

Site Class III Thick soil sites. This includes those sites having a soil deposit of more than 300 ft over the bedrock. The mean and COVs of the shear wave velocity among a set of 14 sites are 2115 fps and 26% respectively. The median value of soil thickness was found to be 650 ft with a COV of 40%. The mean shear wave velocity of the bedrock is 5700 fps with a COV of 45%.

At these sites, profiles show a great deal of variability in site parameters and a generic site class can only be defined in a loose manner. Since the variation of shear wave velocity with depth for a till-like soil is not significant, a constant mean shear wave velocity was assumed in each site class for the generalized till-like site model for response calculation. However, because the shear modulus for cohesionless soils is more sensitive to the soil depth, it is assumed that the shear modulus varies with the square root of the effective overburden pressure for the sand-like site models.

In order to investigate the significance of such a classification system we attempted to apply it to a typical strong motion data set. For application we chose the Joyner and Boore (1981) data set and attempted to put each entry into its proper category based primarily on soil depth. We found that it was not generally possible to do this. About the best that we could do is determine that:

- 17% fall into the rock category.
- 22% fall into the intermediate depth category. (Site Class II all sub-categories)
- 61% fall into the deep soil category.

Our results in Section 4 suggest that the rock category should be broken up into several sub-categories. However, once again too few records are available at sites with boring logs to do this in any useful way.

The results in Bernreuter et al. (1985) can be used to estimate the errors that we might introduce by having to average over a number of categories. Bernreuter et al. developed an estimate of the relative amplification seen at the top of each category relative to the rock category as is schematically represented in Figs. 6.1 a and b. Basically, a set of 20 time histories recorded at rock sites with various magnitudes and distances were used as input at the rock outcrop as shown in Figs. 6.1 a and b.

AVAILABLE

The site response was calculated by assuming one-dimensional vertically propagating SH waves. Sites were modeled as a system of horizontal layers of infinite extent. A viscoelastic material model for each layer was assumed--shear modulus, density, Poisson's ratio, and material damping. The input was one of 20 rock outcrop time histories. The site response for each of the S1,S2,S3,T1,T2,T3 and deep soil categories was computed using the SHAKE Program. Amplification (or correction factors) were then computed relative to the computed spectrum at the top of the deep soil column.

To account for the range of site parameters in a given category Bernreuter et al. performed repeated deterministic analyses. Each analysis simulates an earthquake occurrence. By performing many such analyses and by varying the values of the input parameters, a mean response and its coefficient of variation can be obtained. Variability in the seismic input is included by sampling from the twenty time histories to obtain a different earthquake time history for each simulation. As illustrated in Fig. 6.1b, variability in the dynamic modeling was introduced for each simulation by sets of input parameters (mainly shear wave velocities of soil and rock, damping ratio of soil and the depth of soil deposit) from assumed probability distributions. A lognormal distribution was assumed for their study.

For each category there is a distribution of amplification factors (AF) - one for each of the 20 time histories. Under the assumption that the distribution of AF generated from the 20 time histories and variation in rock and soil shear wave velocities is lognormally distributed, median correction factors for each category were computed relative to the rock input. Fig. 6.2 shows the median AF for the sand-like categories. The distribution can be approximately modeled with the standard deviation of the natural log of the AF equal to 0.5.

It is important to keep in mind that Fig. 6.2 shows median AF, not median spectra. For any one of the 20 sets of AF used to compute the median, a relatively large value for the AF can occur in some period ranges even if the spectral levels are relatively low compared to the other 20 sets of spectra used in the analysis. Thus, if we computed the ratio between the median spectrum for one of the site categories to the median spectrum at the rock outcrop, we would most likely not obtain the AF curve shown in Fig. 6.2, but one much lower. This is also true for the SSSP categories that are developed in Section 6.3. If the only source of uncertainty is the range of sites used to represent a category, then we would obtain a result similar to the AF shown in Fig. 6.2. Clearly, the results of Section 5 show that the uncertainties due to source variations and travel path variations are also large, hence, the final SSSP most likely would not show such a strong amplification relative to the rock SSSP, at least for a relatively limited data set such as is available. One can speculate that if a very large data set were available then we would obtain a ratio approaching the AF shown in Fig. 6.2.

It is also easy to see from Fig. 6.2 what the effect would be if the criteria were too broad by averaging over two or three categories. Fig. 6.3 shows the difference in AF between the use of a range of sites (in this case, category S-2) and a fixed site. As expected, the AF for the S-2 category are lower than for the fixed site, however, the computed uncertainty for the category

BEST COPY AVAILABLE

case is larger so that the differences between the maximum 84th percentile AF are smaller than between the median AF.

The above results indicate that it is possible to use a relatively broad definition to define what makes two sites similar, i.e., fall into the same category, particularly if 84th percentile spectra are used. The uncertainty added by the use of a range of sites is large, but no larger than the uncertainty added by source and travel path variations. The analytical results presented in Bernreuter et al. (1985) are consistent with the results presented in Section 5 of this report.

6.3 Development of Base Cases

To select the suites of records to be used to develop the SSSP for our base cases we proceeded as follows. As discussed in Section 6.1, based on NRC past practices, we attempted to collect all digitized time histories that were recorded within 25 km of the epicenter within the following magnitude ranges:

MM VII Case
$4.6 \leq M_L \leq 5.8$

MM VIII Case
$5.3 \leq M_L \leq 6.3$

Case 1 represents the case for a SSE level of MMVII and Case 2 represents the case for a SSE level of MMVIII. The lower limit magnitude range is somewhat smaller than the 4.8 limit used in earlier studies. We expanded the range to include smaller magnitude earthquakes for rock and shallow soil sites to increase the number of records available. In addition, as discussed in Section 4, smaller magnitude WUS earthquakes appear to better model ENA earthquakes than larger WUS earthquakes, thus we gain the additional advantages of increasing our sample size and better models of ENA earthquakes. The selected records were then sorted into potential site-type categories based on data available for each accelerograph location. Unfortunately, for many of the accelerograph sites, no data is available and one must rely on judgment and regional geology maps. This is generally not adequate to determine if a site is a rock site or what the depth of the soil is. We defined three site-type categories:

1) Rock Category- Accelerograph sites are considered rock sites if a boring log or good geological evidence exists to indicate that the sites are indeed rock. Sites with highly weathered rock were considered rock sites, e.g., Golden Gate Park station.

2) Deep Soil Sites- Accelerograph sites are considered deep soil if the soil depth is greater than 200 ft deep, generally larger. The 200 ft depth was chosen because it is the depth where many of the boring logs terminated. There simply was not sufficient data to separate the site into stiff or soft site types.

BEST COPY AVAILABLE

3) Shallow Soil Sites- Accelerograph sites are considered shallow sites if depth of soil was known to be 120 ft or less.

Table 6.1 lists the records that fell into the rock-site category, Tables 6.2 and 6.3 list the records that fell into the deep soil site category and Table 6.4 lists the records that fell into the shallow soil site category; however only those records marked as used were, for reasons discussed in the next section, used in the analysis.

Figure 6.4a shows the envelope of all of the spectra of the horizontal components of rock records falling into the MM VII case and the resultant median and 84th percentile spectra. Figure 6.4b shows the envelope, 84th percentile and median spectra for the vertical component of the MM VII rock set. Similarly Figs. 6.5a and b show the MM VIII case for rock; Figs. 6.6a and b show the MM VII case for deep soil; Figs. 6.7a and b show the MM VIII case for deep soil and Figs. 6.8a and b shows the MM VII case for shallow soil. For reasons discussed in the next section, there are not enough records to generate a shallow soil SSSP for the MM VIII case.

In Fig. 6.9 we compare the median SSSP for a deep soil site to that for a weathered rock site for a SSE level of MM VII and in Fig. 6.10 for a SSE level of MM VIII. The major difference between the weathered rock case and the deep soil case is at periods longer than 0.2 seconds the deep soil SSSP is higher than the rock SSSP. Interestingly enough, there does not appear to be a large difference between the deep soil and weathered rock SSSP at short periods. Some care was taken in the selection of the records to insure that the soil records were all obtained on relatively deep (deeper than 200 ft) soil. The rock records have a range of rock types, but mostly soft weathered rock.

In Fig. 6.11, we compare the median SSSP for our shallow soil site to that for the deep soil site for the MM VII case. The shallow soil case shows considerable amplification over the deep soil case at short periods as would be expected from our discussion in Section 6.2.

Figure 6.12, shows that the total uncertainty, σ_T, for the rock and deep soil SSSP plotted in Figs. 6.4a and 6.6a. Because of the large uncertainties in the estimated SSSP, it is of some interest to see if the range of sites used had a significant impact on σ_T. One way to get a handle on this is to develop SSSP using data from only one site. Figure 6.13 shows σ_T for a SSSP suite for the Oroville Airport based on six earthquakes all with $M_L = 4.7 \pm 0.5$ at an average distance of 13 km. The value of σ_T is very similar to that shown in Fig. 6.12 suggesting that the variation in sites used to develop the SSSP shown in Figs. 6.4a and 6.6a has not significantly increased σ_T over the contribution from source and travel path uncertainties.

COPY AVAILABLE

6.4 Sensitivities of the SSSP

The "ideal case" for each of our SSSP is to represent an average distance of 15 km and a m_{bLg}= 5.3 earthquake for the MM VII case and a m_{bLg}= 5.8 earthquake for the MM VIII case. It must be kept in mind that there is potential for considerable error in the estimated distances given in Tables 6.1 - 6.4, however based on the estimates given in Tables 6.1 - 6.4 the average distance for each set is:

Case	Average Distance-km	Average Magnitude
MM VII Rock	8.4	5.2
MM VII Deep Soil	10.9	5.1
MM VII Shallow Soil	9.3	5.1
MM VIII Rock	13.3	5.8
MM VIII Deep Soil	12.5	5.9

Each set has approximately the right average magnitude. However, the average distance of each set is smaller than desired. There are several ways one can attempt to determine if the SSSP are very sensitive to distance. The ideal way would be to add more records in the 15-25 km range; however, none are available. A second approach would be to delete records; however, considering how few records we have this is not an acceptable alternative. A third approach, used in Bernreuter et al. (1984) for the Hope Creek site would be to use a weighted averaging approach. The difficulty with the weighted averaging approach is that the uncertainty may be significantly altered by such an approach if one set of a few records must be very heavily weighted relative to the other records. This is the case for our use here. A final alternative would be to fit a simple regression model to the data and use it to estimate the median and 84th percentile spectral at the desired distance. However, the regression model approach might also have problems if the fact that we have used a range of distances and magnitudes to develop our SSSP is one of the significant contributors to the uncertainty. That is if σ_M or σ_R in Eq. 5.6 are significant, then the estimated median and 84th percentile spectra obtained using a regression model that explicitly accounts for distance and magnitude could be quite different than the median and 84 percentile spectra obtained by direct averaging. Such a comparison would allow us to assess the significance of the uncertainty introduced by the range of distances and magnitudes used.

At each period, p, we fit a model of the form:

$$\text{Ln}(S_V(p)) = C_1(p) + C_2(p)\, M + C_3(p)\, \text{Ln}(D) + E(p) \qquad (6.1)$$

where $C_i(p)$ = constants as a function of the period to be determined by the data

M = magnitude

BEST COPY AVAILABLE

D^2 = $R^2 + H^2$

R = epicentral distance

H = 7.3 km based on Joyner and Boore (1981) paper

S_V (p) = spectral velocity at period p

E (p) = error term

to the spectral ordinates in each category.

Figure 6.14 compares the median and 84th percentile spectra predicted from the fitting of Eq. (6.1) to the data for the rock SSSP for the MM VII case at the average distance (8.4 km) and average magnitude (5.2) for this case to the SSSP (Fig. 6.4a) for this case. It is seen from Fig. 6.14 that the two are in good agreement indicating that σ_M and σ_R are small.

Figure 6.15 shows a comparison of the rock SSSP for the MM VII case to the SSSP predicted using the regression model at distance of 15 km with the same average magnitude of 5.2. There is little change indicating a relatively weak sensitivity to distribution of distance used. Figures 6.16 and 6.17a show similar comparisons for the MM VII case for deep soil sites. It is observed from Fig. 6.16 that explicitly accounting for distance and magnitude reduces the uncertainty in the prediction based on a regression model as compared to the SSSP approach. Thus, there are considerable differences between the spectrum predicted by our fit to the data at 15 km and the SSSP (Fig. 6.17a). Examination of the fit of Eq. (6.1) to the data indicated that the predictive model was not very reliable, e.g., at the short period end the coefficents C_2 were negative and there was a very large scatter for the residuals at both the short and large distances. Given the very limited data set and the large uncertainties it is not surprising that the fitted model is suspect.

We also employed a weighted averaging approach. To develop the weights we assumed that typically the SSSP should model the case where earthquakes are assumed to occur randomly around a site. If the area is modeled by a series of rings, in our case four rings, then the number of earthquakes in each ring should be proportional to the area of each ring. Thus, the weights can be easily computed based on the number of records in each ring relative to the desired number of records for each ring. For the case at hand the records in Table 6.2 were sorted into four rings:

Ring No.	Distance Range	No. of Earthquakes	Weight for Ring
1	$0 \leq R \leq 5$	3	0.1
2	$5 \leq R \leq 10$	10	0.1
3	$10 < R \leq 15$	7	0.23
4	$15 < R \leq 20$	4*	0.57

BEST COPY AVAILABLE

* The record labeled CM75 in Table 6.2 was included in Ring 4.

With the given weights, the average distance works out to be 15 km and the average magnitude 5.25. Figure 6.17b shows a comparison of the SSSP for deep soil sites for the MM VII set to the median and 84th percentile spectra obtained from the weighted averaging approach. There is little difference between the two sets of spectra suggesting that the average distance is not an important parameter given all of the uncertainties and the rather narrow distance range of interest.

In Section 4 we concluded that the smaller earthquakes appear to have more short period content than large earthquakes. In Fig. 6.18 we compare the median spectrum for a rock site obtained by using the eight records with magnitudes 5.1 or less to median spectrum based on the seven records with magnitudes between 5.3 and 5.7. We see from Fig. 6.18 that the median spectrum of the set of records with magnitudes 5.1 or less have more short period energy and less long period energy than the median spectrum of the set of records with magnitudes between 5.3 and 5.7. In Fig. 6.19 we compare the median SSSP for rock sites for the MM VII case to the MM VIII case and in Fig. 6.20 we make the same comparison for deep soil SSSP.

We see from Figs. 6.19 and 6.20 that the larger magnitude sets have more long period energy than the smaller magnitude sets. For the rock sets, the smaller magnitude set has more short period energy. This does not appear to hold true for the deep soil sets. However, given the uncertainties and the relatively few earthquakes included in the analysis, it is not possible to reach any generic conclusions.

In Section 6.2 we noted the criteria to say that site A is similar to site B for the case of shallow soil sites should not be too broad. Initially in selecting records to form shallow soil sets we selected all records obtained at sites with less than 150 ft of soil over bedrock. A number of records had to be rejected because no boring logs were available to define the depth to bedrock. Table 6.4 lists the records that more closely met the criteria and Table 6.7 gives the depth of soil. Because of the importance of depth we only used the stations that we were reasonably sure had shallow soil of less than 80 ft. A number of stations were rejected because we could not reasonably infer that they fit our criteria. Figure 6.21 illustrates the importance of not using too broad of a criteria for shallower soil sites. In Fig. 6.21 we compare the median and 84th percentile spectra obtained by using all of the records listed in Table 6.4 with magnitudes less than 5.8 to the median and 84th percentile spectra for the more restricted data set used to generate the SSSP for shallow soils. As expected, based on the discussion in Section 6.2, averaging over a broader range of sites reduces the amplification effect of shallow soils. Other parameters, such as the shear wave velocity contrasts between bedrock and soil and between the layers of soil are as important as depth of soil. However, it is not possible with the limited data set available to investigate these factors.

The above discussion relative to soil depth also suggests that we should examine the set of sites used to generate the rock SSSP. The problem is that

BEST COPY AVAILABLE

almost all of the stations are on weathered rock and for many of these no boring log/shear wave velocity log exist. Thus, it is not possible to subdivide the rock set and still have a sufficient number of records to perform a meaningful analysis. About the best we can hope for is that we have two compensating errors. First, the highly weathered surface layers tend to amplify the short periods as was illustrated in Fig. 4.10. However, typically such weathered surface layers are underlain by deeper softer rocks (i.e., rock with lower shear wave velocity and lower Q) than less weathered sites. As illustrated in Fig. 4.13, the lower shear wave velocity/Q damps out the short period energy, thus there is less short period energy to amplify in the top layers. The hope is that the two factors will compensate for each other.

We noted earlier that the vertical SSSP have the problem that most of the records used to generate them were not obtained on modern data systems with a memory so that some of the initial P-wave train was lost, and in few cases even some of the S-wave train. Thus, it is not possible to determine how "good" the vertical SSSP are. In assessing the vertical SSSP is worthwhile to note that if the maximum vertical motion occurs in the initial P-wave train it is missed because the horizontal motion is generally small. In the stress analysis of the structure the stresses obtained using the vertical spectra are generally included with the maximum stresses obtained using the horizontal spectra. Thus, the vertical SSSP generated above may be more appropriate to use in the analysis than SSSP which may be higher due to the inclusion of the earlier part of the P-wave train.

BEST COPY AVAILABLE

TABLE 6.1
Rock Records Used

Earthquake	Date/Time (1)	Station	Distance(km) (2)	Magnitude
Oroville	8/8/75/0700	Station 6	6	4.9
Oroville	9/27/75	Station 8	11	4.6 (3)
Oroville	8/1/73	Seismograph Sta.	15	5.7
Oroville	9/27/75	DWR	3	4.6
Parkfield	6/27/66	Temblor	5	5.5 (4)
Friuli	9/11/76/1631	S.Rocco	16	5.5
C. Mendocino	6/7/75	Cape Mendocino	20	5.3
Helena	10/3/35	Carroll College	7	5.7 (5)
Helena	11/28/35	Federal Bldg.	5	5.0 (5)
Ancona	6/14/72	Rocco	6	4.7 (3)
Coalinga	5/9/73	Skunk Hollow	4	5.1
Coalinga	5/9/83	Anticline Ridge	2	5.1
Coalinga	7/22/83	Skunk Hollow	12	6.0
New Brunswick	3/31/82	Mitch. Lake Rd.	4	4.8
Westmoreland	4/26/81	Superstition Mt.	13	5.7
Daley City	3/22/57	Golden Gate Pk.	8	5.3
Friuli	5/6/76	Tolmezzo	25	6.2
Friuli	9/11/76:1635	S.Rocco	16	5.9
Friuli	9/15/76:315	S.Rocco	10	6.1
Friuli	9/15/76:921	S.Rocco	20	6.0
Coyote Lake	8/6/79	Gilroy 6	9	5.9
Coyote Lake	8/6/79	Gilroy 1	4	5.9
Morgan Hill	4/24/84	Gilroy 6	14	6.1
Morgan Hill	4/24/84	Gilroy 1	18	6.1

(1) Time is given only if required to identify earthquake.

(2) Distance is usually closest surface approach or epicentral

(3) Somewhat lower than range desired but used because so few rock records are available.

(4) In recent years values of M_L larger than the 5.5 have been assigned to the Parkfield earthquake. Nuttli et al. (1979) examined the seismograms of this earthquake and calculated its m_b as 4.9. Correcting for the difference between an earthquake which occurred in the CUS and one in the WUS, Chung and Bernreuter (1980), would make it equivalent to a m_b of 5.2. It is our opinion that this record should be included because the m_b value of 5.2 for the Parkfield earthquake was computed by the same group which has done much to establish the magnitudes of EUS earthquakes.

(5) Kanamori and Jennings, BSSA (68), 1978.

BEST COPY AVAILABLE

TABLE 6.2

Records Selected for Deep Soil Case for the Ensemble of Earthquakes Centered at m_{bLg} = 5.25

EQ-ID (1)	Station ID (2)	Distance km	Magnitude
H60	HCH	6	5.0
075-1	OAP	15	5.1
075-2	OAP	15	5.2
075-4	OAP	11	4.9
H61	HCH	20	5.7
H61a	HCH	20	5.6
F76-3	B	7	5.0
M72-2	ER	5-10	5.1
H74	HCH	11	5.2
CM75	FCH	10-20	5.3
C83a	PVP	10	5.1
C83a	BC	13	5.1
IV79a	EL6	9	5.0
IV79a	ELDIFF	9	5.0
IV79a	EL5	10	5.0
IV79a	EL8	10	5.0
IV79a	EL4	11	5.0
IV79a	EL2	18	5.0
ML80-2	CC	3	5.6
ML80-3	CC	9	5.3
SB78	SBCH	10	5.6
MV-1	V	5	4.8
MV-1	D	12	4.8
MV-2	V	5	4.8

Notes:

(1) See Table 6.5
(2) See Table 6.6

COPY AVAILABLE

TABLE 6.3

Records Selected for the Deep Soil Case for the Ensemble of Earthquakes Centered at m_{bLg} = 5.75

EQ-ID (1)	Station ID (2)	Distance km	Magnitude
SB41	SBCH	10-36	5.9
H61	HCH	20	5.7
H61a	HCH	20	5.6
F76-1	B	14	5.9
F76-2	B	6	6.1
F76-4	B	19	6.0
M72-1	ER	5-11	5.6
CL79	GA2	8	5.9
CL79	GA3	6	5.9
CL79	GA4	5	5.9
ML80-1	CC	9	6.0
ML80-2	CC	3	5.6
ML80-4	CC	12	6.3
W81	PTF	8	5.7
W81	SS	20	5.7
W81	BAP	18	5.7
C83b	PVP	11	6.0
C83b	BC	12	6.0
MH84	GA2	17	6.1
MH84	GA3	16	6.1
MH84	GA4	15	6.1

BEST COPY AVAILABLE

TABLE 6.4

Records Selected for Shallow Soil Cases

EQ-ID[1]	Station ID [2]	Distance (km)	Magnitude	Used
075-3	DJR	10	4.7	Y
075-4	DJR	10	4.9	Y
075-4	S7	10	4.9	Y
075-5	DJR	12	4.6	Y
NH82	FFD	7	4.7	Y
NB82	HL	6	4.8	Y
S72	BVFS	10	4.9	N
S72	MR	8	4.9	Y
S72	SC	5	4.9	N
CM75	GS	11	5.3	N
P66	S12	15	5.5	N
F76-5	FC	10	5.3	N
F76-6	FC	16	5.5	N
F76-1	FC	15	5.9	N
F76-2	FC	10	6.1	N
F76-4	FC	20	6.0	N
F76-6	Tar	9	5.5	Y
F76-4	Tar	20	6.0	Y
SB78	GOL	8	5.6	Y
H74	GGC	11	5.2	Y
MH84	GGC	18	6.1	N

Notes:
(1) See Table 6.5
(2) See Table 6.7
N = Not used to generate the shallow soil SSSP shown in Fig. 6.8
Y = Used to generate the shallow soil SSSP shown in Fig. 6.8

COPY AVAILABLE

TABLE 6.5

Data for the Earthquakes Identified in Tables 6.2, 6.3 and 6.4

Earthquake ID	Magnitude M_L Unless Noted	Location	Date & Time if Needed for ID
LB33	6.3	Long Beach CA	3/10/33
SB41	5.9	Santa Barbara, CA	6/30/41
LA41	5.4	Los Angeles, CA	11/14/41
IV51	5.6	Imperial Valley, CA	1/23/51
NC54	6.5 M_S	Northern California	12/21/54
SJ55	5.5-5.8	San Jose, CA	9/4/55
SF57	5.3	San Francisco, CA	3/22/57
H60	5.0	Central California	1/19/60
H61	5.7	Central California	4/8/61
H61a	5.6	Central California	4/8/61 (After Shock)
P66	5.5*	Parkfield, CA	6/27/66
NC67	5.8	Northern California	12/10/67
LC70	5.4	Lytle Creek, CA	9/12/70
SF71	6.4	San Fernando, CA	2/9/71
S72	4.9	Salinas, CA	9/4/72
M72-1	5.6 m_b 6.2 M_S	Managus, Nicaragua	12/23/72 - 0629
M72-2	5.1 m_b	Managua, Nicaragua	12/23/72 - 0720
H74	5.2	Central California	11/28/74
O75-1	5.1	Oroville, CA	8/2/75 - 2022
O75-2	5.2	Oroville, CA	8/2/75 - 2059
O75-3	4.7	Oroville, CA	8/6/75 - 350
O75-4	4.9	Oroville, CA	8/8/75 - 0700
O75-5	4.6	Oroville, CA	9/27/75
CM75	5.3	Cape Mendocino, CA	6/7/75
F76-1	5.9	Friuli, Italy	9/11/76 - 1635
F76-2	6.1	Friuli, Italy	9/15/76 - 0315
F76-3	5.0	Friuli, Italy	9/15/76 - 0438

BEST COPY AVAILABLE

TABLE 6.5 (Cont.)

Earthquake ID	Magnitude M_L Unless Noted	Location	Date & Time if Needed for ID
F76-4	6.0	Friuli, Italy	9/15/76 - 0921
F76-5	5.3	Friuli, Italy	5/11/76
F76-6	5.3	Friuli, Italy	9/11/76 - 1631
SB78	5.6	Santa Barbara, CA	8/13/78
MV-1	4.8	Mexicali Valley, Baja	3/11/78
MV-2	4.8	Mexicali Valley, Baja	3/12/78
CL79	5.9	Coyote Lake, CA	8/6/79
IV79a	5.0	Imperial Valley, CA	10/15/79 (After Shock)
ML80-1	6.0	Mammoth Lake, CA	5/25/80 - 0949
ML80-2	5.5 Pas 5.7 Bk	Mammoth Lake, CA	5/25/80 - 1336
ML80-3	4.9 Pas 5.7 Bk	Mammoth Lake, CA	5/26/80 - 1158
ML80-4	6.3 Pas 6.2 Bk	Mammoth Lake, CA	5/27/80 -0751
W81	5.7	Westmoreland, CA	4/26/81
NH82	4.7	Gaza, N.H.	1/19/82
NB82	4.8	New Brunswick	3/31/82
C83a	5.1	Coalinga, CA	5/9/83 (After Shock)
C83b	6.0	Coalinga, CA	7/22/83
MH84	6.1	Morgan Hll, CA	4/24/84

* See Footnote (4) Table 6.1

BEST COPY AVAILABLE

TABLE 6.6

Deep Soil Stations

Site Information for Sites Identified in Tables 6.2 and 6.3

Station ID	Station Name & Location	Station Geology/Basis
B	Buia, Italy	Inferred from regional geology
BAP	Brawley Airport, Brawley, CA	Inferred from regional geology
BC	Burnett Construction Co., Coalinga, CA	Inferred based regional geology
CC	Convict Creek, Mammoth Lakes	Alluvium > 200 meters
D	Delta- part of the Mexicali Valley, Baja, CA array	Deep soil inferred from geology of region
EL 2,4,5, 6,8, Diff. Array	Imperial Valley, CA	Deep soil based
EFB	Eureka Federal Building Eureka, CA	>350 ft quaternay sediments boring Log
ER	ESSO Refinery, Nicaragua	Inferred
FCH	Ferndale City Hall	Deeper than 260 ft based on boring log
GA2	Gilroy Array No.2- Mission Trails Motel	Deeper than 200 ft based on boring log and the geology of area
GA3	Gilroy Array No.3 - Sewage Treatment Plant	Deeper than 200 ft based on boring log
GA4	Gilroy Array No. 4 San Ysidro School	Deeper than 200 ft based on boring log and the geology of the area
HCH	Hollister City Hall	Boring log shows soil at least 350 ft deep
HSPL	Hollywood Storage Building Parking Lot	Boring log shows deep soil
LH #1	Lake Huges Array #1	Deep soil base on boring log
OAP	Oroville, CA Airport	Inferred from regional geology
PFS	Palmdale Fire Station	Inferred from boring log showing at least 30M of soil and regional geology

BEST COPY AVAILABLE

TABLE 6.6 (Cont.)

Station ID	Station Name & Location	Station Geology/Basis
PTF	Parachute Test Facility Imperial Valley, CA	Deep soil based on regional geology
PVP	Pleasant Valley Pumping Plant Pleasant Valley, CA	Inferred from regional geology and location of station. Free-field station had some possible topography affect.
SBCH	County Court House Santa Barbara, CA	Boring log shows soil at least 400 ft deep
SS	Salton Sea, Wildlife Refuge Imperial Valley, CA	Based on regional geology
V	Victoria, part of the Mexicali Valley, Baja California	Deep soil inferred from geology of the region

BEST COPY AVAILABLE

TABLE 6.7

Site Information for Shallow Soil Sites

Station ID	Station Name and Location	Station Geology
S7	Station 7, Oroville, CA	Inferred shallow soil
DJR	Johnson Ranch, Oroville, CA	Inferred shallow soil
S12	Cholame, Shandon No.12	100' alluvium over Pasco Rables formation
FC	Forgaria-Cornino, Italy	120 ft of alluvium over sandstone
Tar	Tarcento, Italy	Estimate 33' of alluvium over sandstone
BVFS	Bear Valley Fire Station	Inferred shallow soil
MR	Melendy Ranch	20 ft alluvium over siltstone
SC	Stone Canyon	Inferred shallow soil
GGC	Gilroy, Gavilen College Physical Science Bldg.	40 ft of alluvium over sandstone
GS	General Store, Petrolia, CA	120 ft of alluvium over siltstone
GOL	Goleta, UCSB	14 ft of alluvium over soft siltstone
FFD	Franklin Falls Dam, N.H. Down stream	100 ft of alluvium over bedrock
HL	Holmes Lake	10 to 16 ft of fill over bedrock

BEST COPY AVAILABLE

BEST COPY AVAILABLE

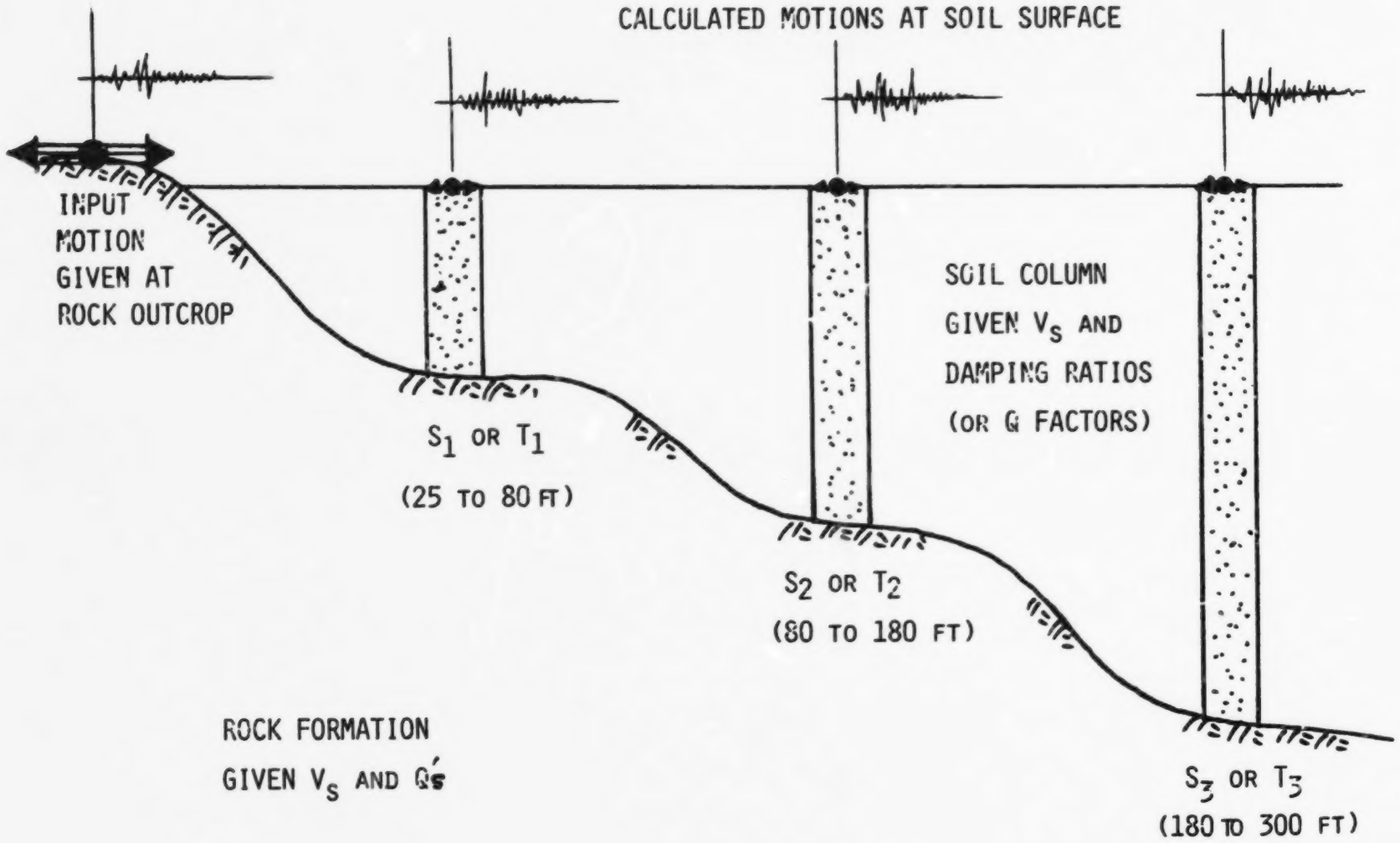
CALCULATED MOTIONS AT SOIL SURFACE
INPUT MOTION GIVEN AT ROCK OUTCROP
SOIL COLUMN GIVEN V_S AND DAMPING RATIOS (OR G FACTORS)
S_1 OR T_1
(25 TO 80 FT)
S_2 OR T_2
(80 TO 180 FT)
S_3 OR T_3
(180 TO 300 FT)
ROCK FORMATION
GIVEN V_S AND Q's

Fig. 6.1a Schematic representation of the overall computation scheme used by Bernreuter et al. (1985).

89

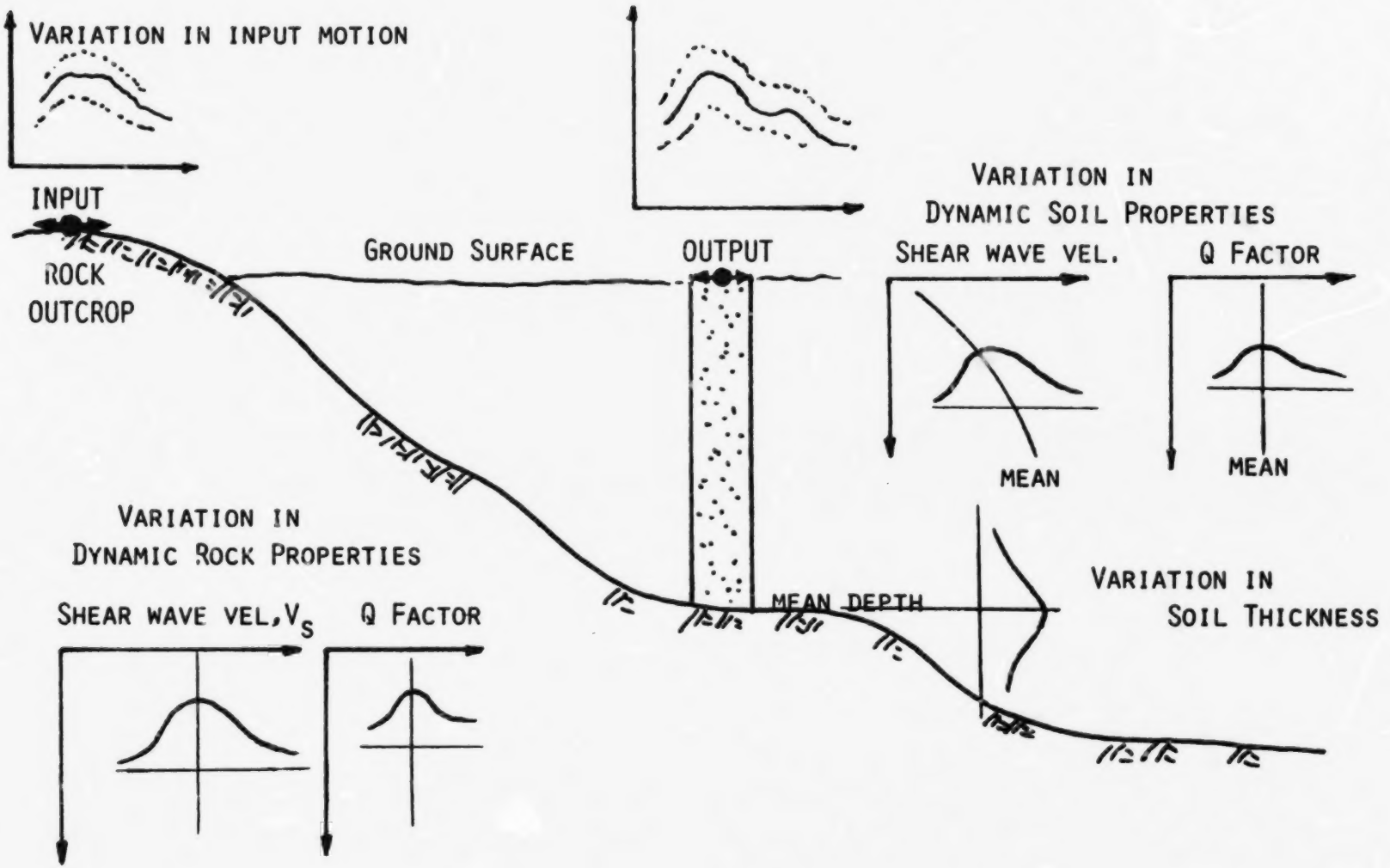

Fig. 6.1b Schematic representaton of the overall simulation approach used in Bernreuter et al. (1985) to model the range of sites within a given category.

- 90 -
BEST COPY AVAILABLE

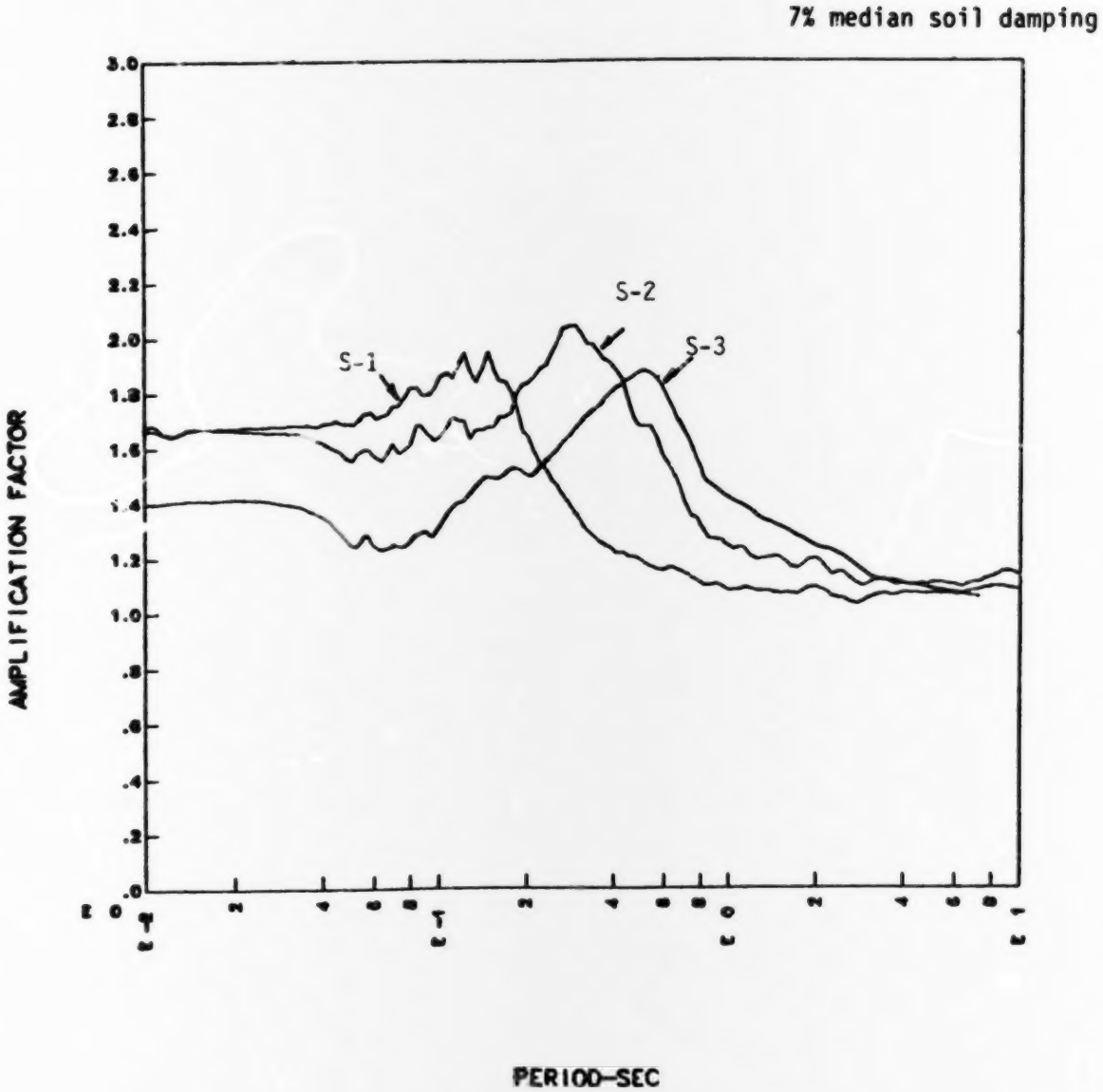

Fig. 6.2 The median amplification factors for the sand-like site categories S-1,S-2 and S-3 defined in Bernreuter et al. (1985).

BEST COPY AVAILABLE

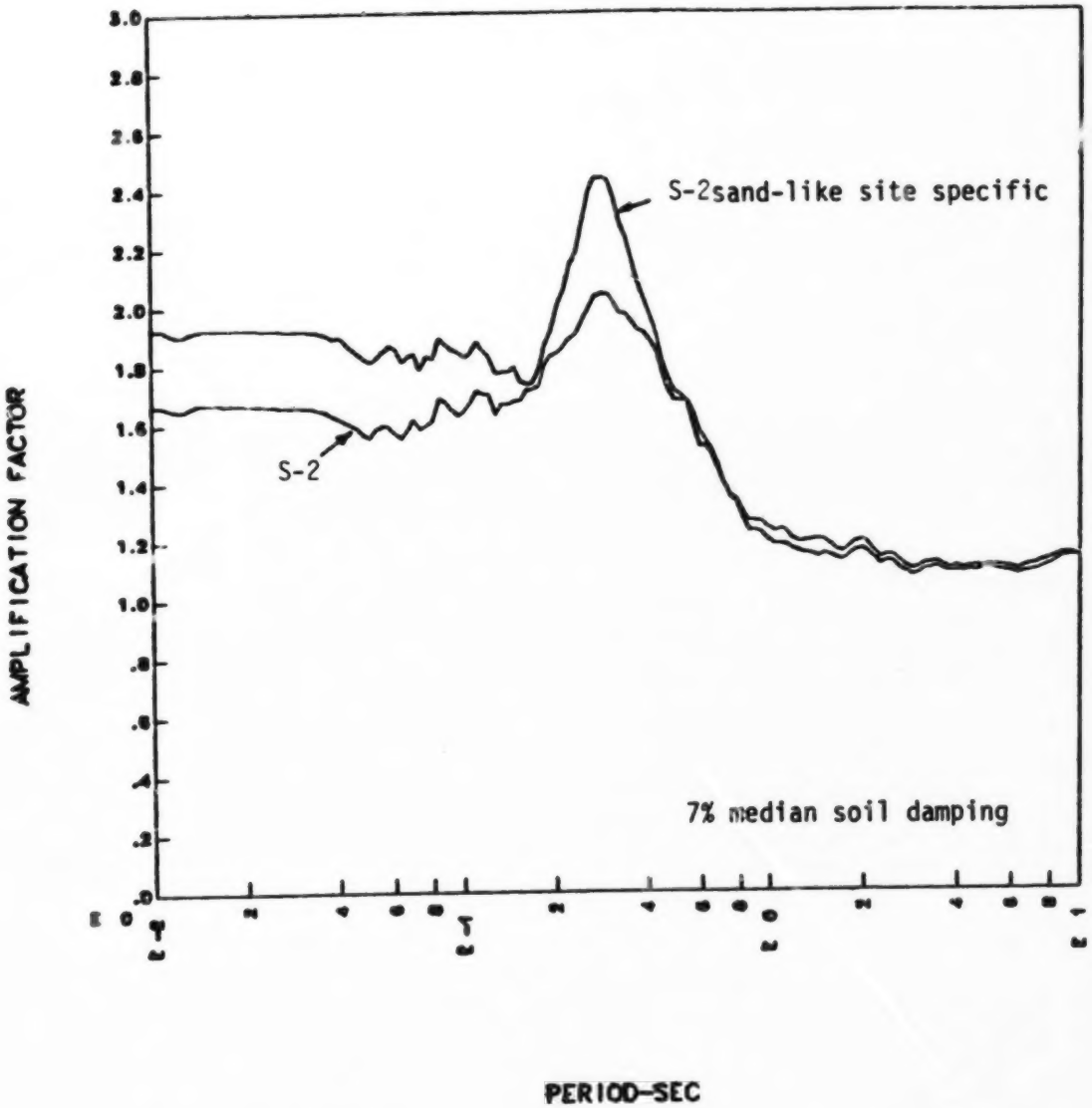

Fig. 6.3 A comparison of the median amplification factor for a fixed site falling into category S-2 and the median amplification factor based on the range of sites in category S-2.

BEST COPY AVAILABLE

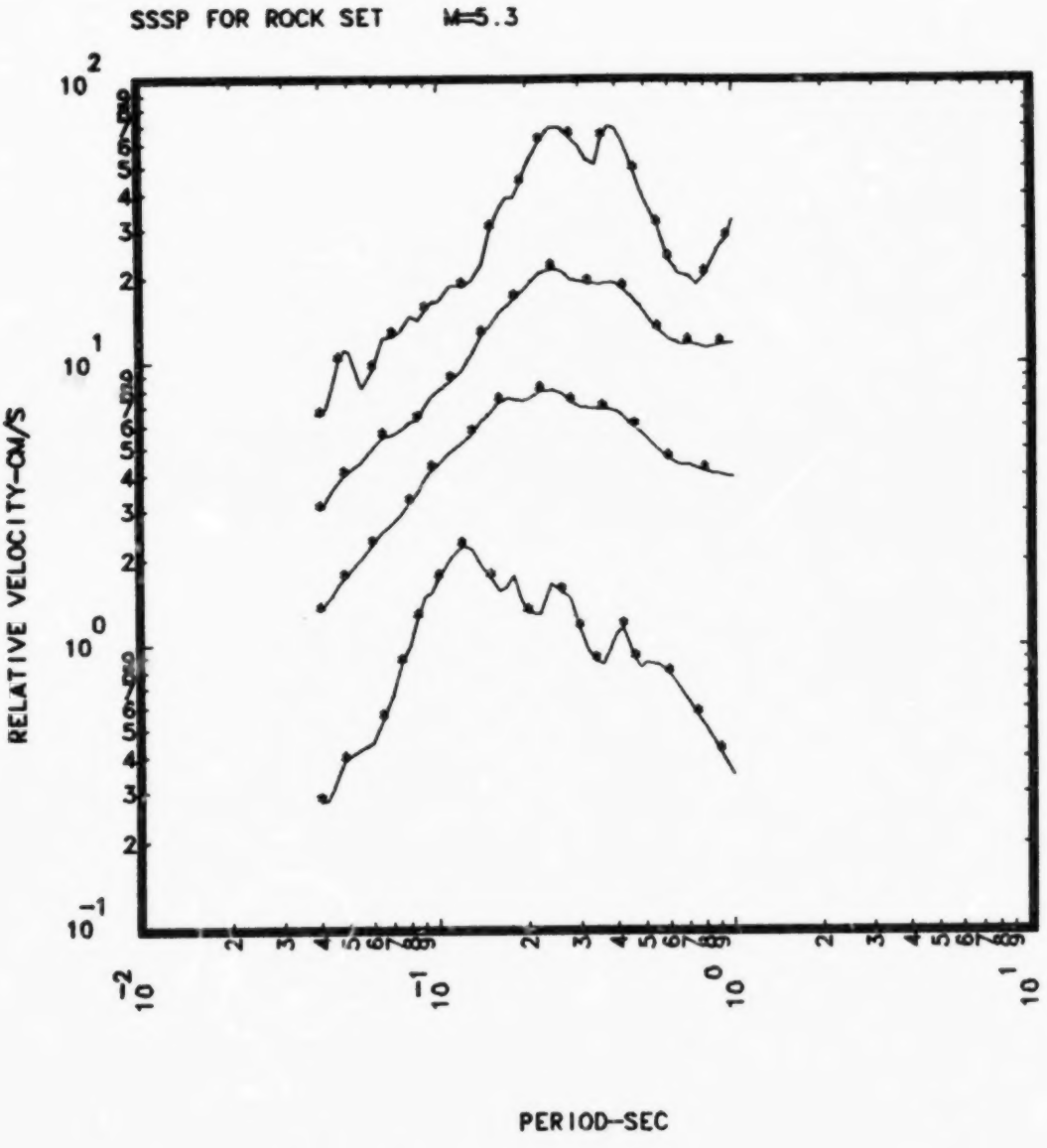

Fig. 6.4a Envelope, 84th percentile and median spectra of the set of records falling into the MM VII case for rock sites- horizontal components.

BEST COPY AVAILABLE

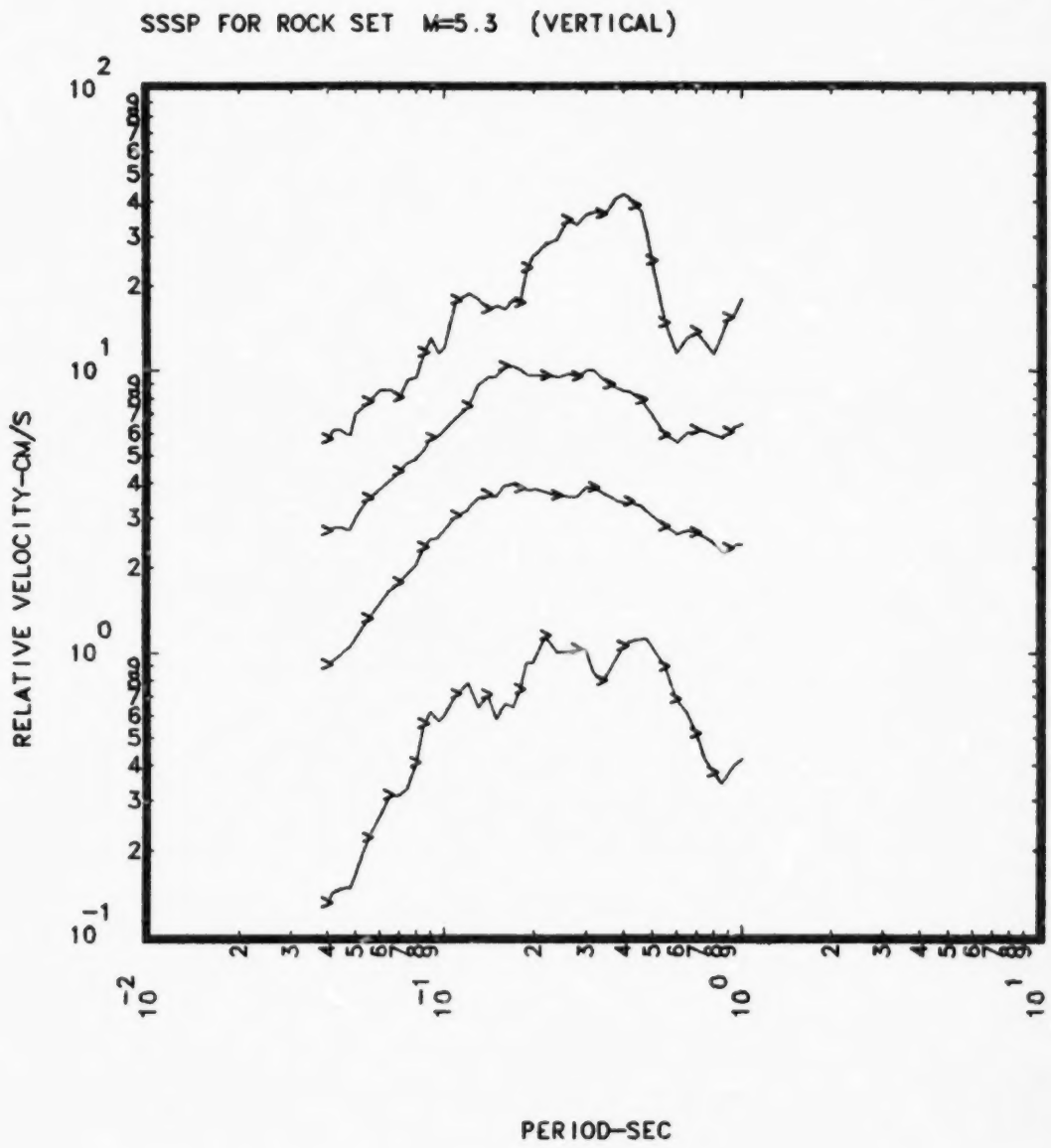

Fig. 6.4b Envelope, 84th percentile and median spectra of the set of records falling into the MM VII case for rock sites- vertical components.

BEST COPY AVAILABLE

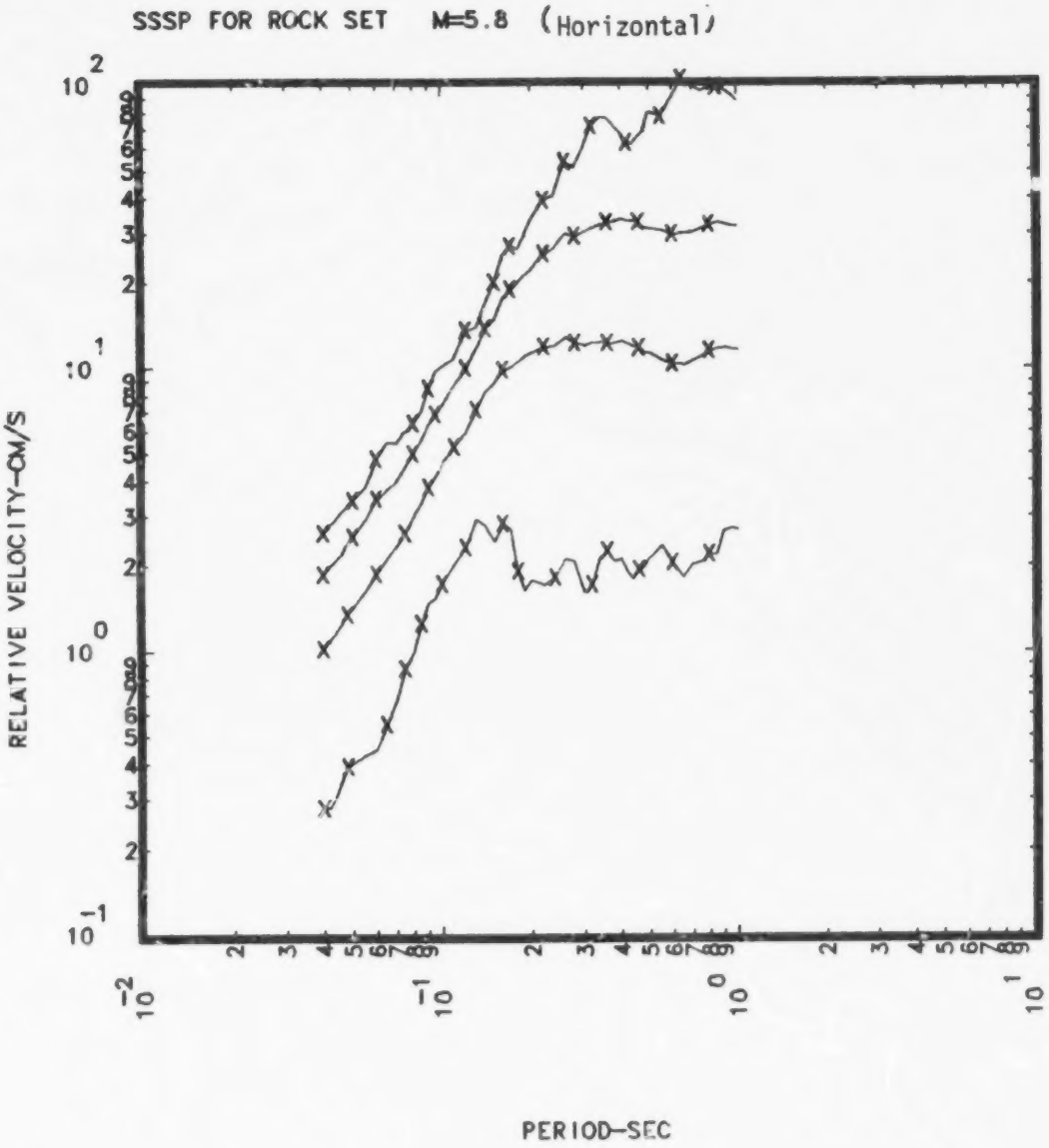

Fig. 6.5a Envelope, 84th percentile and median spectra of the set of records falling into the MM VIII case for rock sites- horizontal component.

BEST COPY AVAILABLE

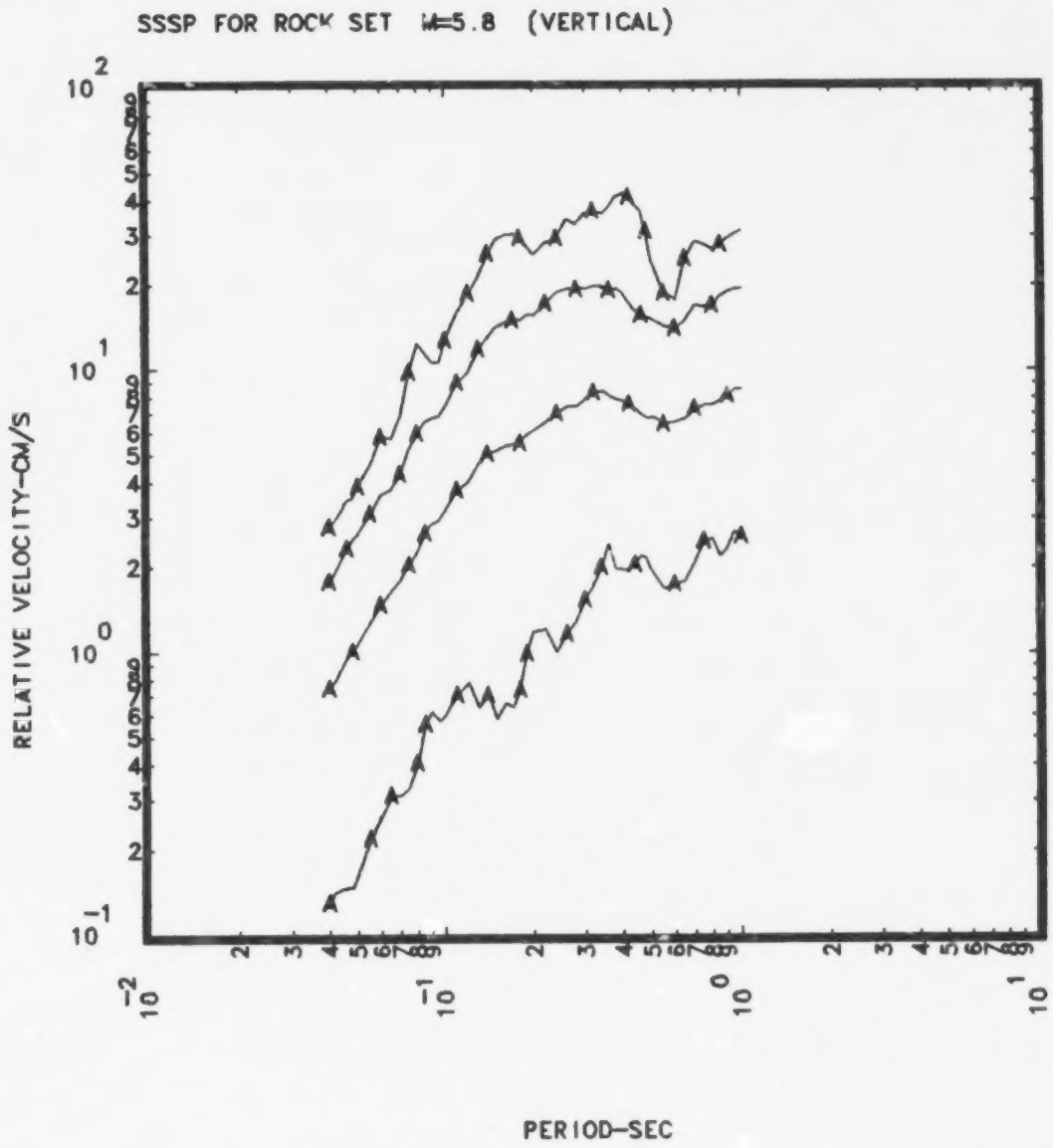

Fig. 6.5b Envelope, 84th percentile and median spectra of the set of records falling into the MM VIII case for rock sites- vertical components.

BEST COPY AVAILABLE

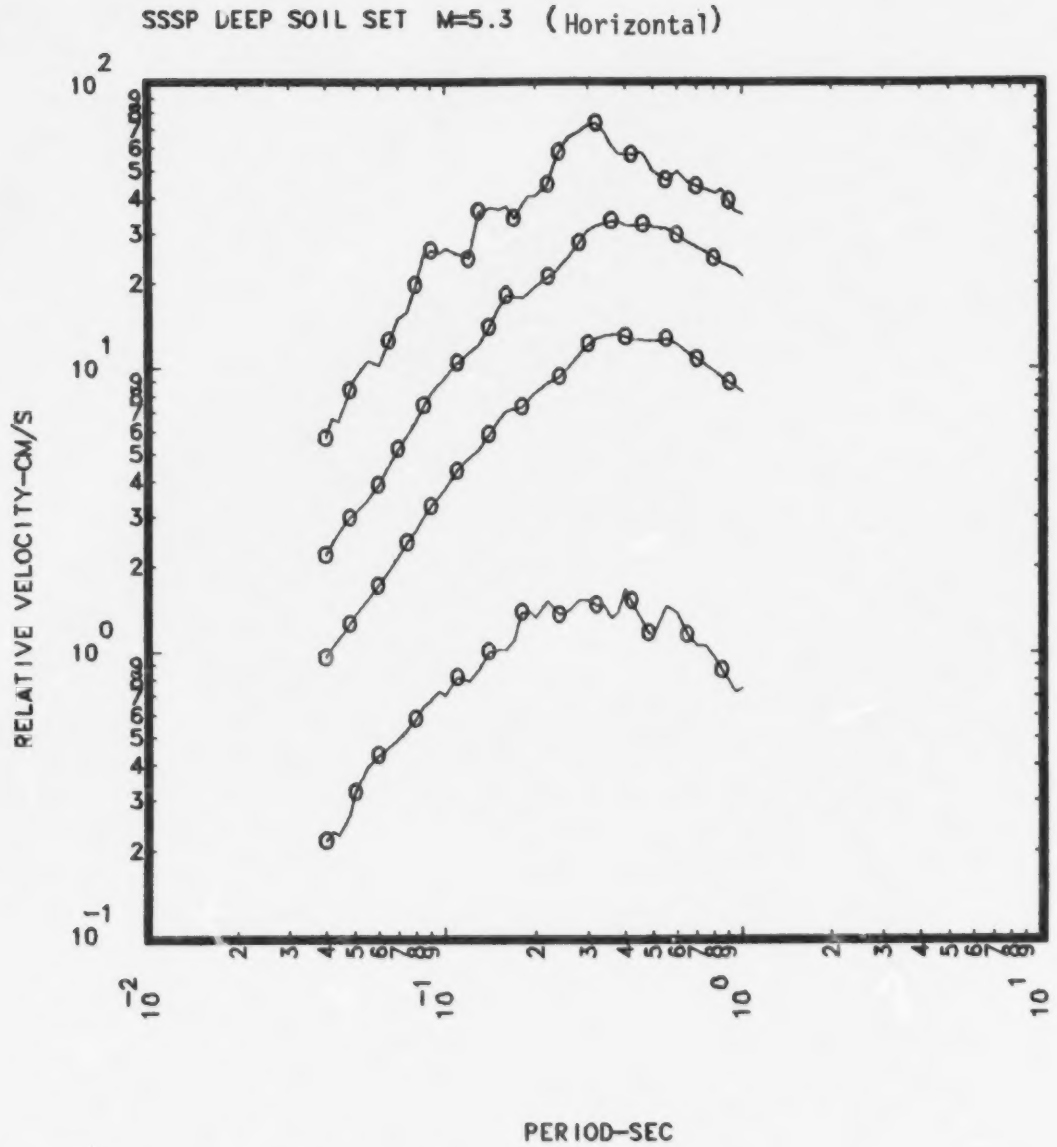

Fig. 6.6a Envelope, 84th percentile and median spectra of the set of records falling into the MM VII case for deep soil sites- horizontal components.

BEST COPY AVAILABLE

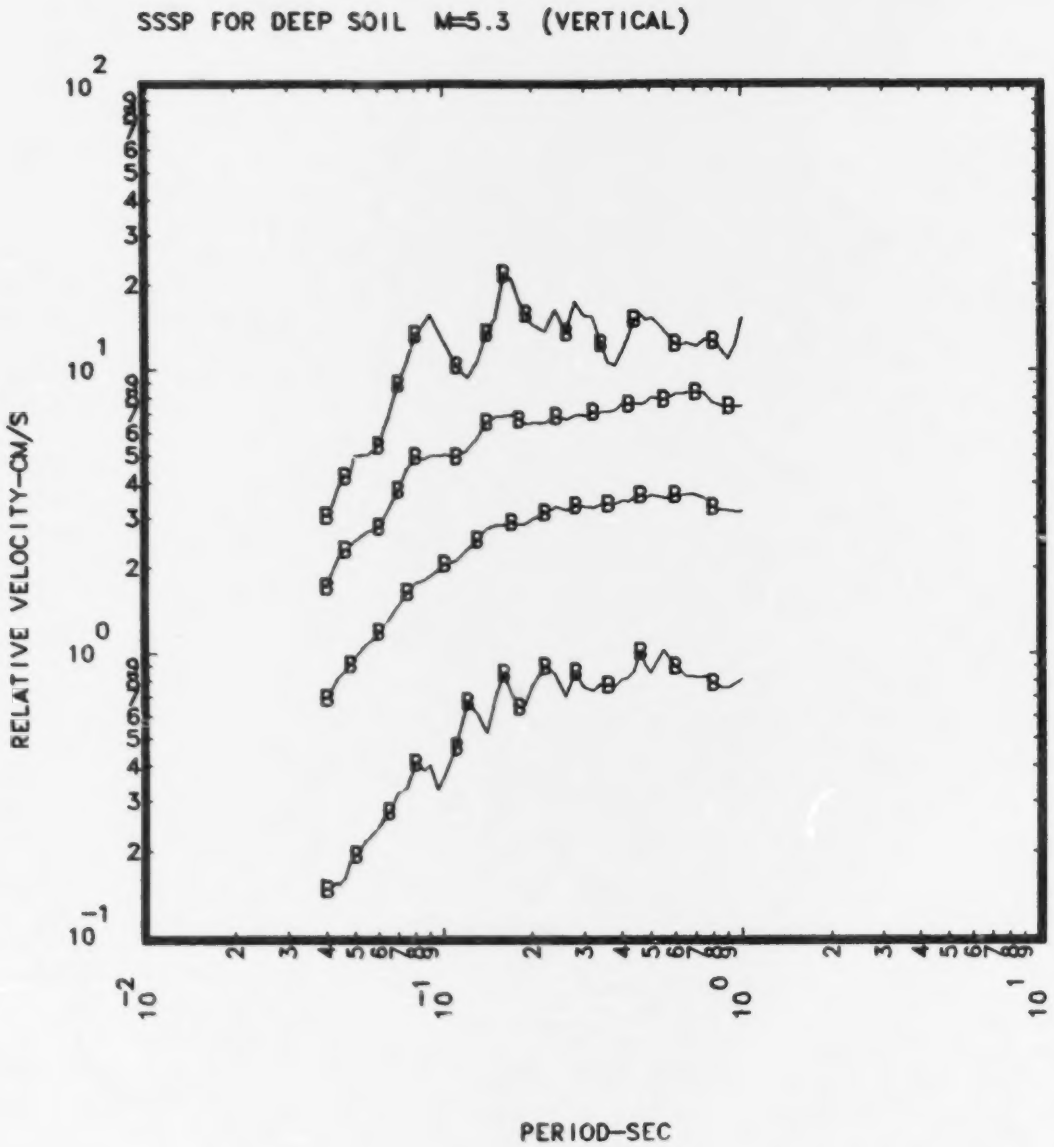

Fig. 6.6b Envelope, 84th percentile and median spectra of the set of records falling into the MM VII case for deep soil sites- vertical components.

BEST COPY AVAILABLE

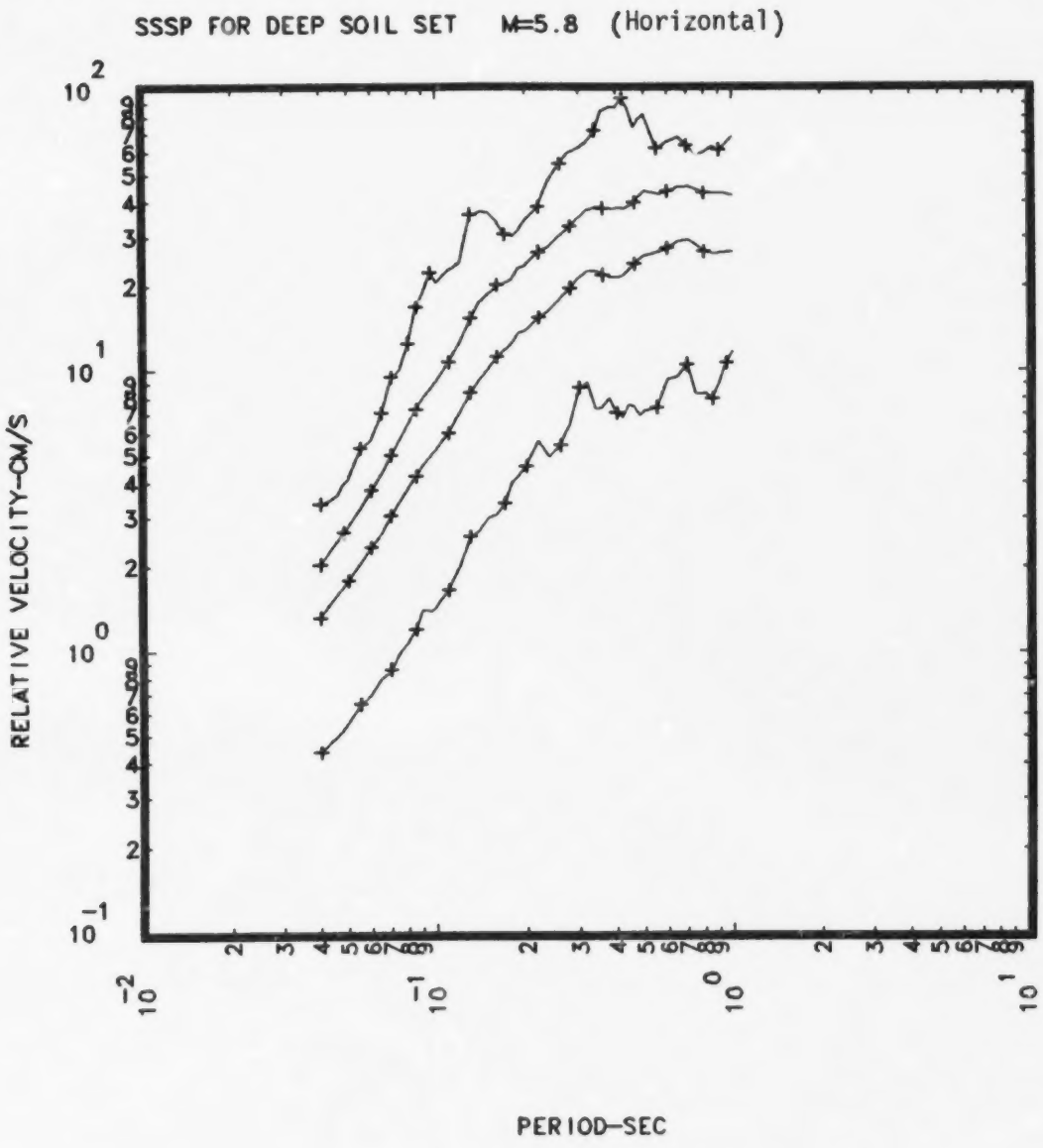

Fig. 6.7a Envelope, 84th percentile and median spectra of the set of records falling into the MM VIII case for deep soil sites- horizontal components.

BEST COPY AVAILABLE

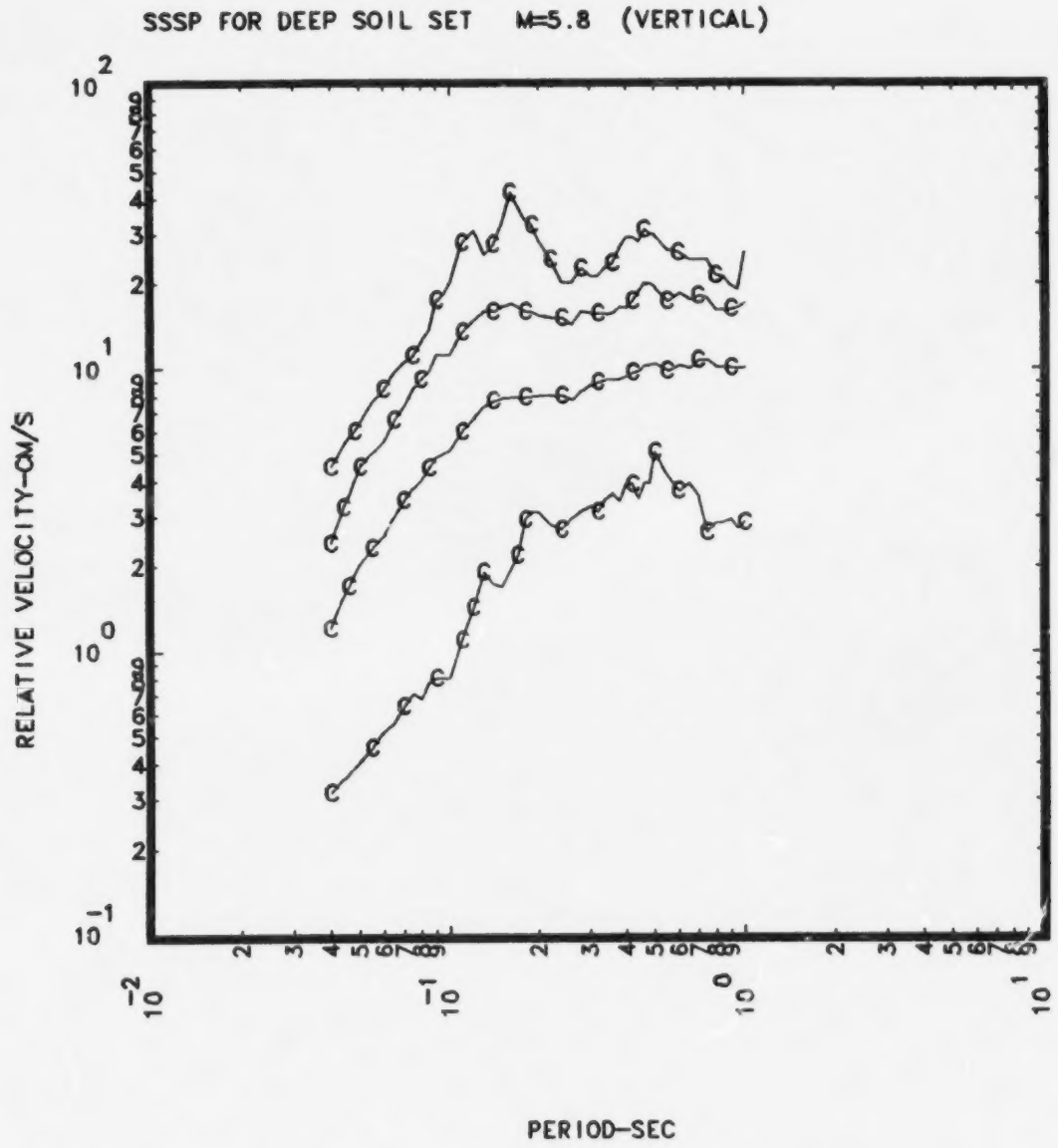

Fig. 6.7b Envelope, 84th percentile and median spectra of the set of records falling into the MM VIII case for deep soil sites- vertical components.

BEST COPY AVAILABLE

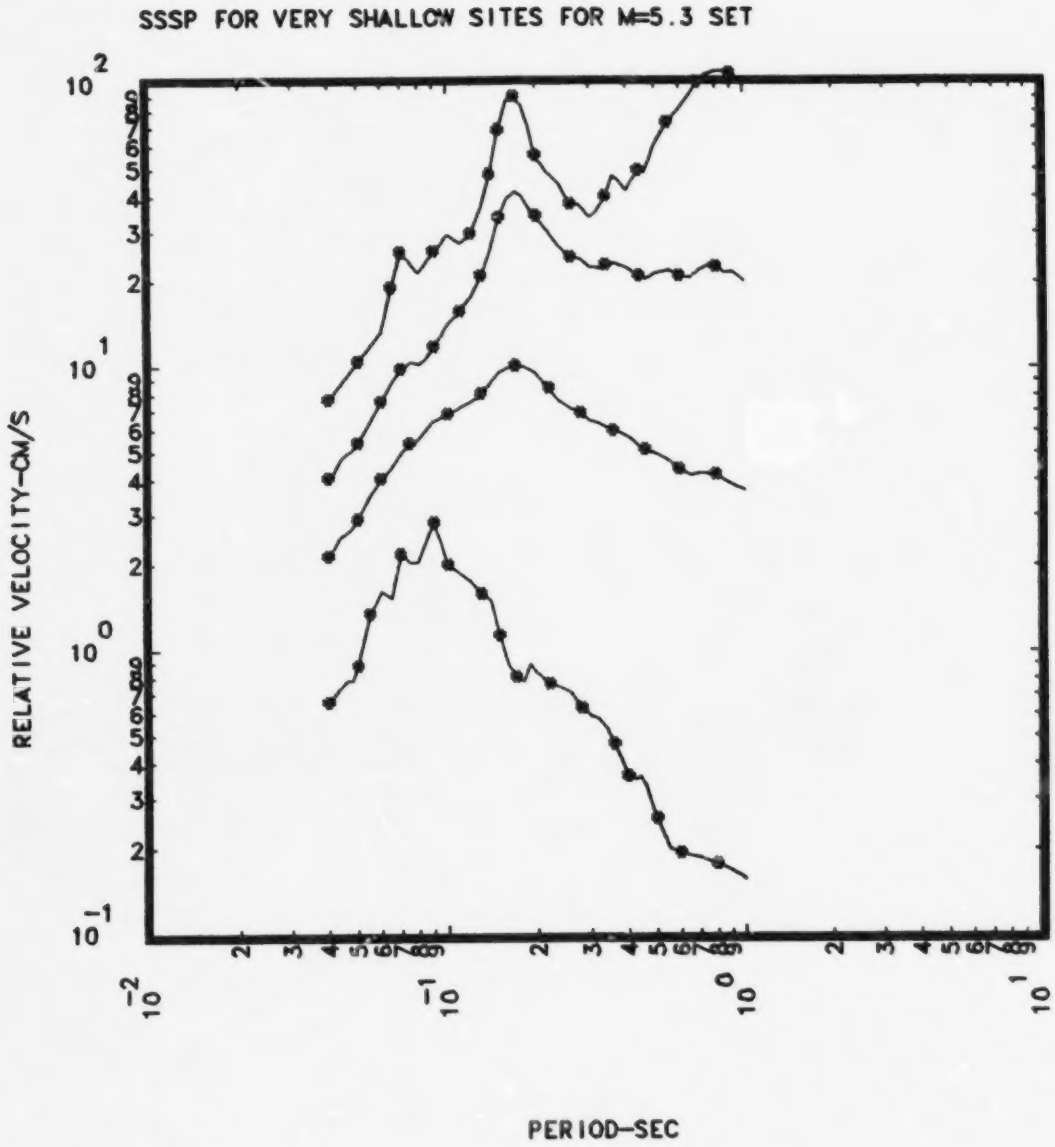

Fig. 6.8a Envelope, 84th percentile and median spectra of the set of records falling into the MM VII case for <u>shallow soil</u> sites- horizontal components.

BEST COPY AVAILABLE

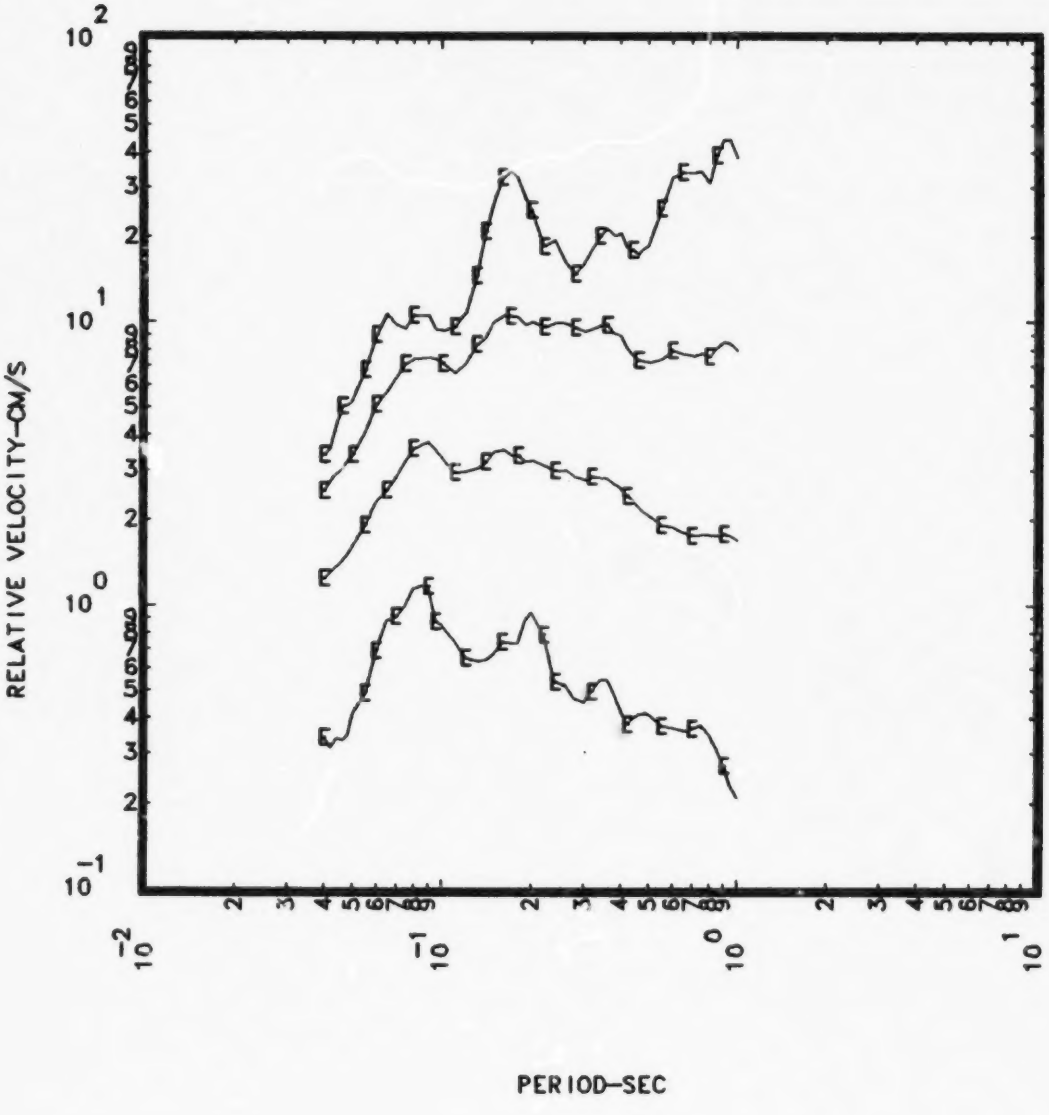

Fig. 6.8b Envelope, 84th percentile and median spectra of the set of records falling into the MM VII case for shallow soil sites- vertical components.

BEST COPY AVAILABLE

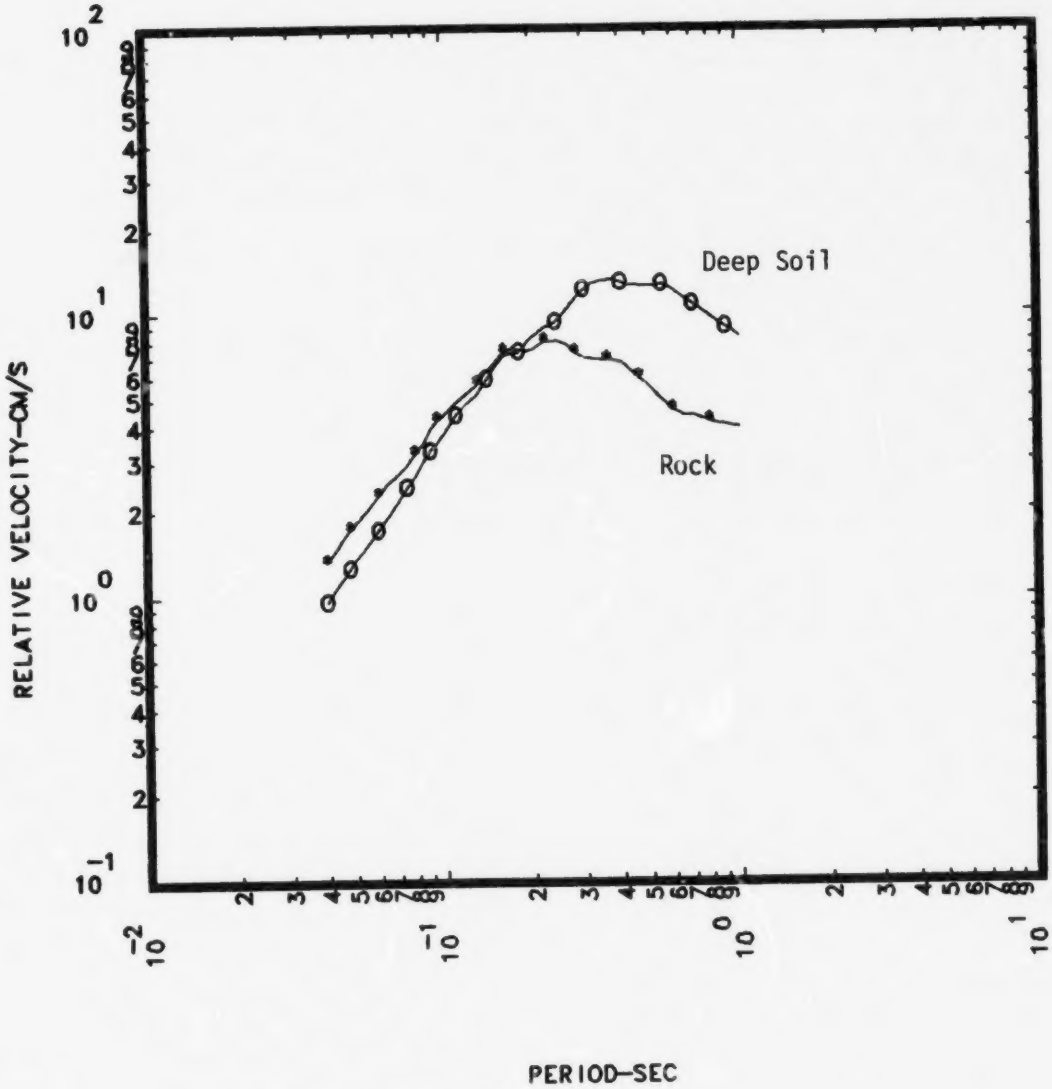

Fig. 6.9 Comparison of the median SSSP for a deep soil site weathered to a rock site for the MM VII case.

BEST COPY AVAILABLE

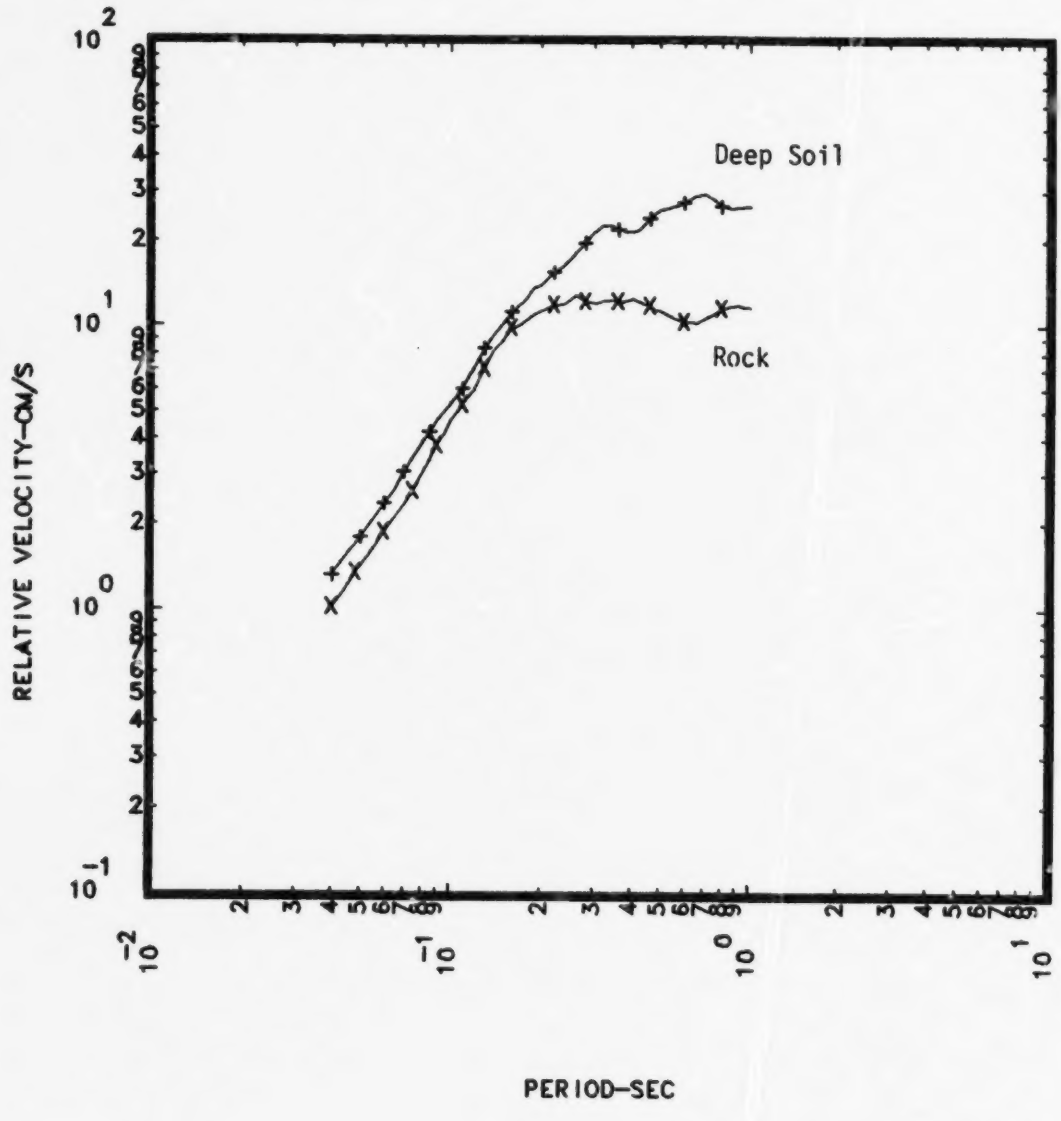

Fig. 6.10 Comparison of the median SSSP for a deep soil site to a rock site for the MM VIII case.

BEST COPY AVAILABLE

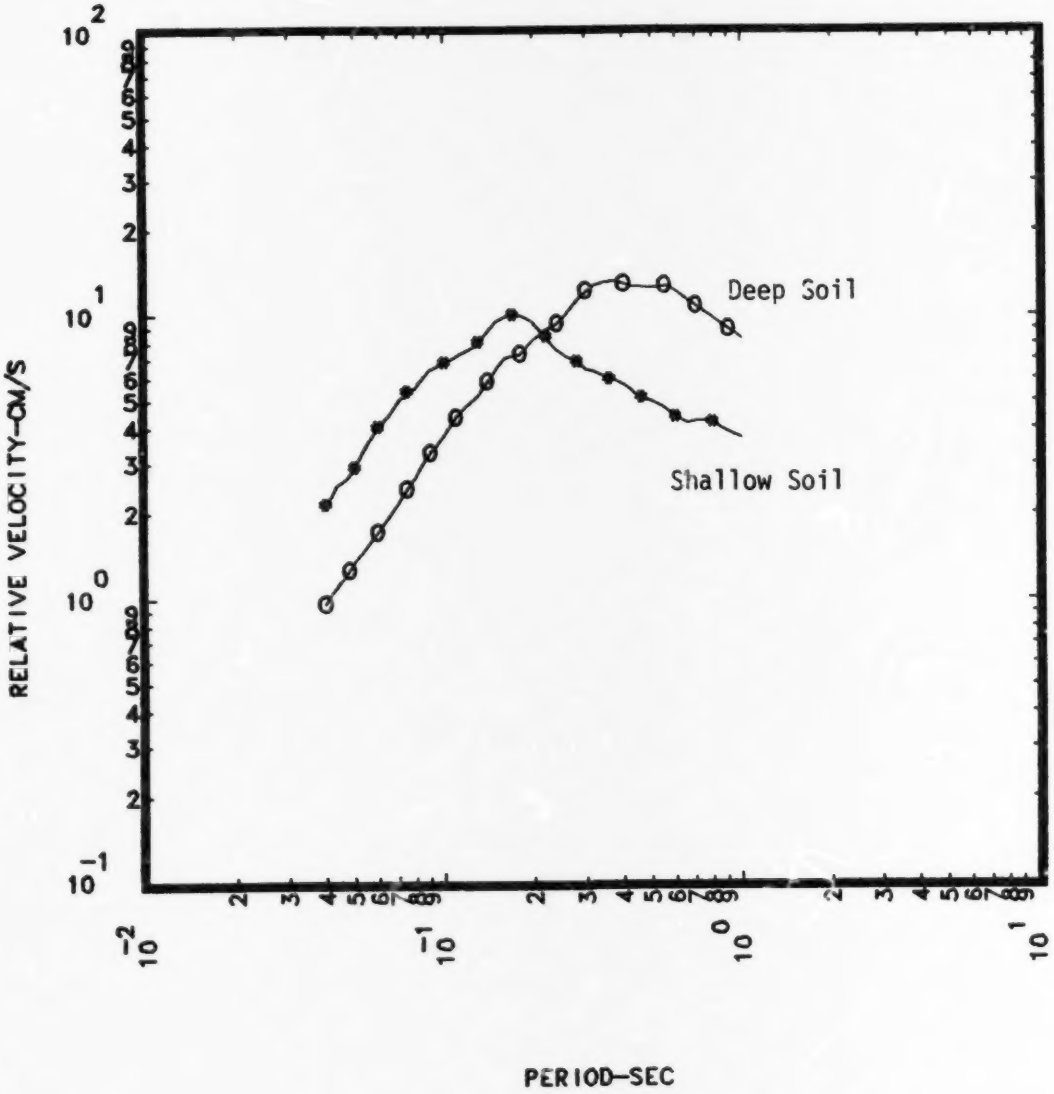

Fig. 6.11 Comparison of the median SSSP for a shallow soil site to a deep site for the MM VII case.

BEST COPY AVAILABLE

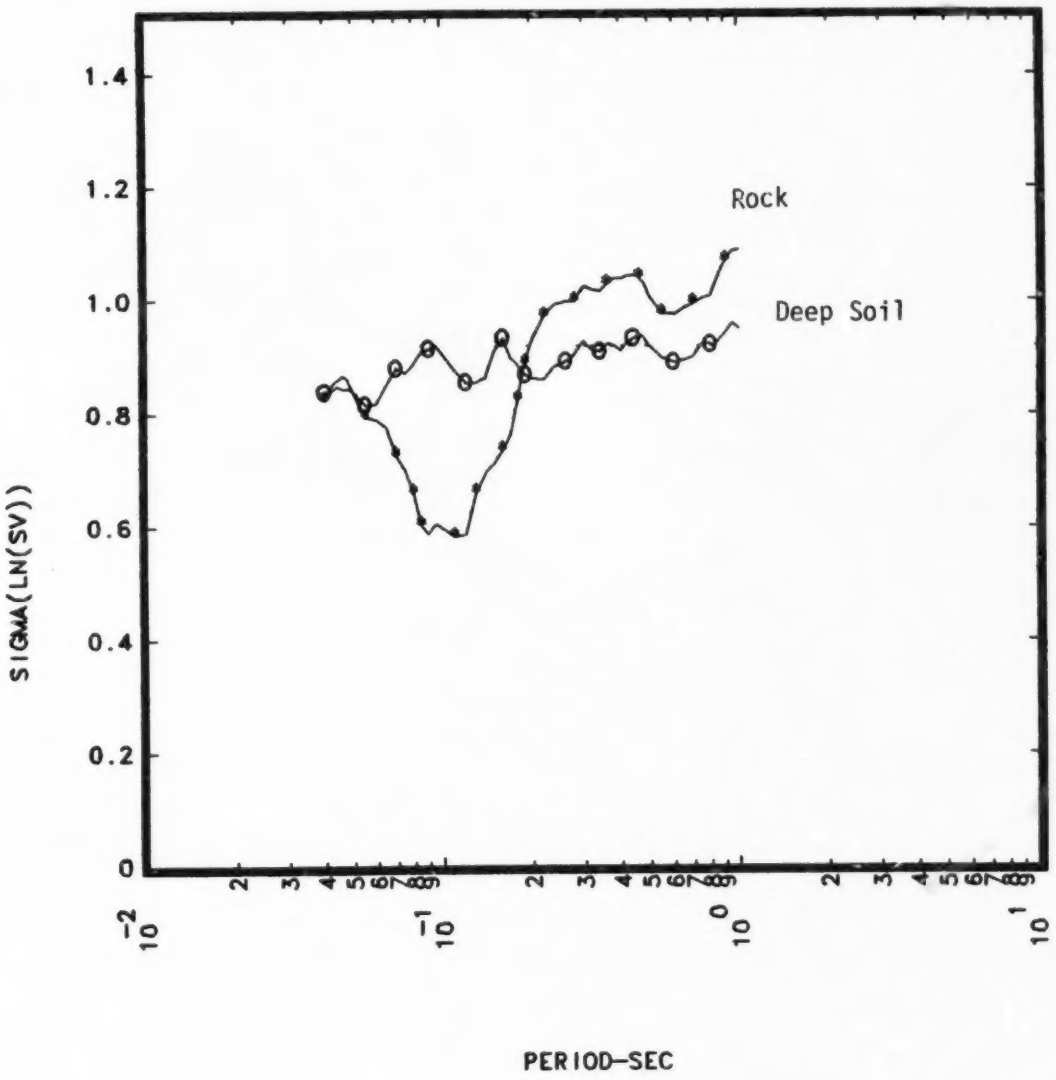

Fig. 6.12 The uncertainty of the SSSP estimate as measured by σ_T for deep soil and rock sites for the MM VII case.

BEST COPY AVAILABLE

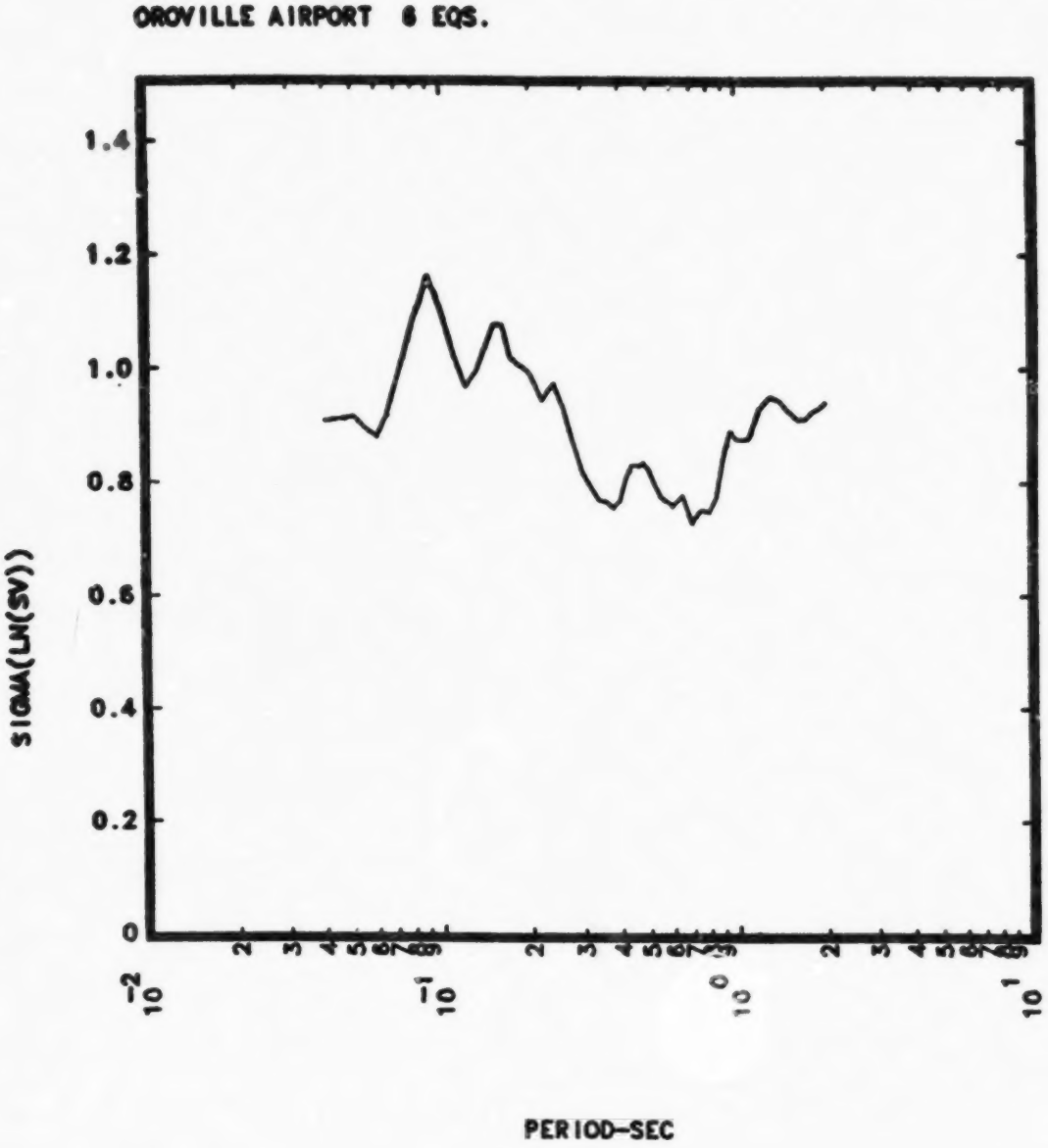

Fig. 6.13 The uncertainty of the SSSP estimate as measured by σ_T for records obtained at the Oroville Airport site based on six earthquakes.

BEST COPY AVAILABLE

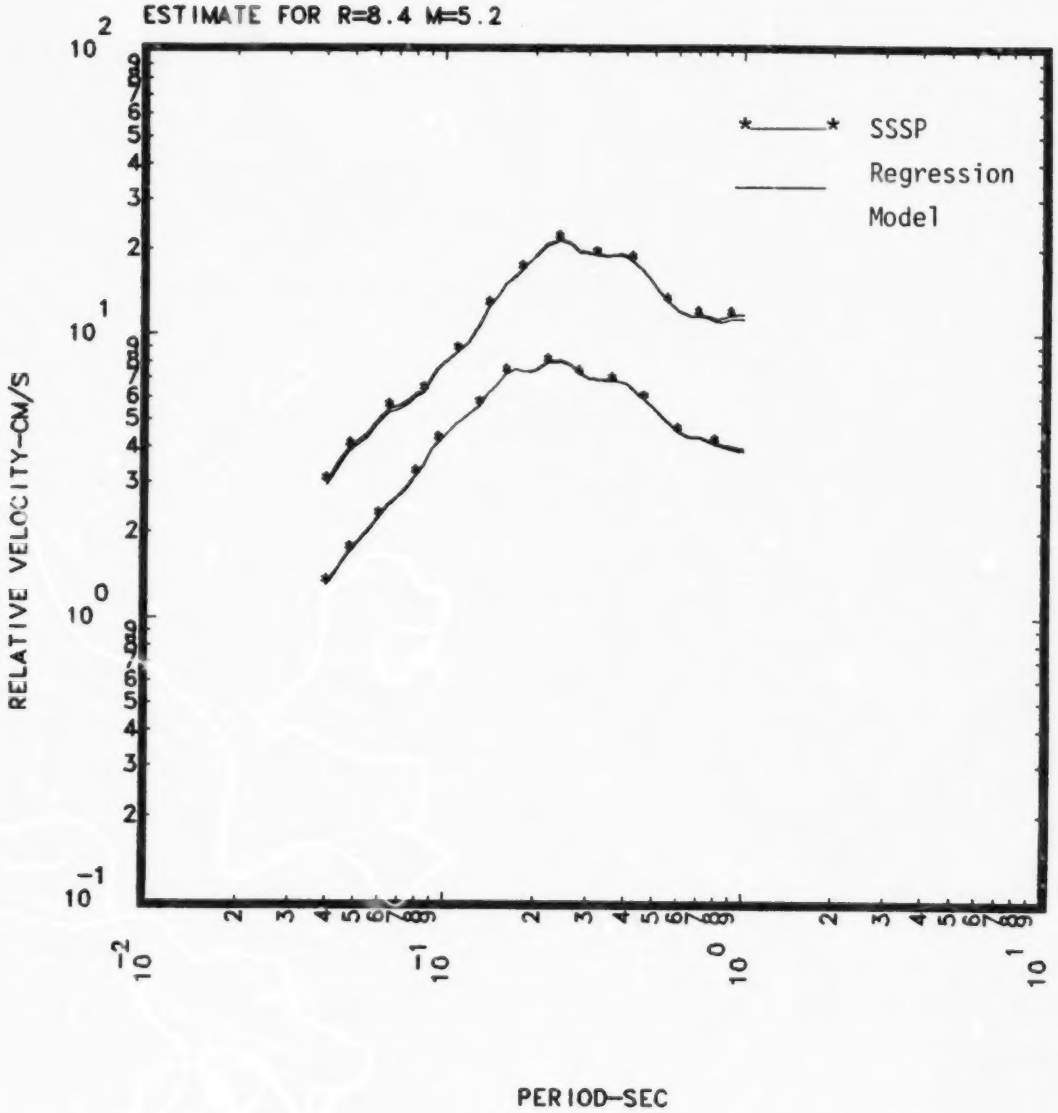

Fig. 6.14 Comparison of the median and 84th percentile spectra predicted by the regression model fit to the MM VII data for rock sites using distance of 8.4 km and a magnitude of 5.2 to the median and 84th percentile spectra for the SSSP for rock sites for the MM VII case.

BEST COPY AVAILABLE

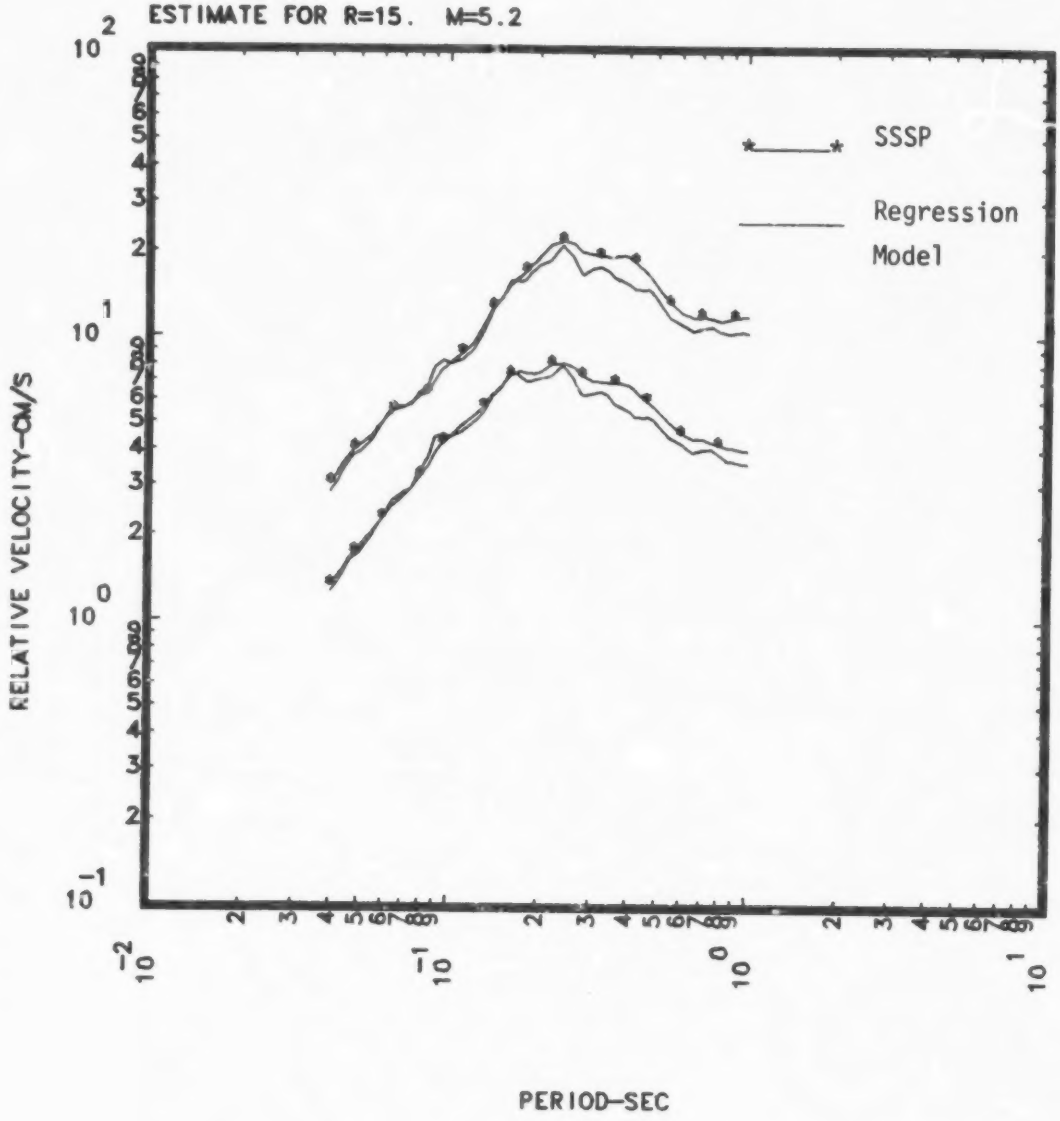

Fig. 6.15 Same as Fig. 6.14, except the prediction is for a distance of 15 km and a magnitude of 5.2.

BEST COPY AVAILABLE

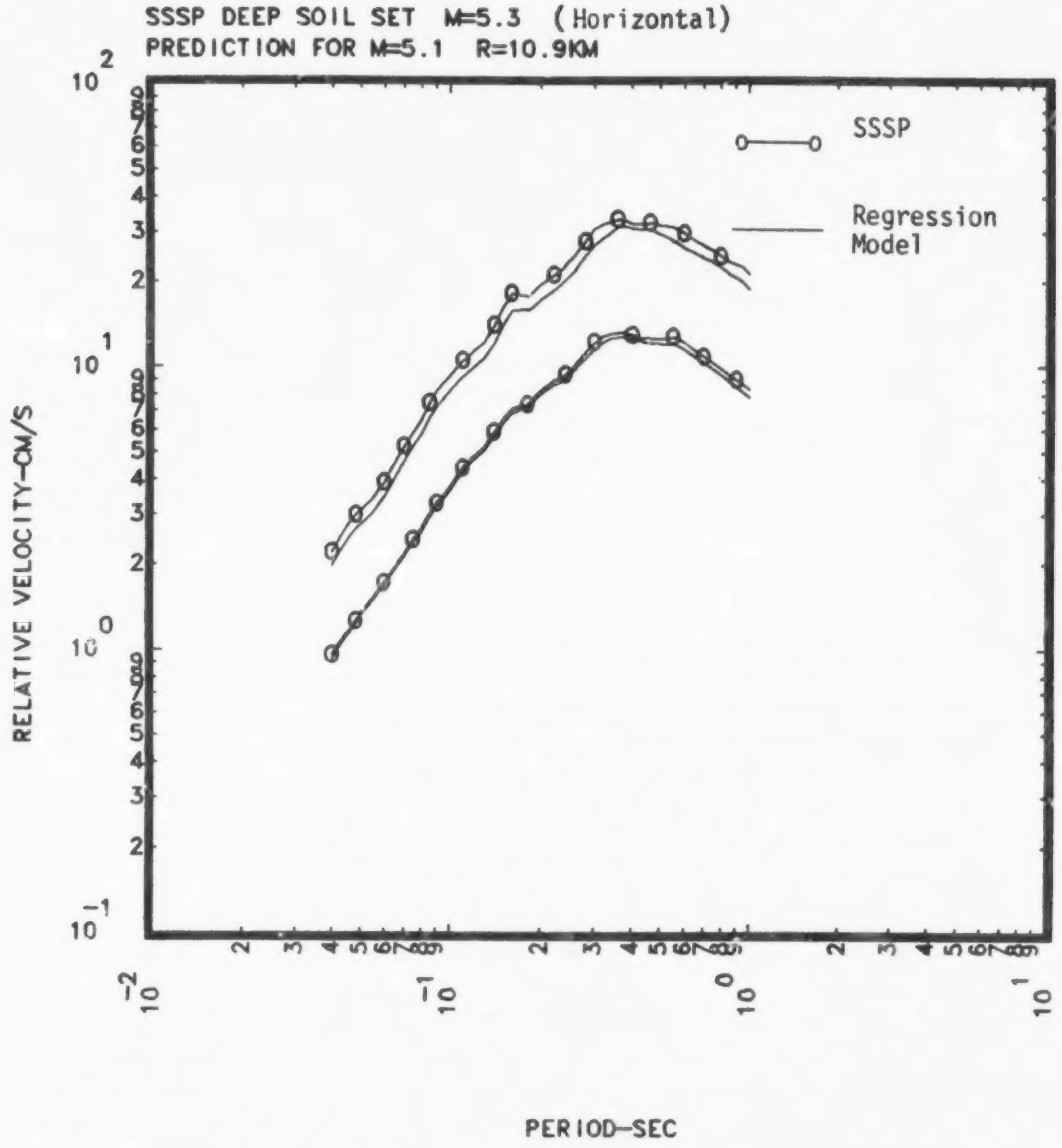

Fig. 6.16 Comparison of the median and 84th percentile spectra predicted by the regression model fit to the MM VII data for deep soil sites using a distance of 10.9 km and a magnitude of 5.1.

BEST COPY AVAILABLE

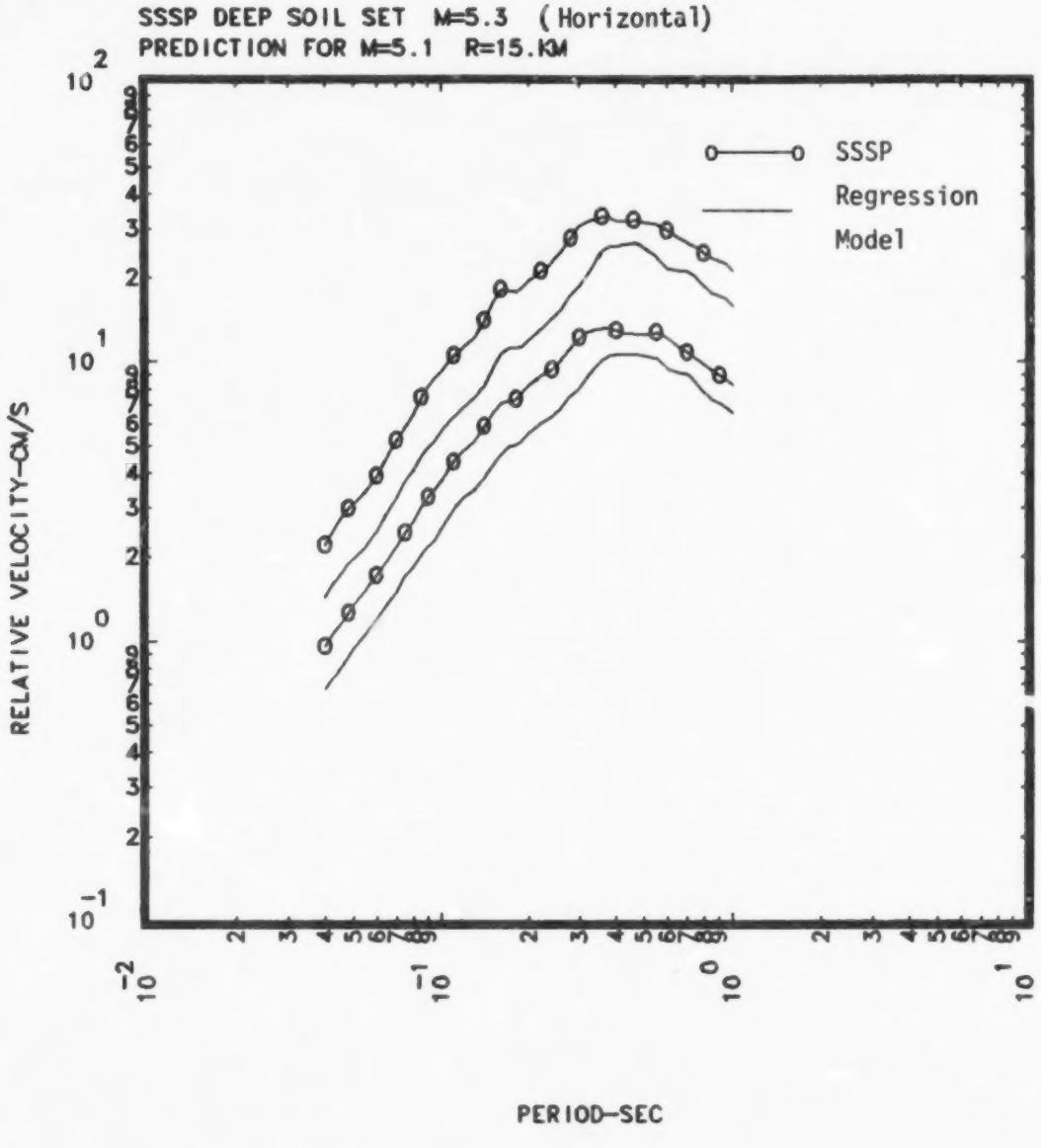

Fig. 6.17a Same as Fig. 6.16, except the prediction is for a distance of 15 km and a magnitude of 5.1.

BEST COPY AVAILABLE

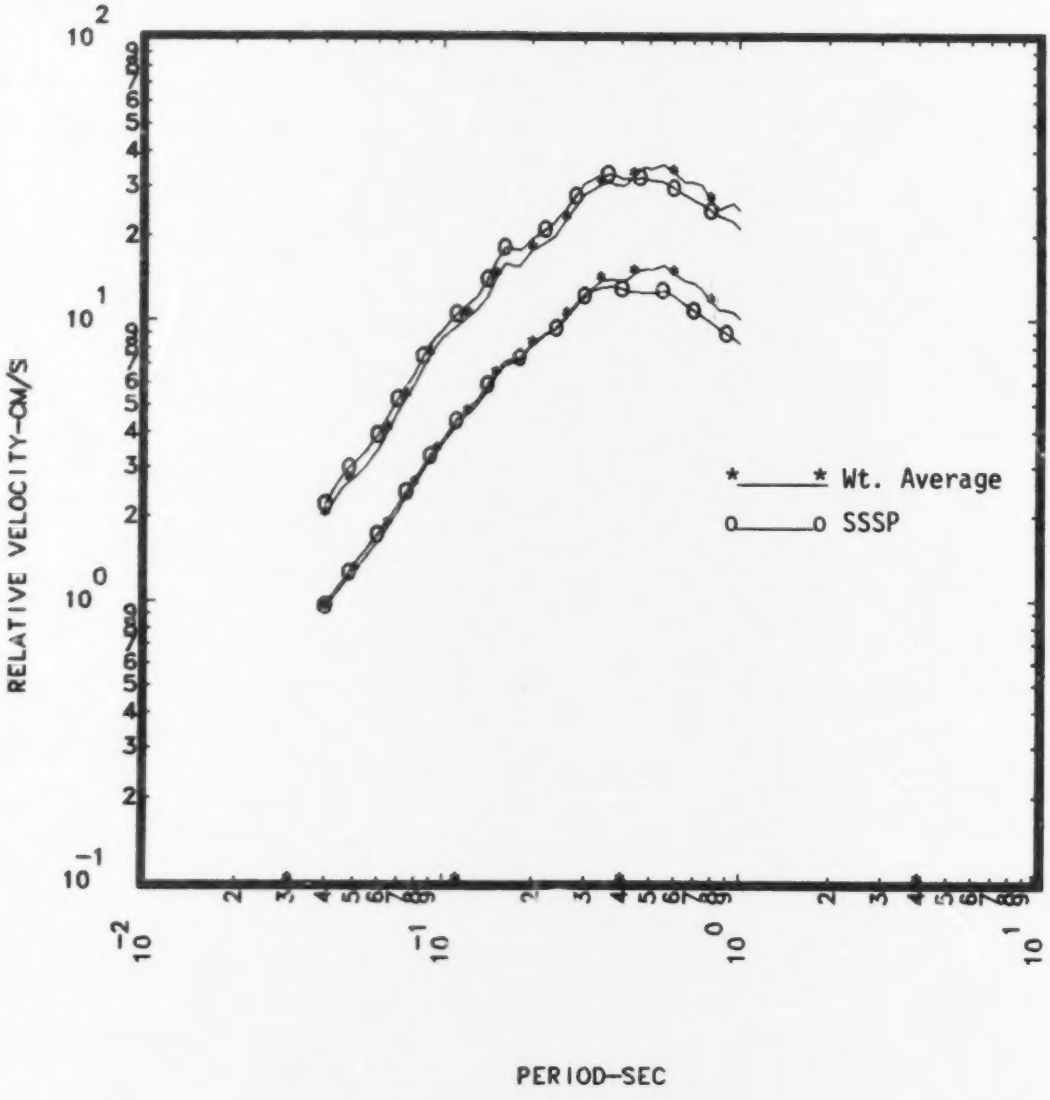

Fig. 6.17b Comparison between the median and 84th percentile SSSP for deep soil sites for the MM VII case and the median and 84th percentile spectra obtained by the weighted averaging approach. The weights were based on four rings.

BEST COPY AVAILABLE

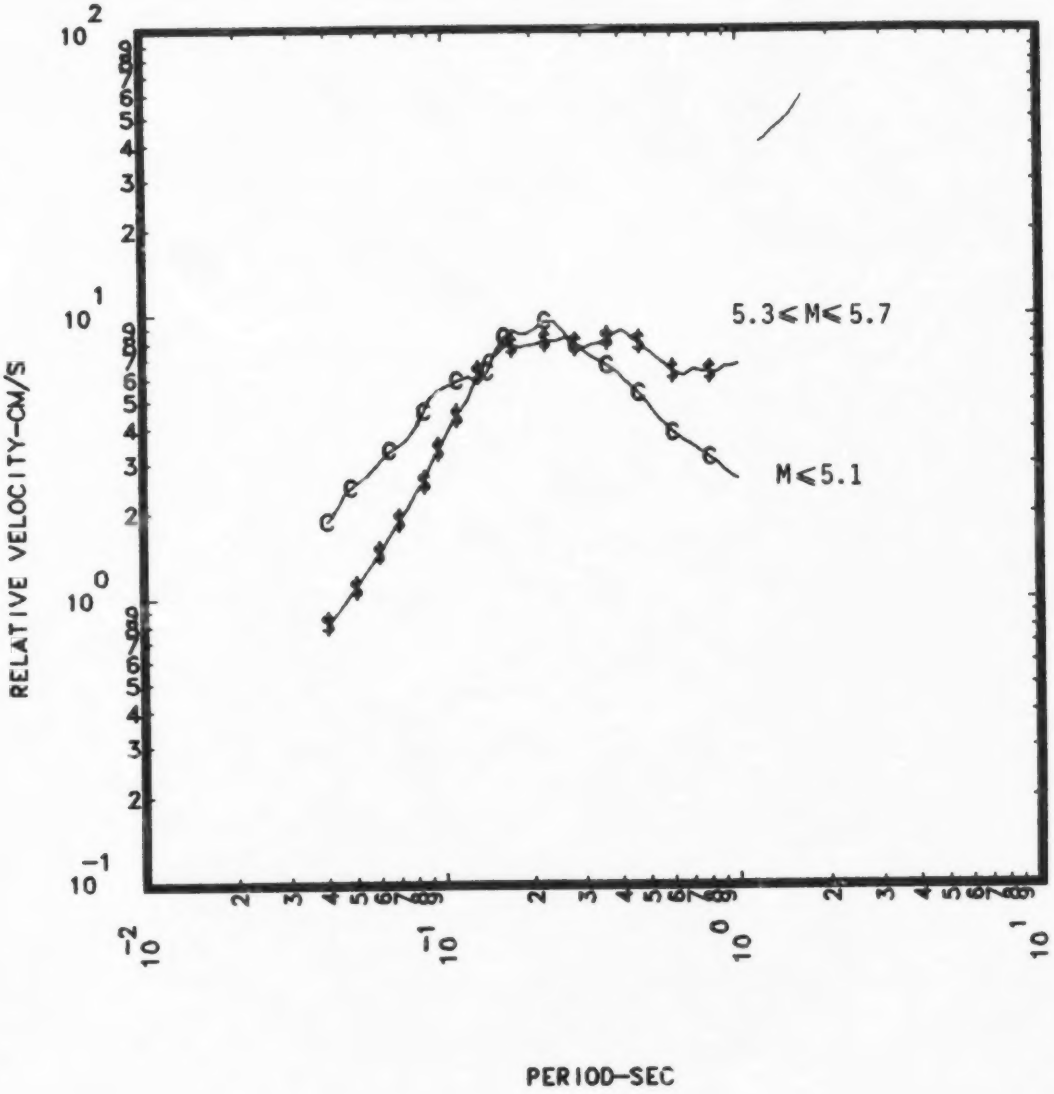

Fig. 6.18 Comparison of the median spectrum of the rock set with magnitudes 5.1 or less to the set with magnitudes between 5.3 and 5.7.

BEST COPY AVAILABLE

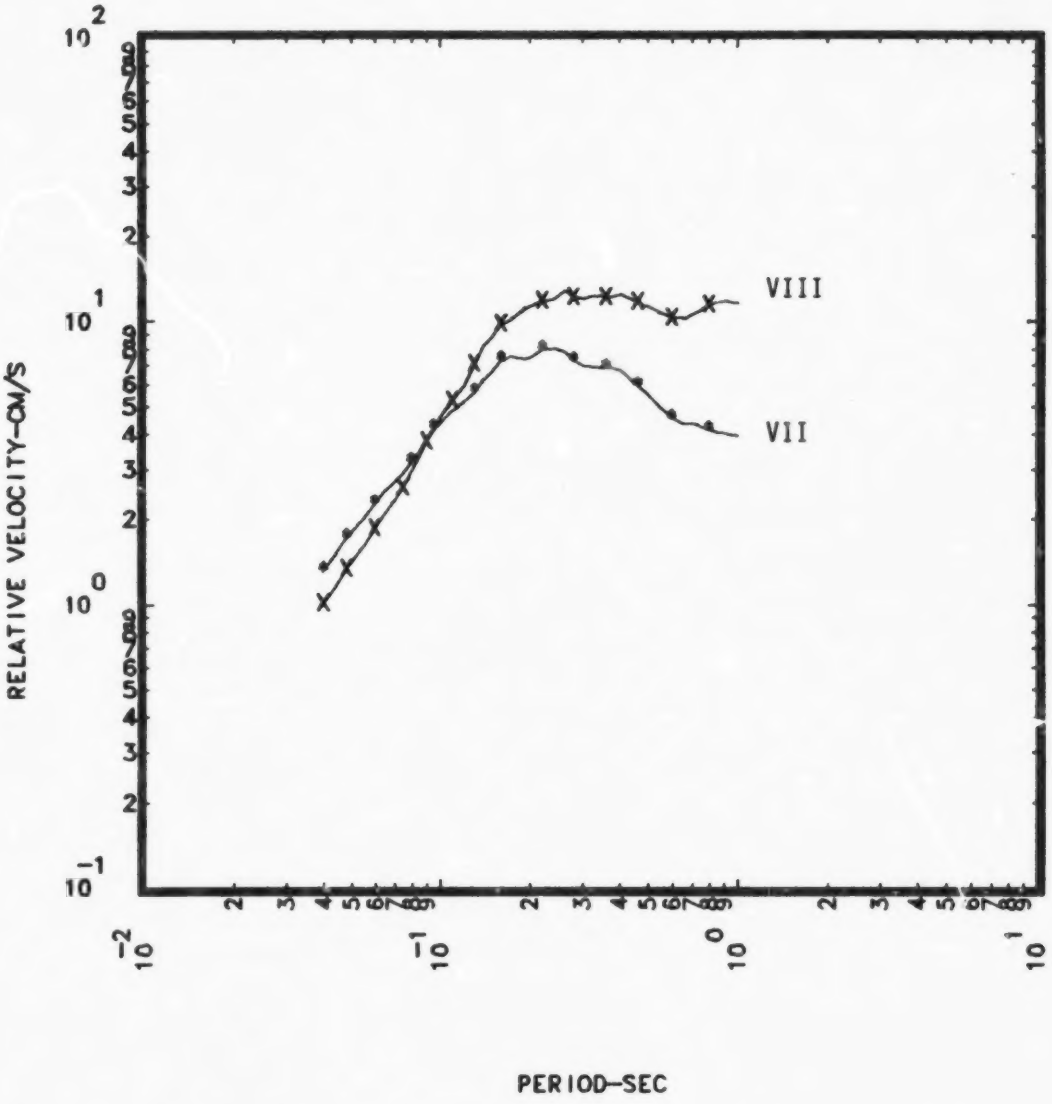

Fig. 6.19 Comparison of the median SSSP for rock sites for the MM VII and MM VIII cases.

BEST COPY AVAILABLE

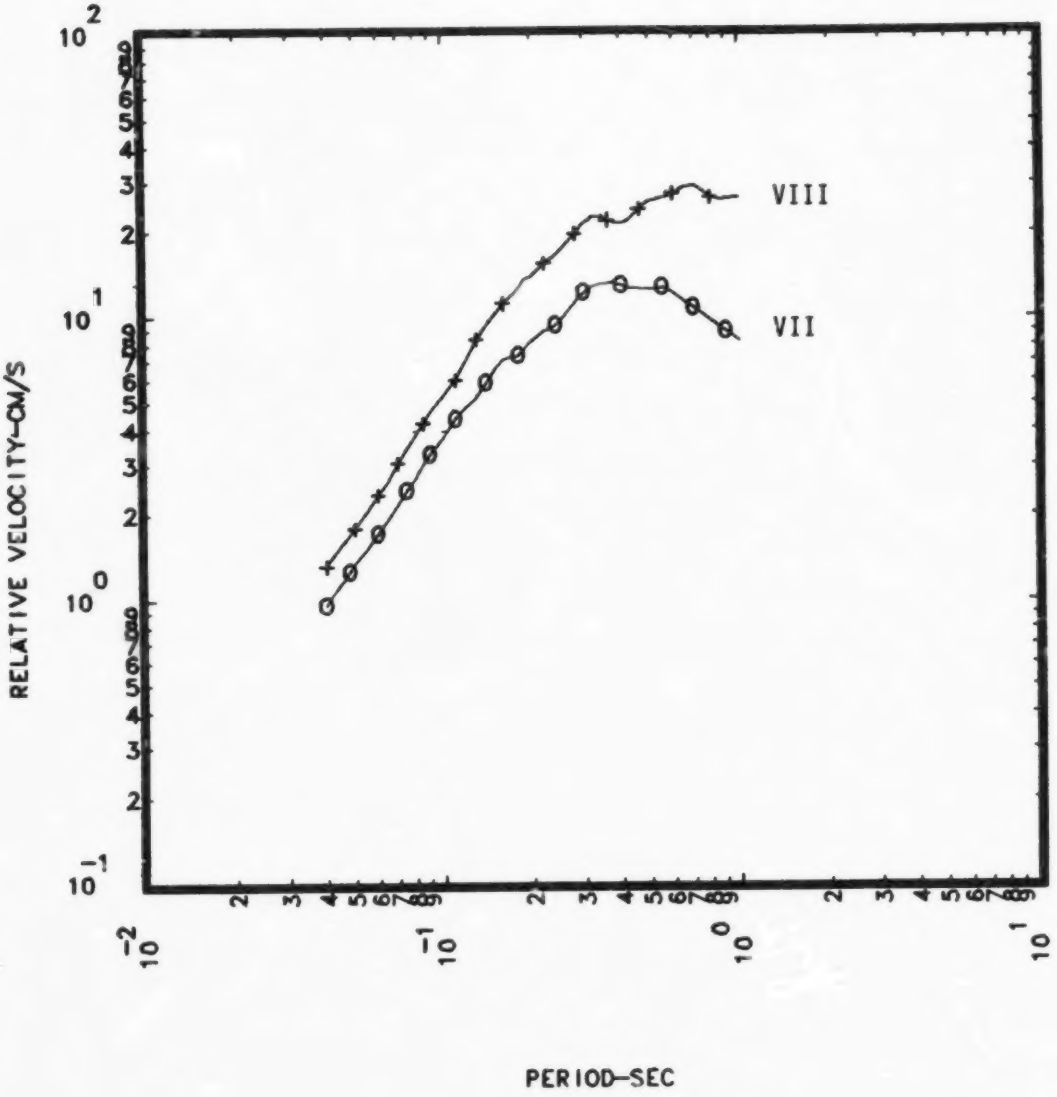

Fig. 6.20 Comparison of the median SSSP for deep soil sites for the MM VII and MMM III cases.

BEST COPY AVAILABLE

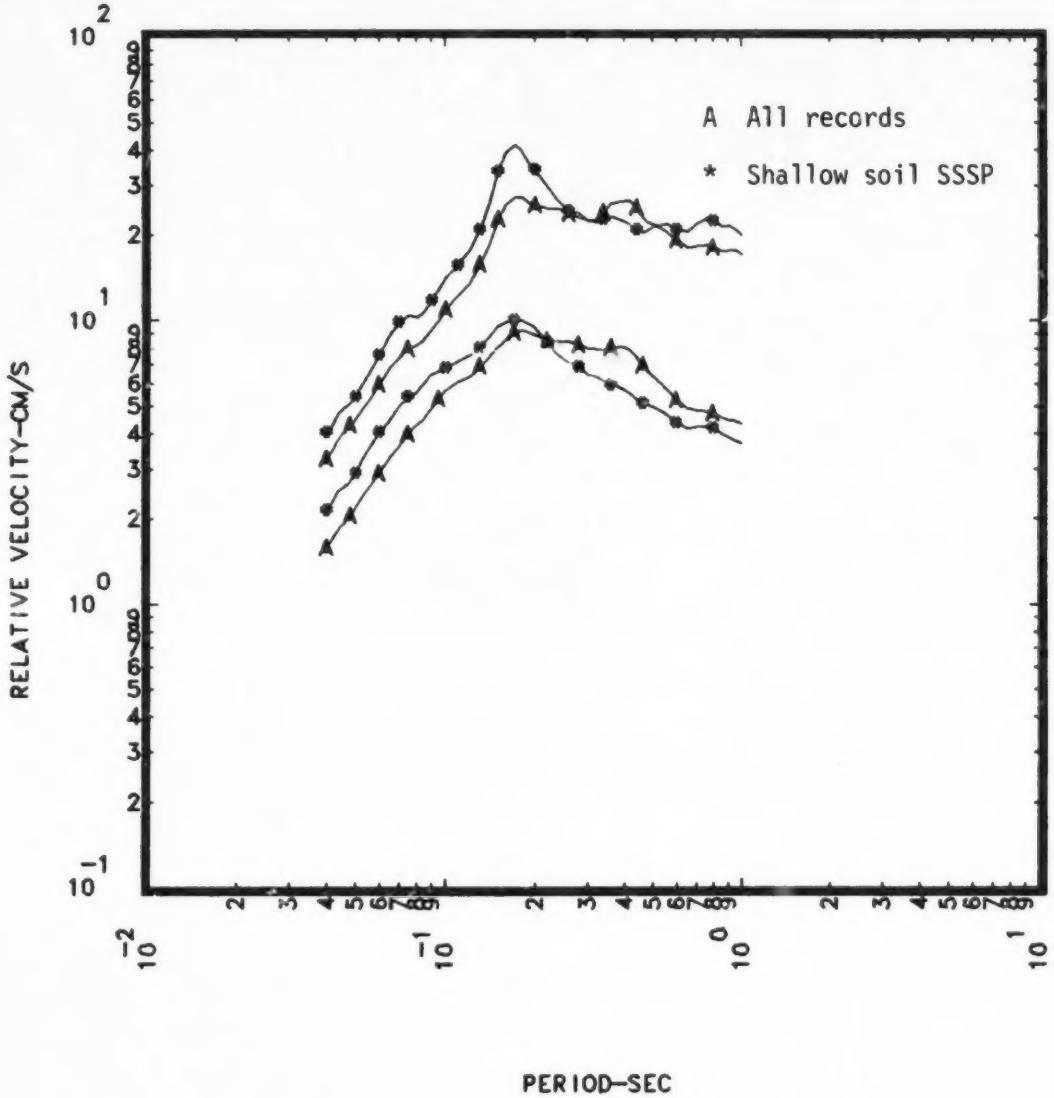

Fig. 6.21 Comparison of the median and 84 percentile spectra for the shallow soil SSSP to the median and 84th percentile spectra obtained using all of the records with magnitudes less than 5.8 in Table 6.4.

BEST COPY AVAILABLE

7. DISCUSSIONS AND CONCLUSIONS

The major conclusion reached in this study is that the ground motion at a site will exhibit large variablility between earthquakes due to source and travel path variabilities. Thus, any approach used to estimate the ground motion at a site will have large uncertainties and the only way to reduce these uncertainties is to include the important source and travel path parameters in the model. We also found that site parameters are very important and should be modeled. These are not new conclusions, but we believe that in Section 5 we have better defined the relative contribution of each of the major sources of uncertainty in the method used to estimate the ground motion. We found that the uncertainty, expressed by the standard deviation of the logarithm of the acceleration, for a fixed site was approximately .5 and the uncertainty introduced by having a variety of sites is .3, which is in agreement with results obtained independently by very different methods by other researchers. (i.e., McCann, 1983). The uncertainty introduced by the paths was found to be on the order of .2 and that of the source was found to be on the order of .3.

Because of large and, at present, unreducible uncertainties, it is not possible to reach conclusions on EUS vs WUS ground motions based on relatively small data sets. For example, in Section 1 we noted that some of the ENA records have more short period energy than WUS records. In Section 2 we noted that this could, in part, be due to the relatively shallow depth of the ENA earthquakes in Section 4 we found high frequencies are not due to site effects but the quality factor Q could be a factor, and given the large variabilities between earthquakes of the same magnitude, it is not possible to test this observation in a meaningful way. We also noted that smaller earthquakes appear to have relatively more short period energy than large earthquakes.

The main task of this report was to update the existing SSSP and generate vertical SSSP. New records were added to the sets initially generated in Bernreuter (1981) where only rock and soil sets of SSSP were generated. In the present study this was refined to include rock, shallow soil and deep soil SSSP as well as vertical spectra.

We concluded that the SSSP were not very sensitive to the distance distribution. That is, the variablity (uncertainty) introduced by the range of distances used was relatively small compared to the variability introduced by other factors. We also concluded that the SSSP are not very sensitive to the distribution of magnitudes used. At rock and, by inference, at shallow soil sites, we found that one important criterion in selecting records to generate SSSP is the depth of soil.

We also concluded that in generating estimates of the ground motion, it is necessary to include data from as many earthquakes as possible with a large number of travel paths. It is also important not to use too much data from a single earthquake.

As more data becomes available, (both strong motion data and equally important data about the soil/rock conditions at the recording site) it will be possible to update and improve the SSSP developed in this report. It is unlikely that the relative difference between the median and 84th percentile spectra will

BEST COPY AVAILABLE

change significantly (i.e., it is unlikely that the uncertainty will be significantly reduced) with the addition of new data. However, it is likely that the absolute location of the medians, and other central tendency measures, will change (more so for the rock and shallow soil SSSP than for the deep soil SSSP). With new data, it should be possible to subdivide the rock set and introduce new shallow soil categories. It should be noted that this will only be possible if the new data includes boring logs and shear wave velocity data.

BEST COPY AVAILABLE

8. REFERENCES

Aki, K, "Attenuation of Shear Waves in the Atmosphere for Frequencies From 0.05 to 25 Hz," Phys. Earth Plant Inter., 21, 50-60, 1980.

Apsel, R. J., Hadley, D. M., Hart, R. S., "Effects of Earthquake Rupture Shallowness and Local Soil Conditions on Simulated Ground Motions," NUREG/CR-3102, UCRL-15495, March 1983.

Apsel, R. J., Frazier, O. A., Jurkevics, A., and Fried, J.C., "Application of Earthquake Source Modeling to Assess the Relative Differences Between Seismic Ground Motion in the Eastern and Western Regions of the United States and to Characterize the Type and Direction of Incoming Seismic Waves," UCRL-15279, September 30, 1980.

Bard, P.Y., and Bouchon, M. (1985), "The two-dimensional Resonance of Sediment Filled Valleys", Bull., Seism., Soc. Am., Vol.75, No.2, pp. 519-541, April.

Bernreuter, D.L., (1979a), "Methods to Develop Site Specific Spectra and a Review of the Important Parameters that Influence the Spectra", Lawrence Livermore National Laboratory, UCRL-52548.

Bernreuter, D.L., (1979b), "Site Soil Column Considerations in Seismic Hazard Analysis" Proceedings of 3rd ASCE Speciality Conference on Structural Design of Nuclear Power Plants, Boston, Mass, April 3-5, 1979.

Bernreuter, D.L. (1983), "Letter Report Documenting work for The Limerick Site", Letter to R. Jackson, June 21, 1983.

Bernreuter, D.L., Savy, J.B., Mensing, R.W., Chen, J.C., and Davis, B.C. "Seismic Hazard Characterization of the Eastern United States", UCID 20421 Vol. 1 & 2, Apr. 1985

Bernreuter, D.L., Chen. J.C., and Bergantz, G. (1984), "Site Specific Spectra for the Hope Creek Site", LLNL Report to NRC.

Bernreuter, D.L., Chen, J.C., and Savy, J.B. (1986) "A Methodology to Correct for the Effect of the Local Site's Characteristics in Seismic Hazard Analysis" Proceedings of 3rd US National Conference on Earthquake Engineering, Charleston, S.C., Aug. 24-27, 1986.

Bernreuter, D.L., (1981) Seismic Hazard Analysis: Application of Methodology, Results and Sensitivity Studies. NUREG/CR 1582 (UCRL-53030, Vol. 4).

Brune, J.N., (1970), "Tectonic Stress and the Spectra of Seismic Shear Waves from Earthquakes", J. Geophys. Res. 75, 4997-5009.

BEST COPY AVAILABLE

Campbell, K.W. (1984), "An Empirical Assessment of near-source Strong Motion for a 6.6m_b (7.5M_s) Earthquake in the Eastern United States", US NRC Report NUREG/CR-3839.

Eisenberg, A. and McEvilly, T.V., (1971), "Comparison of Some Widely-Used Strong-Motion Earthquake Accelerometers", Bull. Seism., Soc., Am., Vol. 61, No. 2, April.

FSAR of Diablo Canyon Nuclear Power Plant.

Hudson, D.E. (1980) "Measurement of Ground and Building Motion". Conference on Advances in Earthquake Engineering", University of CA., Berkeley, June 16-20.

Johnson, D.A. and Hanks T.C., (1976), "Strong Motion Earthquake Accelerograms at Brawley, CA., January 25, 1975" Bull. Seism. Soc. Am. No. 66, pp 1155-1158.

Joyner, W.B. and Boore, D.M., (1981), "Peak Horizontal Accelerations and Velocity from Strong Motion Records Including Records from the 1979 Imperial Valley, California Earthquake", Bull. Seism. Soc. Am., 71, pp 2011-2038.

Kimball, J., (1983), "The Use of Site Dependent Spectra" Proceedings of Conference XXII A Workshop on "Site-specific Effects of Soil and Rock on Ground Motion and the Implication for Earthquake-Resistant Design" USGS Open-file Report 83-845.

Kurata, et.al (1978), "Annual Report on Strong Motion Earthquake Records in Japanese Ports (1976 &1977)", Technical Note No. 287, The Port and Harbor Institute, Ministry of Transport, Japan.

Lynch, R.D., (1969), "Response Spectra for Pahute Mesa Nuclear Events" Bull. Seism., Soc. Am., Vol. 59, pp 2295-2309.

Lynch, R.D., (1971), Covariance Analysis of Response Spectra, AEC Report NVO-1163-TM-24.

Lynch, R.D. and Williams, S.L., (1972), Comparison of Response Spectra from Yucca Flat and Pahute Mesa Underground Nuclear Detonations, AEC Report NVO-1163-TM-32.

McCann, M.W. and Boore, D.M., (1983), "Variability in Ground Motions: Root Mean Square Acceleration and Peak Acceleration for the 1971 San Fernando, California Earthquake", Bull. Seism. Soc. Am., Vol. 73, pp 615-632.

BEST COPY AVAILABLE

McCann, M.W., (1983), "Uncertainty in Ground Motion Predictions" Proc. of Conf. XXII, A Workshop "Site-Specific Effect of Soil and Rock on Ground Motion and the Implication for Earthquake-Resistant Design" USGS Open-file Report 83-345.

McGuire, R.K., (1978), "Seismic Ground Motion Parameter Relations," J. Geotech, ASCE paper 13661, pp 481-490.

Nuttli, O. W., "Seismic Wave Attenuation and Magnitude Relations For Eastern North America," J. Geophys. Res. 78, 876-885, 1973a.

Nuttli, O. W., "The Mississippi Valley Earthquake of 1811 and 1812: Intensities, Ground Motion and Magnitudes," Bull., Seism., Soc. Am., 63, 227-248, 1973b.

Reiter, L., and Jackson, R.E., "Seismic Hazard Review for the Systematic Evaluation Program - A Use of Probability in Decision Making," U.S. Nuclear Regulatory Commission, Division of Engineering, NUREG/0967 (1983).

Schnabel, P. D., Lysmer, J. and Seed, H. B., "SHAKE-A Computer Program For Earthquake Response Analysis of Horizontal Layered Sites," EERC 72-12, U.C. Berkeley, December 1972.

Seekins, L.C., and Hanks, T.C., (1978), "Strong Motion Accelerograms of the Oroville Aftershocks and Peak Acceleration Data," Bull. Seism. Soc. Am. Vol. 68, 677-690.

Shannon & Wilson, Inc. and Agbabian Associate, "Geotechnical Data From Accelerograph Stations Investigated During the Period 1975-1979," Summary Report, NUREG/CR-1643, September 1980.

Shannon & Wilson, Inc. and Agbabian Associate, "Verification of Subsurface Conditions at Selected "Rock" Accelerograph Stations in California," Vol. 2, NUREG/CR-0055, September 1980.

Singh, S., Hermann, R. B., "Regionalization of Crustal Code Q in the Continental United States," J. Geophys., Res. 88, 527-538, Jan 1983.

Sunder, S.S. (1980) "On the Standard Processing Strong-Motion Earthquake Signals", Report R80-38, Mass. Inst. of Tech., School of Engineering, Dept. of C.E.

Thatcher, W., and Hanks, T.C., (1973), "Source Parameters of Southern California Earthquakes," J. Geophys. Res. 78, 8547-8576.

Trifunac, M.D., Udwadia, F. E. and Brady, A.G., (1973) "Analysis of Errors in Digitized Strong-Motion Accelerograms", Bull. Seism. Soc. Am., Vol. 63, No.1, February.

BEST COPY AVAILABLE

Tucker, B.E and King, J.L. (1984) "Dependence of Sediment Valley Response on Input Amplitude and Valley Properties", Bull. Seism. Soc. Am. 74, pp 153-166.

U.S.G.S., "Geologic Description of Selected Strong-Motion Accelerograph Sites," Part 1. Open-File Report 78-1005, 1978.

BEST COPY AVAILABLE

NRC FORM 335 (2-84) NRCM 1102 3201, 3202

U.S. NUCLEAR REGULATORY COMMISSION

BIBLIOGRAPHIC DATA SHEET

SEE INSTRUCTIONS ON THE REVERSE

1 REPORT NUMBER (Assigned by TIDC, add Vol No., if any)

NUREG/CR-4861
UCID-20980

2 TITLE AND SUBTITLE

Development of Site Specific Response Spectra

3 LEAVE BLANK

4 DATE REPORT COMPLETED

MONTH: July YEAR: 1986

5 AUTHOR(S)

D.J. Bernreuter, J.C. Chen, J.B. Savy

6 DATE REPORT ISSUED

MONTH: March YEAR: 1987

7 PERFORMING ORGANIZATION NAME AND MAILING ADDRESS (Include Zip Code)

Lawrence Livermore National Laboratory
7000 East Avenue
Livermore, CA 94550

8 PROJECT/TASK/WORK UNIT NUMBER

9 FIN OR GRANT NUMBER

A0454

10 SPONSORING ORGANIZATION NAME AND MAILING ADDRESS (Include Zip Code)

Division of Engineering Safety
Office of Nuclear Regulatory Research
U.S. Nuclear Regulatory Commission
Washington, DC 20555

11a TYPE OF REPORT

Technical

b PERIOD COVERED (Inclusive dates)

12 SUPPLEMENTARY NOTES

13 ABSTRACT (200 words or less)

For a number of years the USNRC has employed site specific spectra (SSSP) in their evaluation of the adequacy of the Safe Shutdown Earthquake (SSE). As the data set has considerably increased for Eastern North America (ENA) and as more relevant data has become available from earthquakes occurring in other parts of the world (e.g., Italy), together with the fact that recent data indicated the importance of the vertical component, it became clear that an update of the SSSP's for ENA was desirable. This study used actual earthquake ground motion data with magnitudes within a certain range and recorded at distances and at sites similar to those that would be chosen for the definition of an SSE. An extensive analysis of the origin and size of the uncertainty is an important part of this study. The results of this analysis of the uncertainties is used to develop criteria for selecting the earthquake records to be used in the derivation of the SSSP's. We concluded that the SSSPs were not very sensitive to the distribution of the source to site distance of the earthquake records used in the analysis. That is, the variability (uncertainty) introduced by the range of distances was relatively small compared to the variability introduced by other factors. We also concluded that the SSSP are somewhat sensitive to the distribution of the magnitudes of these earthquakes, particularly at rock sites and, by inference, at shallow soil sites. We found that one important criterion in selecting records to generate SSSP is the depth of soil at the site.

14 DOCUMENT ANALYSIS - a KEYWORDS/DESCRIPTORS

site specific spectra
earthquakes

b IDENTIFIERS/OPEN ENDED TERMS

15 AVAILABILITY STATEMENT

Unlimited

16 SECURITY CLASSIFICATION

(This page) Unclassified

(This report) Unclassified

17 NUMBER OF PAGES

18 PRICE

*U.S. GOVERNMENT PRINTING OFFICE: 1987-181-682:60005

123

BEST COPY AVAILABLE